

Investigating methods for assessing erosion and landform stability on rehabilitated mining waste dumps in the Pilbara region, Western Australia

Analysing the potential of remote sensing and
ground-based methods for erosion assessment with
GIS and modelling at the hillslope and gully scale



MSc thesis by Beatriz Nofuentes Martínez

August 2015 - February 2016

Investigating methods for assessing erosion and landform stability on rehabilitated mining waste dumps in the Pilbara region, Western Australia

Analysing the potential of remote sensing and ground-based methods for erosion assessment with GIS and modelling at the hillslope and gully scale

Master thesis Soil Physics and Land Management Group
submitted in partial fulfillment of the degree of Master of
Science in International Land and Water Management at
Wageningen University, the Netherlands

Study program:

MSc International Land and Water Management

Student registration number:

900810606150

Supervisors:

WU Supervisor: Jerry Maroulis
Host supervisor: Rob Loch
Evan Howard

Examinator:

Jerry Maroulis
Jantienne Baartman

Date:

28/02/2015

**Soil Physics and Land Management Group, Wageningen
University**

PREFACE

To the best of my knowledge and belief, the information within this thesis has not been published or written by another person except where due reference is made. Furthermore, the information contained is true, correct and addresses all the requirements of the Guidelines for the MSc Research Thesis Course.

The specific name or location of the study sites are not revealed for reasons of confidentiality. This research has been undertaken in collaboration with Landloch Pty Ltd, BHP Billiton and Wageningen University and Research Centre (WUR).

ACKNOWLEDGEMENT

The author would like to thank Landloch Pty Ltd¹, BHP-Billiton² and Wageningen University (WUR) for providing this research project opportunity. Furthermore, researchers from outside these institutions have also contributed to this project. Thanks to Jerry Maroulis for supervising me and my thesis, during the whole research process.

This research was supported by Landloch Pty Ltd, who provided data, office facilities, all the tools and materials needed for field and office work, airplane tickets, Personal Protective Equipment (PPE) and software required for the project. Furthermore, I thank my colleagues Evan Howard, Brendan Roddy, Dylan Oriley and Anna Reed, who provided insight, expertise and help that greatly assisted the research. I am especially grateful to Evan Howard for supporting and supervising my research whilst in Australia.

I am delighted to have had the opportunity to work on this project and am thus, grateful to BHP-Billiton for their contribution in the provision of data, site access, escort and accommodation during the field work. I would specially like to thank Shayne Lowe, engineer from the rehabilitation department, for providing data and information about the study sites, and in escorting me on site and facilitating my field work. I am also very thankful to Mike Bettison, principal of mining Closure Planning department at BHP-Billiton, for assistance with processing of laser scanner data.

Externally to WUR, Landloch and BHP-Billiton, I am also very thankful to José A. Gómez, author of *Comparing the accuracy of several field methods for measuring gully erosion*, for guiding and sharing with me his expertise in 3D photo-reconstruction; and finally, Stef Verdonk for sharing information about his master thesis *Gully volume calculations using UAV photometry* at the University of Utrecht.

¹ Specialist land, soil, vegetation, and water management consultancy that works collaboratively with clients across a wide range of industries, especially mining, within Australia and internationally. They have work in numerous projects dealing with erosion assessment for BHP-Billiton

² Leading global mining company

TABLE OF CONTENTS

Figures

Tables

Pictures

Hillslope and gully surface assessments

Abbreviations

1. Abstract	1
2. Introduction	2
2.1. Rehabilitation of waste landforms.....	2
2.2. Erosion assessment.....	4
2.2.1. GIS and Erosion modelling	5
2.3. Problem statement.....	6
2.4. Objectives	7
3. Study sites.....	8
3.1. Mining Area C (MAC)	9
3.2. Mount Whaleback (MWB).....	11
4. Methodology	13
4.1. Data collection and pre-processing.....	14
4.1.1. LIDAR	14
4.1.2. UAV	14
4.1.3. Slope transects	15
4.1.4. Laser scanning	16
4.1.5. 3D Reconstruction	17
4.2. Data analysis	18
4.2.1. Surface assessment	18
4.2.2. WEPP erosion modelling	20
4.3. Qualitative analysis and comparison of methods.....	22
5. Results and discussion	23
5.1. Surface assessment.....	23
5.1.1. Hillslope scale: H1	23
5.1.2. Gully scale: G1 and G2	31
5.2. WEPP erosion modelling.....	39

5.3. Qualitative analysis and comparison of methods.....	40
5.3.1. WEPP model	40
5.3.2. LIDAR.....	41
5.3.3. UAV	41
5.3.4. Laser scanning	42
5.3.5. 3D reconstruction.....	42
5.3.6. Slope transects.....	43
6. Conclusions	44
7. References	46
8. Appendices	51
Appendix 1: Project support	51
Appendix 2: Research Planning.....	52
Appendix 2: Rill and gully erosion collection and calculation sheet	53
Appendix 3: Field activities	54
Appendix 4: Field equipment check list.....	55
Appendix 5: Surface assessments.....	56
AP5.1. Hillslope scale.....	56
AP5.2. Gully scale.....	61
Appendix 6: Site pictures.....	71
AP6.1. MAC	73
AP6.2. MWB	77

FIGURES

<i>Figure 1: Non-rehabilitated waste dumps from the Pilbara region</i>	<i>2</i>
<i>Figure 2: Study gully at rehabilitated waste dump</i>	<i>3</i>
<i>Figure 3: Spectral reflectance signatures for bare soil, vegetation and water</i>	<i>5</i>
<i>Figure 4: Location of study areas (BHP-Billiton)</i>	<i>8</i>
<i>Figure 5: Erosion plot (H1) at MAC showing fabric and bucket for collecting erosion and runoff data</i>	<i>9</i>
<i>Figure 6: Satellite image of H1 and G1 (in red)</i>	<i>10</i>
<i>Figure 7: Satellite image of the study waste dump at MWB showing large erosion feature (G2 in red) ...</i>	<i>11</i>
<i>Figure 8: G2 from the bottom</i>	<i>12</i>
<i>Figure 9: Overview of research methodology showing data collection and analysis.....</i>	<i>13</i>
<i>Figure 10: Slope transect method applied on site (Landloch)</i>	<i>15</i>
<i>Figure 11: 3D view of point cloud generated from laser scanning at H1 in Scene showing gullies and the position of the laser scanner (red cross).....</i>	<i>16</i>
<i>Figure 12: 3D reconstruction of G2 at MWB in Cloud Compare</i>	<i>17</i>
<i>Figure 13: Overview of research methodology for data analysis</i>	<i>18</i>
<i>Figure 14: Overview of methodology followed for estimating erosion with WEPP</i>	<i>20</i>

Figure 15: Random roughness versus range in surface elevation along a transect **¡Error! Marcador no definido.**

Figure 16: Satellite image showing H1 (MAC) **¡Error! Marcador no definido.**

Figure 17: Comparison of LIDAR, UAV and laser scanning point clouds at H1 24

Figure 18: 3D view of point cloud generated from laser scanning from the bottom of H1 in Scene..... 24

Figure 19: Comparison of LIDAR, UAV and laser scanning DEM at H1 showing erosion detected features from laser scanning..... 25

Figure 20: Longitudinal slope profiles derived from LIDAR, UAV, laser scanning and field measurements at H1, showing rip lines on laser scanning profile 26

Figure 21: Transverse profile substracted at H1 27

Figure 22: Transverse profiles from LIDAR, UAV, laser scanning and slope transects at H1 showing G1 in blue and another gully in red 27

Figure 23: Comparison of LIDAR, UAV and laser scanning slope maps at H1 (degrees) 28

Figure 24: Comparison of LIDAR, UAV and laser scanning flow accumulation maps at H1 28

Figure 25: Difference of LIDAR and LS DEM at H1 29

Figure 26: Orthophoto June 2012 (on the left) and satellite image September 2015 (on the right) showing how rip lines have been filled in since H1 construction 30

Figure 27: Satellite image of G1 (Sep 2015) 31

Figure 28: Comparison of slope maps derived from 3D reconstruction, laser scanning, UAV and LIDAR at G1 (degrees) 31

Figure 29: Cross section profiles derived from 3D reconstruction, laser scanning, UAV, LIDAR and slope transects at G1 32

Figure 30: Comparison of volume maps created from 3D reconstruction, laser scanning, UAV and LIDAR at G1 33

Figure 31: Satellite image of G2 (Sep 2015) 34

Figure 32: 3D view of point cloud generated from 3D reconstruction at G2, using Cloud Compare software 35

Figure 33: Comparison of DEM profiles derived from 3D reconstruction, laser scanning and LIDAR at G2 35

Figure 34: Maps of surface slope provided by 3D reconstruction, laser scanning and LIDAR at G2 36

Figure 35: Cross section profiles derived from 3D reconstruction, laser scanning, LIDAR and slope transects at G2 37

Figure 36: Comparison of volume map derived from 3D reconstruction, laser scanning and LIDAR at G2 38

TABLES

Table 1: Climatic conditions in MAC (BHP-Billiton)9

Table 2: Soil characteristics at H1, MAC (Landloch) 10

Table 3: Climatic conditions in Newman (Landloch) 11

Table 4: Soil characteristics at G2, MWB 12

Table 5: Erosion calculations from slope transects at H1 29

Table 6: Volume estimations relative to the 3D reconstruction for slope transects laser scanning, UAV and LIDAR at G1 33

Table 7: Volume estimations relative to the 3D reconstruction for slope transects, laser scanning and LIDAR at G2 38

<i>Table 8: Comparison between erosion estimations with WEPP and H1 data from erosion plots</i>	<i>39</i>
<i>Table 9: Comparison between runoff estimations with WEPP and H1 data from erosion plots</i>	<i>39</i>
<i>Table 10: Summary of methods (qualitative characteristics)</i>	<i>40</i>

PICTURES

<i>Picture 1: Results of revegetation efforts at Albatross Flamingo Waste Dump</i>	<i>71</i>
<i>Picture 2: Status of vegetation after rehabilitation on a waste dump in the Pilbara region</i>	<i>71</i>
<i>Picture 3: Rip lines implementation after waste dumps rehabilitation at MWB</i>	<i>72</i>
<i>Picture 4: Eroded waste dump at MWB (1)</i>	<i>72</i>
<i>Picture 5: Eroded waste dump at MWB (2)</i>	<i>73</i>
<i>Picture 6: H1 view from the bottom of the hillslope</i>	<i>73</i>
<i>Picture 7: View of H1 from the top of the hillslope</i>	<i>74</i>
<i>Picture 8: Erosion bucket at H1</i>	<i>74</i>
<i>Picture 9: View from top of H1</i>	<i>75</i>
<i>Picture 10: G1 at MAC from top</i>	<i>76</i>
<i>Picture 11: Precision of the point cloud generated from 3D reconstruction at G1</i>	<i>76</i>
<i>Picture 12: G2 from the bottom of the hillslope</i>	<i>77</i>
<i>Picture 13: G2 from the middle of the hillslope looking downhill</i>	<i>77</i>
<i>Picture 14: G2 from the middle of the hillslope looking uphill</i>	<i>78</i>
<i>Picture 15: G2 from the top of the hillslope (1)</i>	<i>78</i>
<i>Picture 16: G2 from the top of the hillslope (2)</i>	<i>79</i>

HILLSLOPE AND GULLY SURFACE ASSESSMENTS

<i>Plan 1: Hillslope 1 (H1, MAC)</i>	<i>56</i>
<i>Plan 2: LIDAR surface assessment at H1 (MAC)</i>	<i>57</i>
<i>Plan 3: UAV surface assessment at H1 (MAC)</i>	<i>58</i>
<i>Plan 4: Laser scanning surface assessment at H1 (MAC)</i>	<i>59</i>
<i>Plan 5: Cross sections from slope transect data at H1 (MAC)</i>	<i>60</i>
<i>Plan 6: Gully 1 (G1, MAC)</i>	<i>61</i>
<i>Plan 7: LIDAR surface assessment at G1 (MAC)</i>	<i>62</i>
<i>Plan 8: UAV surface assessment at G1 (MAC)</i>	<i>63</i>
<i>Plan 9: Laser scanning surface assessment at G1 (MAC)</i>	<i>64</i>
<i>Plan 10: 3D reconstruction surface assessment at G1 (MAC)</i>	<i>65</i>
<i>Plan 11: Cross sections from slope transect data at G1 (MAC)</i>	<i>66</i>
<i>Plan 12: Gully 2 (G2, MWB)</i>	<i>67</i>
<i>Plan 13: LIDAR surface assessment at G2 (MWB)</i>	<i>68</i>
<i>Plan 14: Laser scanning surface assessment at G2 (MWB)</i>	<i>69</i>
<i>Plan 15: 3D Reconstruction surface assessment at G2 (MWB)</i>	<i>70</i>

ABBREVIATIONS

DEM: Digital Elevation Model

G1: Gully 1. Study gully assessed at H1, MAC

G2: Gully 2. Study gully assessed at MWB

GIS: Geographic Information System

GPS: Global Positioning System

H1: Hillslope 1. Study hillslope assessed at MAC

LIDAR: Laser Imaging Detection and Ranging

LS: Laser Scanning

MAC: Mining Area C (Study mining area)

MWB: Mount Whaleback (Study mining area)

PPE: Personal Protective Equipment

SFM: Surface from Motion

ST: Slope transect

TIN: Triangulated Irregular Network

UAV: Unmanned Aerial Vehicle

WA: Western Australia

WEPP: Water Erosion Prediction Program

WUR: Wageningen University and Research Centre

1. ABSTRACT

Mining can have significant impacts on the local environment, including degraded scenery, landscape degradation, landscape fragmentation, loss of biodiversity and decreased quantity and quality of water resources (Darwish et al., 2010). Apart from being the most visual landform left after mine closure, waste dumps are the most susceptible to erosion (Department of Mines and Petroleum, 2009), leading to landform instability and off-site effects (Evans, 2000). In order to avoid these impacts and thus, convert an area to safe and stable conditions, the effective rehabilitation planning and monitoring of waste dumps becomes essential.

The present research focuses on investigating the potential of methods for assessing erosion and landform stability on rehabilitated waste dumps in the Pilbara region, Western Australia. Various methods for obtaining surface and elevation data – remote sensing (LIDAR and UAV), and ground-based methods (laser scanning, 3D reconstruction and erosion measurements) - were assessed at the hillslope and gully scale by analysing surfaces with *ArcGIS* and modelling them with the Water Erosion Prediction Program (WEPP) model.

The research outcomes provide tools for assessing erosion at different scales, monitoring landform changes over time and supporting or justifying future decision-making in rehabilitation planning of mining waste landforms.

Key words: erosion assessment, rehabilitated mining waste dumps, remote sensing, ground-based methods, WEPP model, GIS, hillslope and gully scale.

2. INTRODUCTION

Mines and their abandonment can have significant impacts on the local environment, including degraded scenery, landscape degradation, landscape fragmentation, loss of biodiversity and decreased quantity and quality of water resources (Darwish et al., 2010). This is especially true in the Pilbara region, located in Western Australia (WA), which is endowed with abundant mineral deposits. Here, the combination of open cut mining activities (changes in landforms, geology and hydrology), erodible soils and very dry conditions result in mining areas which are heavily degraded and vulnerable to erosion. The materials left over from mining give rise to waste dumps (see Figure 1), which apart from being the most visual landform left after mining closure, are the most susceptible to erosion (Department of Mines and Petroleum, 2009). Erosion on waste dumps has a clear impact on landform stability and the pollution of waterways. The combination of erodible material, steep slopes, rainfall events and the concentration of water leads to the formation of rills and gullies on waste dumps; sheet erosion also appears to be a common erosion process on post-mining landforms (Aly, 2010; Morgan, 2009; Singh et al., 1995; Valentin et al., 2005).



Figure 1: Non-rehabilitated waste dumps from the Pilbara region

2.1. Rehabilitation of waste landforms

Although many landholders are conscious about the environmental consequences of mining, more attention should be paid to mine site rehabilitation planning (Claughton, 2014). Rehabilitation is “a process where disturbed land is returned to a stable, productive and self-sustaining condition, taking future land use into account [...] not aspiring to fully replace all of the original components of an ecosystem” (Environmental Protection Authority [EPA], 2006: 33). Environmental approvals for mining activities are granted in accordance with the Mining Act 1978 (State Law Publisher [SLP], 2015), including mine closure plans covering all aspects of mine rehabilitation. Since July 2013, the Department of Mines and Petroleum, WA Government, introduced the Mining Rehabilitation Fund (MRF) so that every mineral exploitation and mining company has to pay an annual levy in order to rehabilitate abandoned mines across the State. This is an incentive for mining companies to generate environmental and financial safety, with interest allocated towards a progressive rehabilitation so that land is restored immediately after use. The sooner the company fulfills its environmental obligations, the lower its annual levy.

Rehabilitation of waste dumps has different objectives such as improving soil properties, reducing erosion rates or supporting future land uses (rehabilitators at BHP-Billiton, pers. comm.). Rehabilitation planning should include an adequate design of landform, revegetation and monitoring

of outcomes that the approach has on the surrounding environment; such as erosion, landscape transformation and recreation of ecosystems. Hence, waste dump rehabilitation must assure, among others, surface stability i.e. that the constructed soil surface shows no signs of significant erosion. Thus, the design of a stable waste dump is essential for minimizing erosion, which could otherwise lead to exposure of encapsulated contaminants, elevated sediment delivery at catchment outlets, and subsequent environmental off-site impacts such as degradation of downstream water quality, soil depletion, sediment deposition or contaminant transport (Evans, 2000; Moliere et al., 2002; Niemiec, 2009; Vrieling, 2005; Woldai, 2001). For this reason, according to the Department of Mines and Petroleum of the Government of Western Australia (2009), the design of waste dump profiles should ensure that the structure is not prone to significant erosion rates, by paying close attention to soil material characteristics, proposed vegetation cover, natural topography and climate. BHP-Billiton installs rip lines on contour across the slope using a wheeled tractor as contour barriers in order to interrupt the hydrological connectivity at the hillslope scale. However, when the landform design is not appropriate, rip lines can lead to completely the opposite effect (Figure 2).



Figure 2: Study gully at rehabilitated waste dump

Waste material can be derived from considerable depths in the mine and thus can be characterized by being very poor soils with low drainage capacity. Therefore, waste soil needs to be mixed with topsoil so that the store of seeds, organic matter, nutrients and soil microbes are present in the soil (Jasper, 1994) and revegetation can succeed. Despite the importance of an effective waste landform design and revegetation plan, the most important factor to take into account when rehabilitating is the material composing the waste dump (rehabilitators at BHP-Billiton, pers. comm.). In order to prevent soil loss and support any possible future land use, revegetation based on enhancing native and local species (BHP Billiton Iron Ore, 2013; Red Dirt Seeds, n.d.) is applied to waste dumps in the region.

BHP Billiton Iron Ore (2013) proposed an overarching framework for the restoration of iron ore mining areas in the Pilbara in order to prevent, control and abate pollution and environmental harm. Vegetation reduces erosion by decreasing the kinetic energy of the raindrops, increasing infiltration (stabilization of the soil, enhancement of porosity and permeability, and organic matter input), and

decreasing runoff speed and depth. However, although vegetation can be an effective solution against erosion, the success of revegetation on waste dumps are varying (United States, 1985).

Current rehabilitation strategies developed by BHP-Billiton are based on 3 principles – stability, safety and no pollution- consisting of defining goals for rehabilitation, site limitations and/or requirements, testing and characterizing materials (e.g. erodibility and fertility), assessing the potential for erosion through modelling, testing design alternatives attending to factors such as cost and practicality, and finally, selecting the most suitable alternative, referring to landform shape, soil and vegetation aspects at the waste landform.

2.2. Erosion assessment

Although erosion assessment on waste dumps have not been subject of much research, several techniques have been applied for assessing erosion for a range of scenarios. Over the last century, directly measuring erosion on site has been the main methodology used in erosion studies. Developed by A.N. Alutin of the United States Soil Conservation Service (USCS), the slope transect method consisting of measuring the cross section of rills found across a fixed-length transect has been applied for estimating erosion in a simple and direct way since 1937 (Hudson, 1993).

A very indirect way of assessing erosion is by remote sensing. “Remote sensing from aircraft and satellites, is a powerful tool used in Earth resources mapping which can be adapted for environmental monitoring of mining induced activities” (Woldai, 2001: 75). According to Miemiec (2009), remote sensing provides homogeneous high-resolution data over large areas that can be widely applied for erosion assessment.

Satellite remote sensing can contribute to surface assessments by providing spatial data (Vrieling, 2005). Optical satellite images, such as Landsat, Ikonos, QuickBird or ENVISAT, have been and can be applied in erosion research for detecting eroded areas, determining their spatial range or assessing erosion factors (Miemiec, 2009). In Australia, there has been some important research undertaken by Raval, Merton and Laurence, who have been working on using satellite remote sensing techniques for assessing revegetation on mine sites since 2010. For instance, Raval and Laurence (Australian Centre for Sustainable Mining Practices (ACSMP), University of New South Wales (UNSW)), have used various satellite imagery for this purpose, especially WorldView-2 satellite imagery. “This satellite based approach clearly identifies subtle changes in vegetation composition and health across an otherwise homogenous revegetated surface and proves a valuable addition for mine rehabilitation management” (Raval et al., 2013: 200). There are other remote sensing techniques that are useful for assessing erosion. For instance, LIDAR can identify ephemeral erosion sites and produce slope estimates for use in erosion estimations (Minnesota Geospatial Information Office Minnesota Geospatial Information Office [MnGeo], 2001) and has the potential to quantify and monitor gully erosion (Perroy et al., 2010). Volumes of gullies can be calculated with UAV platforms and ArcGIS with the aim of creating a better understanding of long-term erosion rates (Verdonk, 2015).

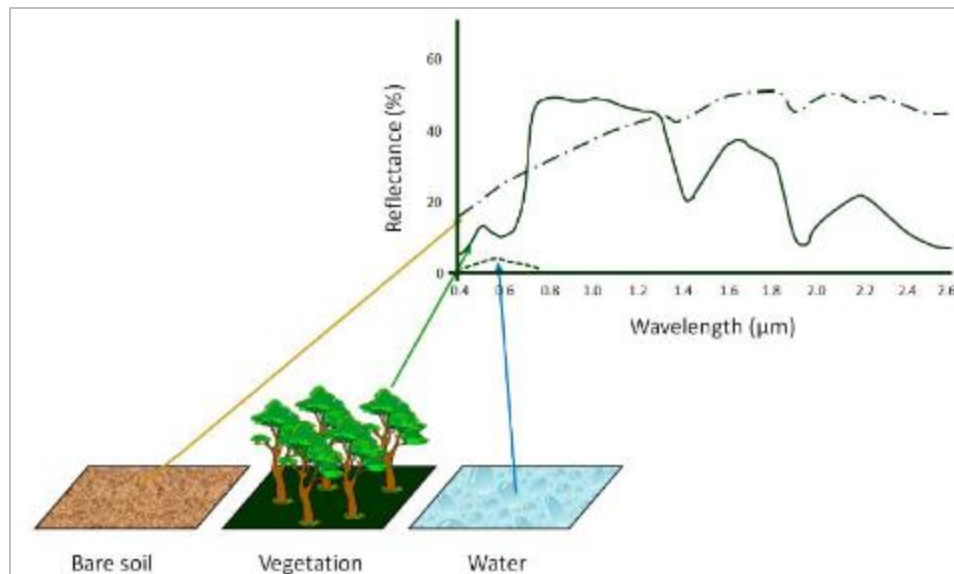


Figure 3: Spectral reflectance signatures for bare soil, vegetation and water

Information from the surface can be derived from the multispectral remotely sensed data, as in the case of LIDAR, making it a potential tool for erosion assessment. The amount and spectral distribution of reflected energy are utilized in remote sensing to infer the nature of the reflecting surface. A basic assumption made in remote sensing is that specific targets have an individual and characteristic manner of interacting with incident radiation which is described by the spectral response of that target, called the spectral signature. Figure 3 shows an idealized spectral reflectance curve for vigorous vegetation, bare soil and water bodies between the visible and the infrared spectra.

There are other ground-based remotely sensed methods that can be applied in erosion studies. For instance, Castillo et al. (2012) compared the accuracy of different ground-based field methods for measuring gully erosion, including 3D reconstruction and laser profilometer among others. 3D photo-reconstruction is an innovative technique based on the Surface from Motion (SfM) approach that has been applied to erosion studies (Castillo et al., 2012; James et al., 2012). This technique is an alternative to other expensive remote sensing techniques (e.g. laser scanning), which consists of creating 3D models from field photographs taken with a standard digital camera, using of open source software. Laser scanners or photogrammetry can produce high resolutions surveys for assessing landform changes and volume losses (Schmid et al., 2004), being useful for detailed studies of erosion processes, despite their high cost (James et al., 2012).

2.2.1. GIS AND EROSION MODELLING

The precision of these methods for erosion assessment can be analyzed through the use of techniques such as modelling to predict or estimate erosion rates, or by applying Geo-Information Systems (GIS). Surfaces can be derived from a limited set of elevation point values in ArcGIS, which enables analysis of raster terrain surfaces and extraction of information from surfaces (e.g. elevation profiles, contour lines or calculation of surface area).

Models are extremely valuable tools for researchers but it is important to keep in mind that the “real” behaviour of the environment is much more complex than can be considered in models. Most erosion models were created to assess erosion in agricultural areas (Aly, 2010). However, although

Landloch has been working on this issue for many years, there is very little reported in the literature about the assessment of erosion from waste dumps through modelling; despite erosion and landform evolution modelling techniques being useful approaches for predicting landform stability (Evans et al., 1998). An overview of erosion models applicable to mining areas was developed by Aly (2010). He stated that the USLE model, the most widely used empirical erosion model, can only be applied for predicting net erosion, as depositional areas and pathways are not considered in the model.

The combination of remote sensing with GIS can also be used for estimating soil erosion. “GIS offers a means by which the data collected during the assessment of possible mining impacts can be stored and manipulated” (Boggs et al., 2001: 7). For instance, a soil erosion model was developed by Hazarika et al. (1999) to integrate the Normalized Difference Vegetation Index (NDVI) and land slope for estimating the annual soil erosion rate. Bagyaraj et al. (2014) also applied NDVI, among other factors, and GIS for estimating erosion based on the Weight Index Overlay (WIO). The USLE model in combination with GIS was used by Printemps et al. (2007) to plan the mitigation of erosion by relating off-site deposition and mining activities.

The WEPP physically-based model “simulates many of the physical processes important in soil erosion, including infiltration, runoff, raindrop and flow detachment, sediment transport, deposition, plant growth, and residue decomposition” (Flanagan et al., 2007: 1603). This model can be applied at hillslope or small watershed scale. It requires a large number of input parameters, mainly classified into four classes: climate, soil, slope and management. Landloch developed guidelines for landform rehabilitation at mine sites to assess erosion potential using WEPP (Landloch Pty Ltd, 2010). Different batters and other slopes were used to identify erosion potential. They could analyze conditions when rehabilitating waste dumps in order to avoid or decrease erosion. Furthermore, WEPP also provides water balance (surface runoff, subsurface flow, and evapotranspiration), soil detachment and deposition at points along the slope, sediment delivery, and vegetation growth outputs.

2.3. Problem statement

Rehabilitation of waste dumps has different objectives such as improving soil properties, reducing erosion rates or supporting future land uses. Ultimately, to correct or reduce the impact that mining has on the environment. However, rehabilitation may not always act as expected due to a number of factors including inadequate design of the landform or failure in the revegetation making landforms susceptible to erosion. Therefore, there is a need to assess the success of any rehabilitation implemented in order to support future rehabilitation planning and monitoring (Department of Industry, Tourism and Resources, 2006), being both essential for ensuring landform stability.

Most rehabilitation monitoring programmes, focused on landform stability assessment, have been based on field work, e.g. trapping and measuring eroded sediments by runoff. Remote sensing can thus represent a potentially more cost-effective approach than fieldwork and allows the study of static and dynamic attributes (Satellite Imaging Corporation [SIC], n.d.), even though remote sensing always requires ground validation. Given the spatial extents and variable nature of post mining substrates, the mining sector realises the potential of remote sensing but they must fully integrate it

with their monitoring methods (Fletcher et al., 2013; Ravalet al., 2011). Therefore, BHP-Billiton views investigation of techniques based on remote sensing for assessing erosion as important because an assessment, only based on field work, can be very laborious, time-consuming and costly (Perroy et al., 2010). BHP-Billiton is looking for a broad-scale method to collect data on erosion, which can be validated and defensible. Furthermore, the data obtained is needed to internally justify the landform design process.

2.4. Objectives

The main objective of this research is to gain insights into the potential of different methods for assessing erosion and landform stability on rehabilitated waste landforms in the Pilbara region, WA. Different methods for obtaining surface and elevation data – remote sensing (LIDAR and UAV), and ground-based methods (laser scanning, 3D reconstruction and erosion measurements) – have been analysed and compared at the hillslope and gully scale by:

- Using GIS for analysing surfaces, calculating erosion volumes, assessing erosion features and comparing methods;
- Modelling with WEPP to predict soil loss that "should have" occurred, for the current structure since construction to present, which can be validated through erosion plot data;
- Qualitative analysis summarising the characteristics and potential of each technique.

This work will enhance future rehabilitation planning and monitoring of waste dumps through methods to control erosion and landform stability at different scales. The outcomes from this work may provide insight into erosion assessment methods that have potential to be accepted by WA regulators and be widely applied not only across the Pilbara, but, eventually, across most WA mining regions. The study approach could also be applied in erosion assessments under a range of other different scenarios. The ultimate goal of this research is to evaluate tools for assessing erosion in order to implement solutions for minimising environmental off-site impacts.

These objectives lead to the main research question: **How can remote sensing (LIDAR and UAV) and ground-based (laser scanning, 3D reconstruction and field measurements) methods be applied for assessing erosion and landform stability on rehabilitated waste dumps in the Pilbara region, WA?**

In order to answer the main research question, several sub-questions have been formulated:

1. What are the characteristics and how precise is each approach for assessing landform surface erosion on mining waste dumps at the hillslope and gully scale?
2. In what ways does WEPP represent a useful tool for estimating erosion on mining waste dumps?
3. What are the strengths and weaknesses of the study methods in the assessment of erosion on rehabilitated waste dumps?

3. STUDY SITES

The Pilbara region in Western Australia is characterized by an arid, tropical climate with very high temperatures and low irregular annual precipitation driven largely by sporadic tropical cyclones that can deliver high intensity rainfall in a short period of time. Typical soils from the region are characteristically red iron-rich and shallow soil and ranging from rocky to stony soils (Department of Agriculture and Food, 2014). Landscapes in the Pilbara are dominated by spinifex (*Triodia* sp.) grasslands spotted with scrublands patches, under *Eucalyptus* sp. and *Corymbia* sp. low open woodlands (Ecoscape, 2011).

Several rehabilitated waste dumps were identified as possible sites of study by BHP-Billiton. The selection of the study sites was based on the available data such as LIDAR, specific soil characteristic information about each rehabilitation area and observations from satellite imagery, orthophotos and the first site visit. The erosion assessment was finally based on 2 mining sites, Mining Area C and Mount Whaleback, within BHP-Billiton leases in the Pilbara region (see Figure 4).



Figure 4: Location of study areas (BHP-Billiton)

3.1. Mining Area C (MAC)

Located 135 km North of Newman, Mining Area C (MAC) contains a number of waste dumps, some of which were not successfully rehabilitated and are currently going through a new rehabilitation plan. The study waste dump contains nine runoff-erosion plots on a hillslope that has been collecting erosion data for the last three years (July 2012-2015). Climatic conditions (Table 1) correspond to the characteristic arid climate in the Pilbara with very high temperatures and low annual precipitation (352 mm) concentrated in the summer months (mainly Jan-Mar). According to available daily climatic series data at 15 minute interval, precipitation at MAC is characterised by high intensity rainfall events in short periods of time, which leads to high erosion rates (Morgan, 2009).

Table 1: Climatic conditions in MAC (BHP-Billiton)

	Jan	Feb	Mar	Apr	May	Jun	Jul	Aug	Sep	Oct	Nov	Dec	
T	32.8	31.3	29.9	26.3	20.9	17.5	16.7	18.8	22.7	27.1	30.0	32.1	
MT	40.0	37.9	36.7	33.1	27.7	24.3	24.1	26.6	31.0	35.4	38.2	39.8	
mT	25.5	24.6	23.0	19.4	14.1	10.7	9.3	11.0	14.4	18.7	21.7	24.4	
SR	571	523	504	439	381	355	395	468	554	616	635	617	
P	89.5	81.3	52.5	20.8	19.6	22.2	10.6	6.6	2.4	4.3	10.1	32.7	352.6

T: Monthly average temperature (°C); MT: Monthly average maximum temperature (°C); mT: Monthly average minimum temperature (°C); SR: Monthly average solar radiation (langleys/day); AND P: Monthly average precipitation (mm).

Data from the experimental erosion plots includes rainfall data, runoff, suspended and bed load, from which we obtain erosion rates for each of the 9 plots. Each plot has an approximate area of 1200 m². The erosion plot edges were built so that they are disconnected from the rest of the waste dump in terms of hydrological connectivity.

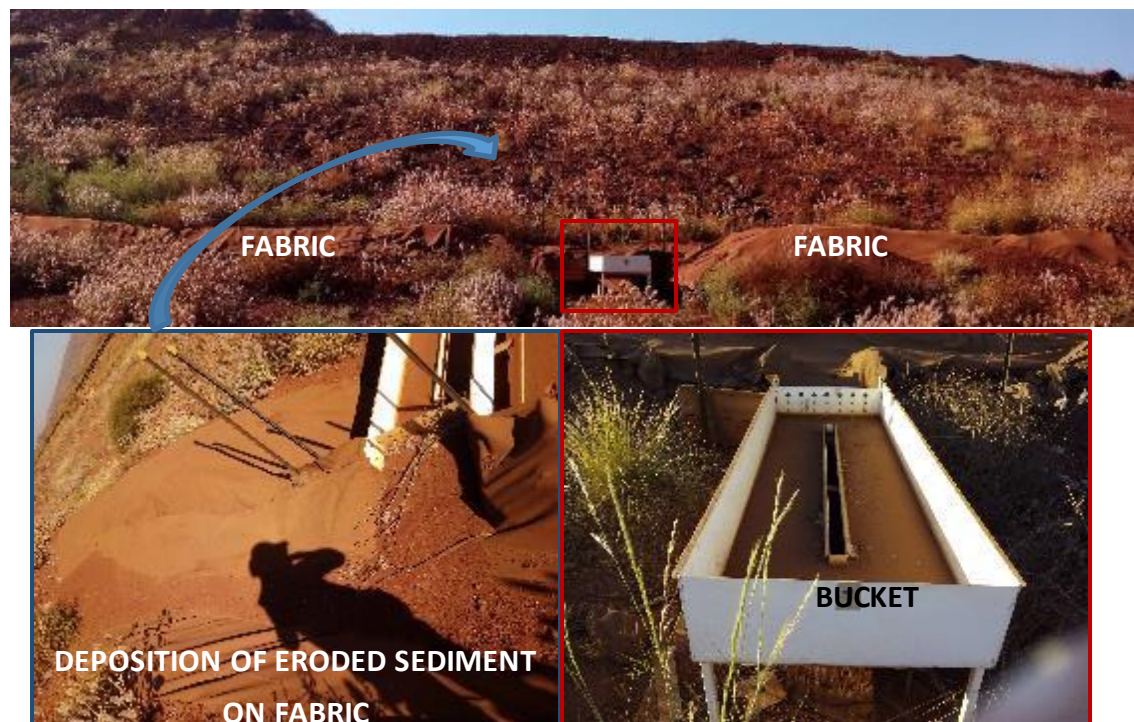


Figure 5: Erosion plot (H1) at MAC showing fabric and bucket for collecting erosion and runoff data

The largest bed load particles (>2mm) eroded are retained by a fabric located at the bottom of the hillslope covering the whole plot width. A bucket collecting runoff and suspended load is located at the plot outlet, after the fabric (Figure 5); it is a tipping bucket with a magnetic counter that counts the number of times the box has tipped to measure runoff volume. Part of the runoff is diverted to another bucket in order to measure the suspended load.

Erosion was assessed at the hillslope and gully scale in MAC. The study focused on one of the erosion plots, H1 (Figures 5 and 6), where more erosion has been experienced compared to the other 8 plots. H1 covers an area of 1145 m², approximately 40 m long and 30 m wide. It is a section of waste dump hillslope characterised by an 18° slope with clear gully and rill erosion features (Figure 6) mainly due to the highly erodible substrate (see Table 2). Vegetation covering H1, mainly perennial herbs of *Ptilotus* (Figure 5), provides very low vegetation cover to protect against water erosion (canopy cover of 15% and ground cover of 5%, estimated from observations). Rip lines implemented on the hillslope when constructed have been considerably filled in over the last three years. An 18.5x1.1 m gully, G1, has been also studied at H1 in MAC- (Figure 6).

Table 2: Soil characteristics at H1, MAC (Landloch)

Soil texture	Albedo	Initial Sat. Level (%)	Interrill Erodibility (kg*s/m ⁴)	Rill Erodibility (s/m)	Critical Shear (Pa)	EHC (mm/h)
Sandy loam	0,23	2	244200	0,03	25	10

EHC: Effective Hydraulic Conductivity

Although this site has not been rehabilitated, there is erosion data available, and so the erosion plots represent an ideal scenario for applying the study techniques.

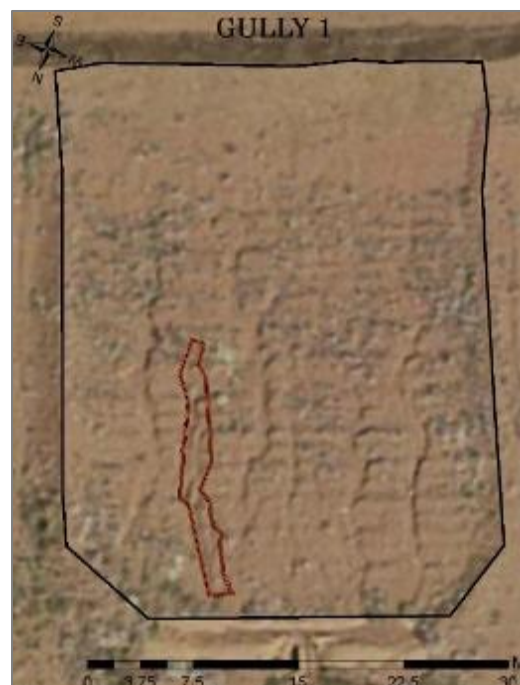


Figure 6: Satellite image of H1 and G1 (in red)

3.2. Mount Whaleback (MWB)

The second study waste dump is located at Mount Whaleback, close to the town of Newman, where mining operations have taken place since 1962. The rehabilitation works on this waste dump started during the 70's but it has been through several re-rehabilitations due to inadequate landform design. The inadequate waste landform design together with uncontoured rip lines have been fostering the concentration of water for 9 years resulting in numerous on and off site effects, with pronounced erosion features (Figure 7) and wash out of waste materials, making this area susceptible to landform instability.

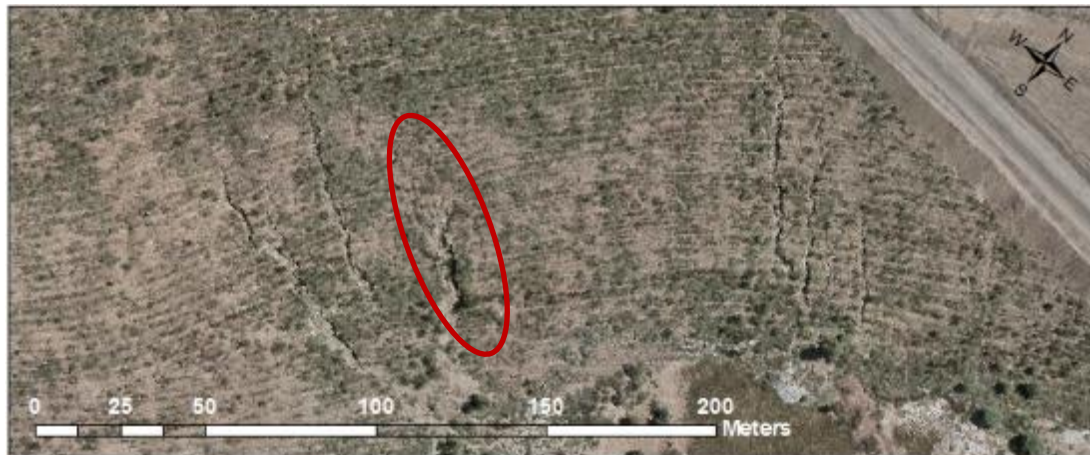


Figure 7: Satellite image of the study waste dump at MWB showing large erosion feature (G2 in red)

The climatic conditions at this mining site are similar to those registered in Newman (Table 3), where the closest weather station is located. As in the case of MAC, this area is characterised by high temperature by high temperatures and low but intense precipitation concentrated in the summer months.

Table 3: Climatic conditions in Newman (Landloch)

	J	F	M	A	M	J	Jl	Au	S	O	N	D	
T	32.4	30.9	28.9	25.0	19.6	15.8	15.2	17.4	21.6	25.9	29.0	31.4	
MT	39.4	37.3	35.6	31.8	26.6	22.8	22.7	25.3	29.8	34.1	36.9	38.8	
mT	25.3	24.4	22.2	18.1	12.6	8.8	7.6	9.5	13.3	17.7	21.1	24.0	
SR	587	533	503	437	378	347	381	459	550	613	633	616	
P	54.9	80.8	40.7	22.7	19.2	18.9	13.1	8.6	4.5	5.3	10.2	52.5	331.4

T: Monthly average temperature (°C); MT: Monthly average maximum temperature (°C); mT: Monthly average minimum temperature (°C); SR: Monthly average solar radiation (langleys/day); AND P: Monthly average precipitation (mm).

The section of hillslope selected for the study is heavily eroded (Figures 7 and 8). Only gully scale assessment was done at this waste dump due to limited time for the field work. In this case a 35x6 m long gully, G2, has been reconstructed and analysed (Figures 7 and 8). Despite the area not being characterised by steep slopes (12°) nor low vegetation cover, large erosion features can be found here.



Figure 8: G2 from the bottom

Soil characteristics, texture and classification derived from soil samples obtained on site are shown in Table 4. Whereas the soil characteristics are similar for all the samples, sample one presented a high electric conductivity according to the Soil Electrical Conductivity Classification developed by Johnson et al. (2002), confirming saline mining waste. This sample was taken from an area of the study gully channel that dominated by white material. In comparison, samples 2 to 4 are largely the same, presenting a low electro-conductivity. Vegetation cover is dominated by various species of Acacia shrubs, providing an estimated canopy and ground cover of 65-70% and 40-50%, respectively. There was an absence of vegetation in the gully channel (see Figure 8).

Table 4: Soil characteristics at G2, MWB

Nº	EC 1:5 (μ S)	R (kg)	Pb (kg)	CG (kg)	5mm (kg)	FINES <2mm (kg)	SAMPLE WEIGHT (kg)	CF >2mm (%)	TEXTURE
1	638	0,13	0,56	1,51	0,51	1,94	4,65	58,28	Sandy Clay Loam
2	82	0,32	0,56	0,97	0,36	1,80	4,01	55,11	Sandy Clay Loam
3	39	0,00	0,34	1,34	0,68	1,87	4,23	55,79	Sandy Loam
4	88	0,00	0,30	1,91	0,81	2,39	5,41	55,82	Sandy Loam

EC: Electro-conductivity (μ S); R: Rock; Pb: Pebbles; CG: Course gravel; and CF: Coarse Fragments

4. METHODOLOGY

During this research, various methods were applied to assess their potential as an effective erosion and rehabilitation assessment tool through different analysis and at different scales.

Before collecting and processing data, the study sites were analyzed using spatial imagery and orthophoto information since the construction of waste dumps to the present day. The first visit to the mining sites took place from October 19th to 21st, where observations were made and pictures taken. The selection of the most suitable study sites was based on the presence of erosion, available LIDAR imagery, climatic and soil data, time available for field work, specific information about each rehabilitation, and direct field observations or from satellite imagery and orthophotos.

Figure 9 shows the methodology followed in the present research for data collection and analysis. While remote sensing data (UAV and LIDAR) was provided for the study, slope transects, laser scanning and 3D reconstruction (i.e. ground-based methods) were applied on site for the collection of surface data at the hillslope and gully scale (except 3D reconstruction, which was only focused at the gully scale). Other field measurements such as slope or rip line characteristics were also collected.

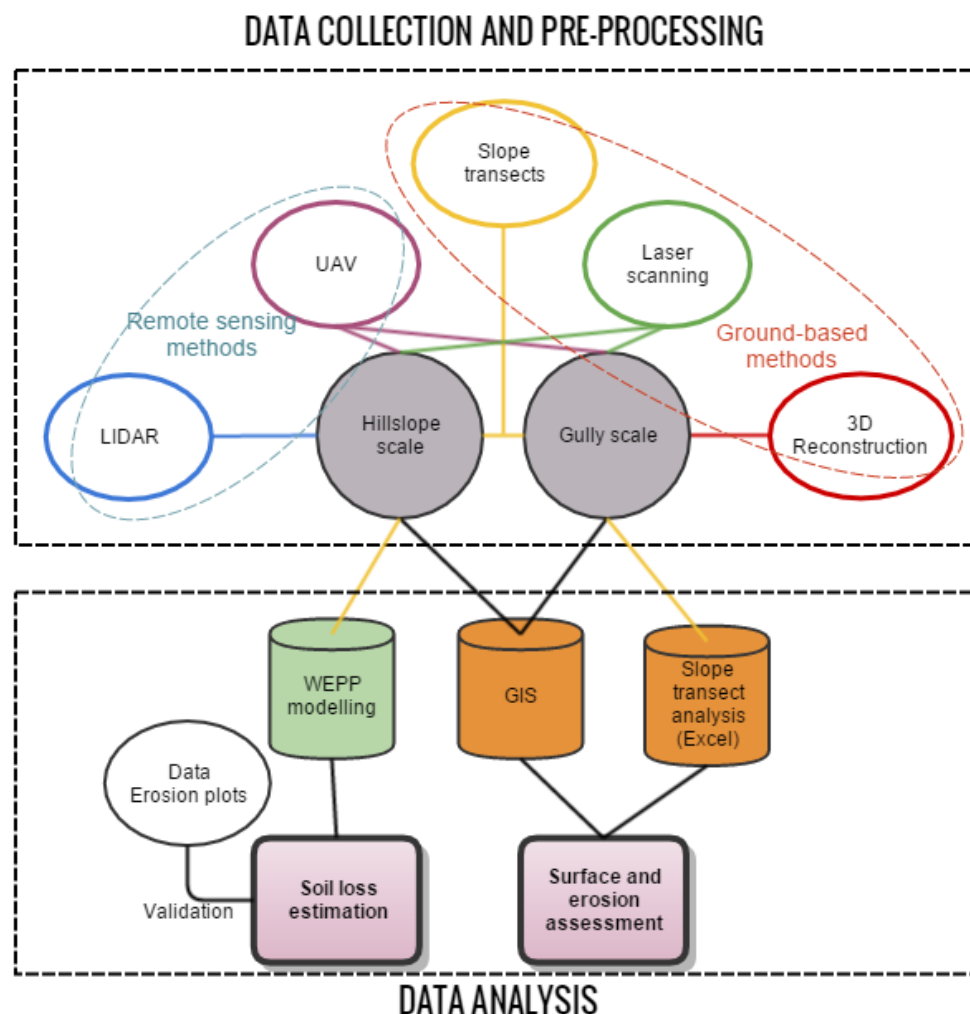


Figure 9: Overview of research methodology showing data collection and analysis

Data analysis consisted of implementing the data collected previously in WEPP for estimating soil loss, ArcGIS for assessing surface erosion and Excel for calculating erosion volumes from slope transect data (Figure 9). WEPP estimations were validated through erosion plot data. Finally, a qualitative analysis and comparison of the study methods based in the most practical experiences was performed.

4.1. Data collection and pre-processing

In this study, the potential of LIDAR, UAV, laser scanning, physical erosion measurements and 3D reconstruction was analyzed, with remotely sensed data – LIDAR and UAV - provided by BHP-Billiton. Fieldwork was undertaken from November 9th to 13th, 2015.

4.1.1. LIDAR

A total of 72-Gb of LIDAR data was provided by BHP-Billiton for MAC and MWB. The format of the elevation data was 00T format and LAS files. The 00T files were converted to DXF format through the software Global Mapper, as the most recent 00T files required the use of Vulcan. But the data was not sufficiently accurate for working at the hillslope scale, as they were already processed elevation files through a rough triangulation. LIDAR data collected in September 2015 and provided as LAS files were used in this research.

4.1.2. UAV

UAV was only available for H1 (MAC) with data applied to the study by combining elevation data from 4 different flights that covered the area. The elevation data from UAV flights was processed on November 17th, with an average ground sampling distance of 3.3 cm and 1067 calibrated images from a total of 1233 images, and provided as LAS files. Before applying this information to the study, UAV data was analyzed using Cloud Compare, a 3D point cloud processing software, as there were a lot of points misplaced, both above and below the main point cloud. This scattering could not be avoided by applying statistical dispersion calculations (e.g. standard deviation) in this case as the point cloud is based on elevation data, so elevation values from the actual hillslope could be discarded. The most evident error points were eliminated by editing the point cloud in 3D view with Cloud Compare, but the noise closest to the surface could not be removed. UAV noise in the point cloud could be due to the presence of vegetation that disturbs the surface data or that the way the provided UAV data was developed and preprocessed had a large scale objective, so that attention to detail or small scale was not paid.

4.1.3. SLOPE TRANSECTS



Figure 10: Slope transect method applied on site (Landloch)

Estimating rill and gully erosion rates deployed the slope transect method developed by Alutin (Hudson, 1993). Field work consisted of several transects along the slope with a measuring tape so that all the study area was covered (Figure 10); measuring width and depth of rills and gullies so that erosion rates could be calculated. Slope transect edges were marked with GPS, but the geolocations resulted not as precise as expected.

In the case of MAC, slope transects were used at the hillslope and gully scale (H1 and G1), covering a complete erosion plot (30 m wide). In MWB, only G2 was measured due to the scarcity of time. From data collected through slope transects on site, erosion rates were calculated

using an Excel spread sheet.

Cross sections were calculated from measured rill widths and depths, using an ellipsoidal section in the case of G1 (1) and rectangular for G2 (2):

$$(1) \text{ Ellipsoidal cross – sectional area (m}^2\text{)} = \frac{\pi * \text{Width (m)} * \text{Depth (m)}}{4}$$

$$(2) \text{ Rectangular cross – sectional area (m}^2\text{)} = \frac{\text{Width (m)} * \text{Depth (m)}}{2}$$

All calculated cross sections were summed and divided into the number of transects (n) to obtain an average cross section per transect (3).

$$(3) \text{ Av [Transect cross – sectional area] (m}^2\text{)} = \frac{\sum_{i=1}^x \text{Transect cross – sectional area}_i \text{ (m}^2\text{)}}{n}$$

This number, the average cross-sectional area covering the whole width of H1, was multiplied by hillslope length (m) to determine the volume of eroded soil (m³) for the study (4) at H1. In the case of G1 and G2, the average cross-sectional area was multiplied by gully length (m).

$$(4) \text{ Soil eroded volume (m}^3\text{/hillslope)} = \text{Av [Transect cross – section area] (m}^2\text{)} * L \text{ (m)}$$

Then, multiplying (4) by the bulk density, erosion rates are obtained (5, 6).

$$(5) \text{ Soil loss } \left(\frac{\text{m}^3}{\text{hillslope}} \right) * \text{Bulk density } \left(\frac{\text{Kg}}{\text{m}^3} \right) = \text{Soil loss } \left(\frac{\text{Kg}}{\text{hillslope}} \right)$$

$$(6) \text{ Soil loss } \left(\frac{\text{Kg}}{\text{hillslope}} \right) * \frac{\text{hillslope}}{x \text{ ha}} = \text{Soil loss } \left(\frac{\text{T}}{\text{ha}} \right)$$

From slope transect data, transverse profiles at the hillslope and gully cross sections could be obtained. The base altitude utilized for creating the profiles was indicative, as it is mainly based on LIDAR data.

4.1.4. LASER SCANNING

Laser scanning was also applied to the study sites. The laser scanner was installed and run at the bottom of the study hillslopes and gullies (Figure 11), after setting the characteristics of the scanning (e.g. precision). The scanner gave fast (8 minutes), accurate long-range measurements up to a distance of 130 meters. Laser scanning provided elevation point clouds that were processed with the software *Scene* (Figure 11).

Various scans were made for H1, however the high density of points provided by one unique scanning results in considerable data for processing. For this reason, the point cloud used for surface assessment at H1 and G1 was created only from one scan (Figure 11). The point cloud was then scaled, georeferenced and edited through the software *Cloud Compare*, on the basis of the LIDAR elevation. It can also be appreciated how point cloud density (i.e. precision) of the laser scan is lower as it is further from the position of the scanner. Hence, whereas gullies in front of the scanner position (including G1) are mostly reconstructed (marked in blue), gullies marked in red in Figure 11 are visible because there is no elevation point data from their channel bed. For performing this technique and the 3D reconstruction, vegetation was removed from the erosion channels. This will not have an effect on future erosion, considering the low amount of canopy and ground cover to protect against water erosion provided by *Ptilotus* species, the dominant vegetation covering H1. At MWB, another scan was run for assessing G2.

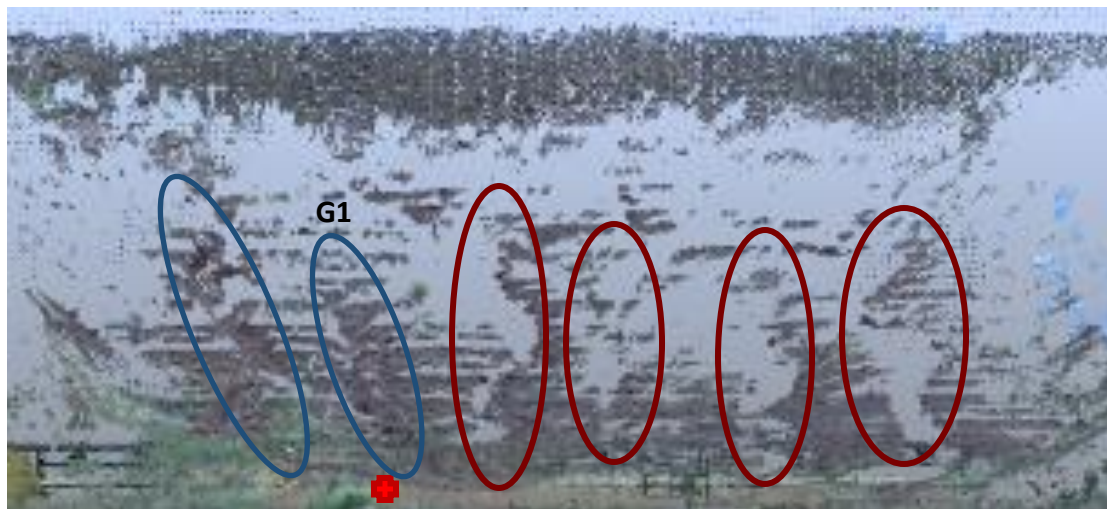


Figure 11: 3D view of point cloud generated from laser scanning at H1 in *Scene* showing gullies and the position of the laser scanner (red cross)

4.1.5. 3D RECONSTRUCTION

This technique is based on creating a 3D reconstruction from pictures taken with a standard digital camera. The field work involved selecting specific gullies from the study waste dumps, implementing control points around the area reconstructed, determining their geographic location with GPS, and finally taking pictures of all the erosion features present in the area.



Figure 12: 3D reconstruction of G2 at MWB in Cloud Compare

When taking the pictures, it is recommended to follow several guidelines to make the reconstruction as accurate as possible. These include using bright but overcast conditions, fixed focal length, cover every feature in at least 3 photos and provide small angle variations (Castillo et al., 2012; James et al., 2012). These requirements were followed despite the bright conditions which characterize the Pilbara region. A total of 245 pictures were taken for G1 and 586 for G2. Moreover, for scaling and georeferencing, even though 3 control points needed to be included in the pictures, 6 were implemented along the edges of each gully.

Once all the data was collected, the reconstruction was performed using the Structure from Motion approach in the software *Visual SFM* (Wu, 2011; Wu et al., 2011). In principle, the resulting point cloud was supposed to be implemented into *SfM GeoRef*. *SfM GeoRef* is software that scales and georeferences the resulting point clouds from *Visual SFM*, by directly marking control point positions on the pictures used for the reconstruction. GPS was applied on site to scale and georeference the 3D point cloud, but the positions given were not sufficiently accurate for this purpose, as happened for the slope transects and soil sample locations. Therefore, *SfM GeoRef* could not be applied to this research, as it requires accurate geographic positions for the control points. The point cloud was thus scaled, georeferenced and edited through the software *Cloud Compare* (Figure 12), on the basis of the LIDAR elevation and observing aerial images. This may have led to errors in scale or georeferencing, as in the case of laser scanning.

4.2. Data analysis

Two different approaches will be applied in order to assess soil surface alteration by erosion from the available elevation information obtained from data collection: erosion surface assessment with *ArcGIS* (*Excel* in the case of slope transect data), both at the hillslope and gully scale, and soil loss estimation modelling using WEPP (Figure 13).

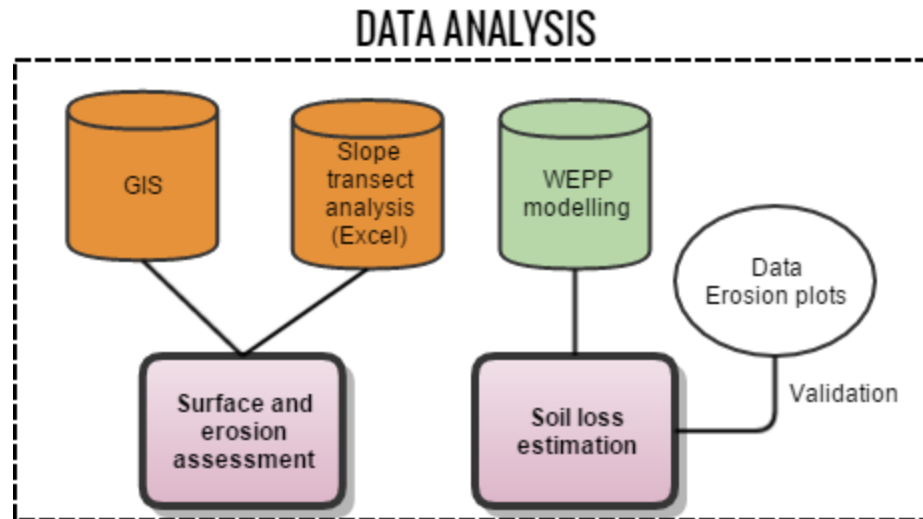


Figure 13: Overview of research methodology for data analysis

4.2.1. SURFACE ASSESSMENT

Surface assessment was performed by processing the data obtained from the study approach using *ArcGIS* at the hillslope and gully scale. All available methods were compared through the reconstruction of surfaces from point clouds and creation of longitudinal and cross-sectional profiles, slope and flow accumulation maps, 3D views, and calculation of erosion volume. In the case of data from field measurements, calculations of gully volumes and creation of profiles were developed in *Excel*.

Surfaces were created by interpolating the available point clouds. The interpolation method applied estimated surface values for each cell using the value and distance of nearby points. The interpolated values are a weighted average (using a Delauney triangulation) of the values of a set of nearby points (ESRI, 2013). In the case of the 3D reconstruction, the interpolation was created as a triangulated irregular network (TIN) from the set of point clouds. *ArcGIS* provides assorted tools for erosion assessment, such as slope, hillshade, flow accumulation and 3D profiles. The slope tool calculates the maximum rate of height change between each cell and its 8 neighbors; the steepest downhill cell in other words. By applying the hillshade tool, hillshade values are computed for a raster surface by considering the illumination angle and shadows, which in this study was azimuth 315 and altitude 45.

Volume calculations

Tomczyk et al. (2012) developed an assessment of soil erosion, explaining surface changes and quantifying soil loss and deposition by subtracting a DEM from subsequent time periods. Overlaying and differencing consecutive DEM over time can provide valuable erosion assessments, from which

ArcGIS creates a map displaying the areas and volumes of surface materials that have been modified by the removal or addition of surface material. This means that the distribution of erosion processes can be observed i.e. where sediment is being eroded, where deposited and where the surface remains the same. Furthermore, this analysis makes it possible to calculate the volume of soil that has been eroded and thus determine the erosion rates.

At the gully scale, as there was no past data to apply the difference of DEM for consecutive years, differencing was applied between LIDAR and laser scanning. Since LIDAR provides a smoother surface, it can act as a “cover” simulating the initial situation of the hillslope, although it does not consider rip lines, unlike laser scanning. Anyway, this analysis can give a rough estimation of soil movement along the hillslope.

Gully volume calculations were performed by creating a raster cover over the available elevation data. A reference plane or “cover” was created with *ArcGIS* simulating the original surface situation i.e. without erosion. By extrapolating elevation data values from each DEM on the boundaries of the gully, a raster cover for the gully can be created and thus, gully volume can be calculated. The process was the following:

1. Delimiting the edges of the gully, with the help of slope and hillshade maps from 3D reconstructions and laser scanning, using a polyline shapefile;
2. Interpolating the edge shapefile with each of the available study DEM; this was done per method, as the complexity and accuracy of the surface is very different between methods. For instance, laser scanning and 3D reconstruction perceive rip lines, whereas LIDAR and UAV do not;
3. Creating a TIN from the interpolated polyline shapefile in order to generate the “cover” surface of the gully, simulating the “original situation”;
4. Creating a raster cover (DEM) from the previous TIN;
5. Differencing the raster cover created in the previous step and the DEM created with each method, provides a volume raster for the area covered by the DEM;
6. Create a polygon shapefile covering the same area as the polyline shapefile;
7. Interpolating the polygon shapefile to the DEM created at step 4;
8. The resulting raster layer from step 5 is cut with the interpolated polygon shapefile, so that the volume of erosion is only calculated for the surface covered by the gully.
9. The average volume value in the cut volume raster and from the known area of the pixel (m^2) we can calculate the average empty volume per pixel. If we multiply it by the number of pixels (7), then we obtain the gully volume.

$$(7) \text{ Gully volume } (m^3) = n^{\circ}pixels \text{ (pix)} * area \text{ pixel } \left(\frac{m^2}{pix}\right) * Av[elevation \text{ difference}] (m)$$

4.2.2. WEPP EROSION MODELLING

The selection of erosion model should be focused on factors such as cost of data collection or possible environmental impact (Evans, 2000). Due to the availability of input data, WEPP was only applied at MAC for hillslope erosion estimations at H1. In this study, modelling has been assessed as a predicting tool and validated through data from erosion plots. Soil loss was estimated from July 2012 to April 2015.

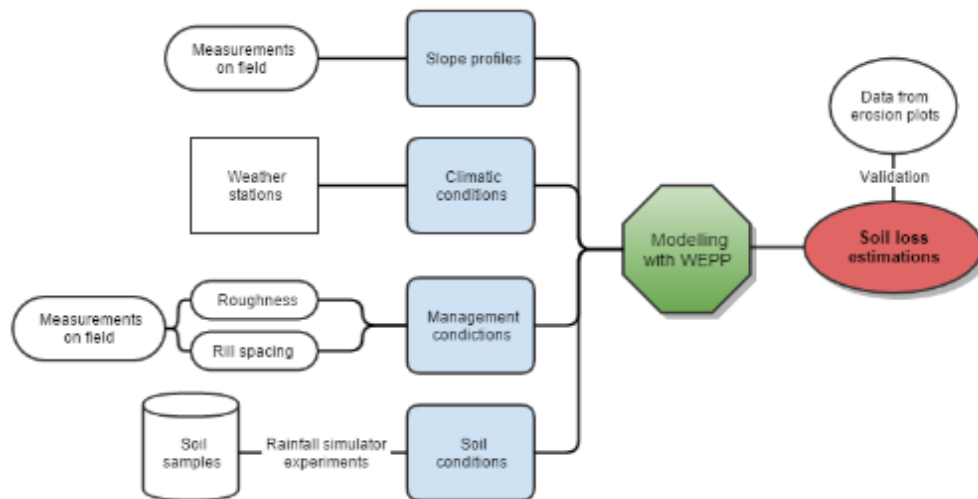


Figure 14: Overview of methodology followed for estimating erosion with WEPP

Modelling with WEPP requires a large number of input parameters, which are classified into four different groups: Climate, management, slope and soil (Figure 14). The synthetic climate data conforms to the same statistics as the observed data which were computed into a text file for predicting erosion; with available climatic data provided by BHP-Billiton from the MAC weather station, from July 2012 (when construction of erosion plots were completed) until April 2015. The climate input was created from daily climatic series data at 15-minute intervals, which is useful for modelling information about peak rainfall and intensity especially when estimating erosion.

WEPP was designed for erosion studies in agricultural lands. Thus, in order to adapt it to a mining waste dump context, Landloch's modelling expertise on mining waste dumps was called on to determine default management conditions: bare soil for the initial conditions, then tillage undertaken each week, in order to maintain the desired roughness conditions constant, among the other soil properties (otherwise there is an uncontrolled sharp change in some parameters).

Following these default conditions, it was essential to correctly define two parameters, as they are very sensitive in erosion assessment: random roughness, and rill spacing. Rill spacing was estimated as an average from the slope transect data collected on site. According to the model, the lower the spacing, the lower the erosion, as it assumes that less water is accumulated.

On the other hand, roughness is how rip lines on the hillslope are considered in the model. From information about rip line height, width and distance between them, a value for random roughness could be determined (Figure 15, Weesies et al., 1997). The lower the roughness value, the less space for water to be stored and thus more runoff is concentrated and more erosion occurs. The model was calibrated by considering different roughness values which were derived from the initial and the

current rip lines characteristics, so that predicted erosion rates could be compared to actual data from erosion plots, thereby validating the model.

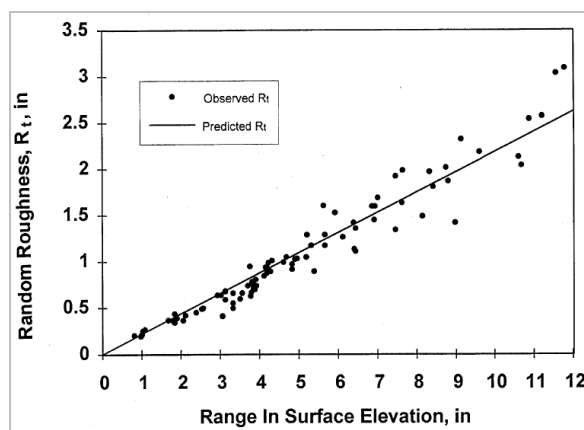


Figure 15: Random roughness versus range in surface elevation along a transect

WEPP key input soil characteristics include soil texture, interrill erodibility, rill erodibility, critical shear and effective hydrological conductivity among others. All relevant data was obtained by Landloch from soil samples in the field and through experiments conducted in the lab with a rainfall simulator.

WEPP is also able to model complex slopes along a hillslope. Slope profiles can be extracted with ArcGIS using the elevation data. However, the available LIDAR files provided by BHP-Billiton from 2012 were not sufficiently accurate for determining the slope profile. Therefore, the initial slope implemented in the model was the one measured on site.

Running and validating the model

WEPP has been used as a tool for erosion assessment or prediction to determine the amount of soil loss from waste dumps since rehabilitation was implemented. Random roughness was used as the calibrating parameter for the model. Different roughness values were considered for WEPP that were derived from initial and current rip lines characteristics.

There was a need for assessing the level of agreement between measured and predicted rates to validate the model. Validation requires actual erosion rates measured on site. Erosion rates are available from the erosion plots installed in MAC and MWB, however, data has been collected only for one year from MWB, not resulting in enough for validating the model. Therefore, soil loss was only predicted and validated at the hillslope scale at H1 (July 2012 to April 2015). H1 erosion plot data could be slightly under-estimated due to a leak at the plot outlet probably associated with its maintenance.

Data from the erosion plots can only be used to validate results from modelling, as both refer to soil loss, i.e. soil leaving the plot, whereas the other study methods do not consider deposition, so that only erosion rates from gully volumes can be obtained. This determines whether the modelling is accurate for predicting and assessing erosion and if it is suitable for being applied to other locations.

4.3. Qualitative analysis and comparison of methods

A summary overview of the main characteristics of all the study methods was generated, based on factors such as the accuracy of the rates obtained, availability of these methods, time needed for generating and processing data, associated errors, cost and computation time in the model under the study conditions. The most practical experiences of the study methods were incorporated to an analysis in which strengths and weaknesses were described, providing a good overview of the advantages and disadvantages of each method for the purpose of assessing erosion on rehabilitated mining waste dumps. Helpful and harmful aspects to achieving the research objective, referring to both internal attributes of the methods application and external attributes of the research environment.

Additional detailed information, including all surface analyses by method and scale, are included in the Appendices.

5. RESULTS AND DISCUSSION

The outcomes from this research address the main research question: *How can remote sensing (LIDAR and UAV) and ground-based (laser scanning, 3D reconstruction and field measurements) methods be applied for assessing erosion and landform stability on rehabilitated waste dumps in the Pilbara region, WA?*

5.1. Surface assessment

The first sub-research question: *What are the characteristics and how precise is each approach for assessing landform surface erosion on mining waste dumps at the hillslope and gully scale?*

The study techniques from Chapter 4.1 have been used to obtain surface data and to analyze landform alteration by erosion at the hillslope and gully scale using ArcGIS. LIDAR, UAV, Laser scanning and 3D reconstructions provided elevation point clouds from the rill to the hillslope scale. Surface information were then derived from slope transects, from which a comparison between the processed data provided an overview of the accuracy and applicability of the study methods for assessing erosion on mining waste dumps, and potentially for other scenarios.

5.1.1. HILLSLOPE SCALE: H1

The surface at H1 (MAC) was analyzed with LIDAR, UAV, laser scanning and slope transects. Hillslope H1 had practically no vegetation cover, and thus the plot presents numerous erosion features (Figure 16).



Figure 16: Satellite image showing H1 (MAC)

While LIDAR and UAV covered several waste dumps and can be applied to a larger scale surface assessment (>1000 ha), a single laser scanning of 5.3 ha and slope transects coverage can be variable, but both were applicable at the hillslope or smaller scale.

Figure 17 shows the elevation point clouds provided by LIDAR, UAV and laser scanning, in increasing order of point density. In the case of LIDAR, cloud density at H1 was 247 elevation points, whereas UAV was 2,340 and laser scanning 6,914,840 points.

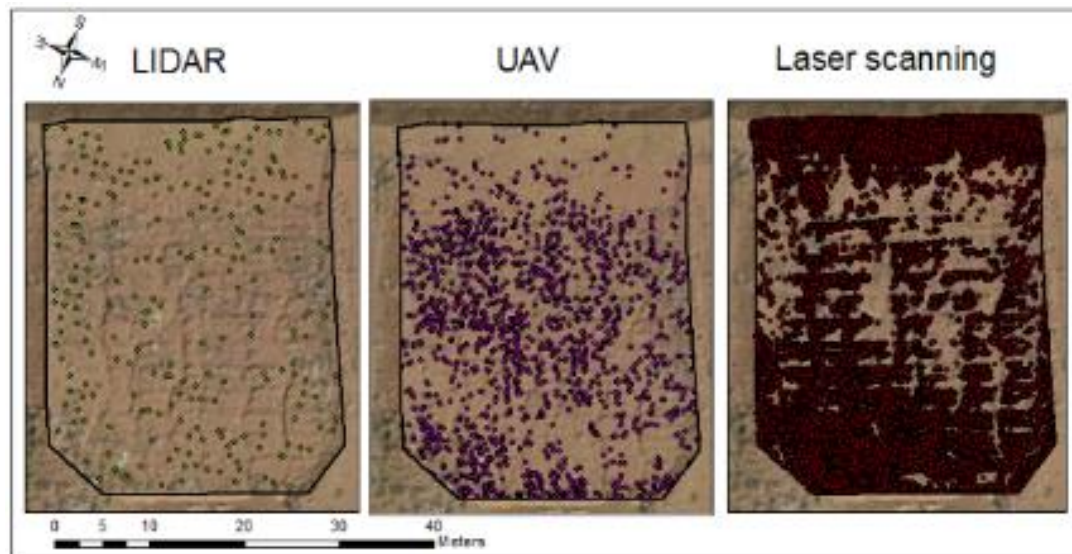


Figure 17: Comparison of LIDAR, UAV and laser scanning point clouds at H1

The high density of laser scanning elevation point cloud allows one to sense where the erosion gullies or even where rip lines are, even before reconstructing the surface (Figures 17 and 18). Laser scanner (located at the northern corner of the plot when run) loses precision for assessing the surface with the distance, as it loses visibility of parts of the surface.



Figure 18: 3D view of point cloud generated from laser scanning from the bottom of H1 in Scene

The Digital Elevation models (DEM) (Figure 19), generated from the point clouds above, are at the same altitude rank, varying from 697 to 711 masl, and follow similar elevation patterns. The east side of the plot is lower, being the northern corner and thus the lowest point of the plot.

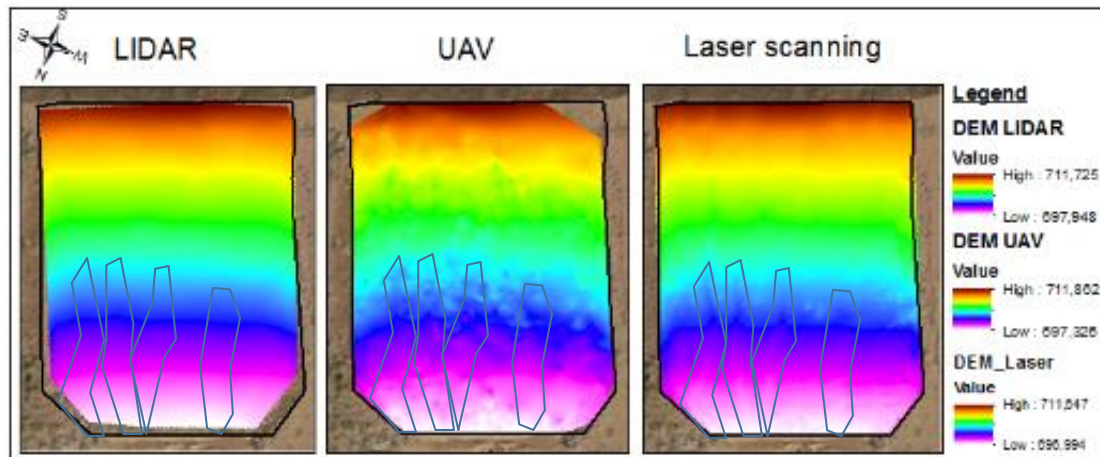


Figure 19: Comparison of LIDAR, UAV and laser scanning DEM at H1 showing erosion detected features from laser scanning

While a smooth surface is obtained from LIDAR data (Figure 19), laser scanning and UAV give more irregular surfaces. Laser scanning provides a clear picture of the gullies, which have been formed towards the lowest point of the plot. UAV provided a more irregular surface than laser scanning, which shows relatively similar elevation patterns as laser scanning where erosion features are. Gullies can also be slightly discerned on the LIDAR DEM, especially to the east of the plot.

Slope and transverse profiles were generated from the study DEM. Slope was also measured on site and compared to the generated slope profiles at H1. LIDAR, laser scanning and slope measured on site provided very similar profiles (Figure 20). Rip lines can be detected on the laser scanning slope profile, especially on the bottom of the hillslope. UAV provided an irregular slope which does not give an accurate hillslope profile. H1 is shaped by two different slopes, the main hillslope and a steeper top slope, 32.5% and 60% on average, respectively.

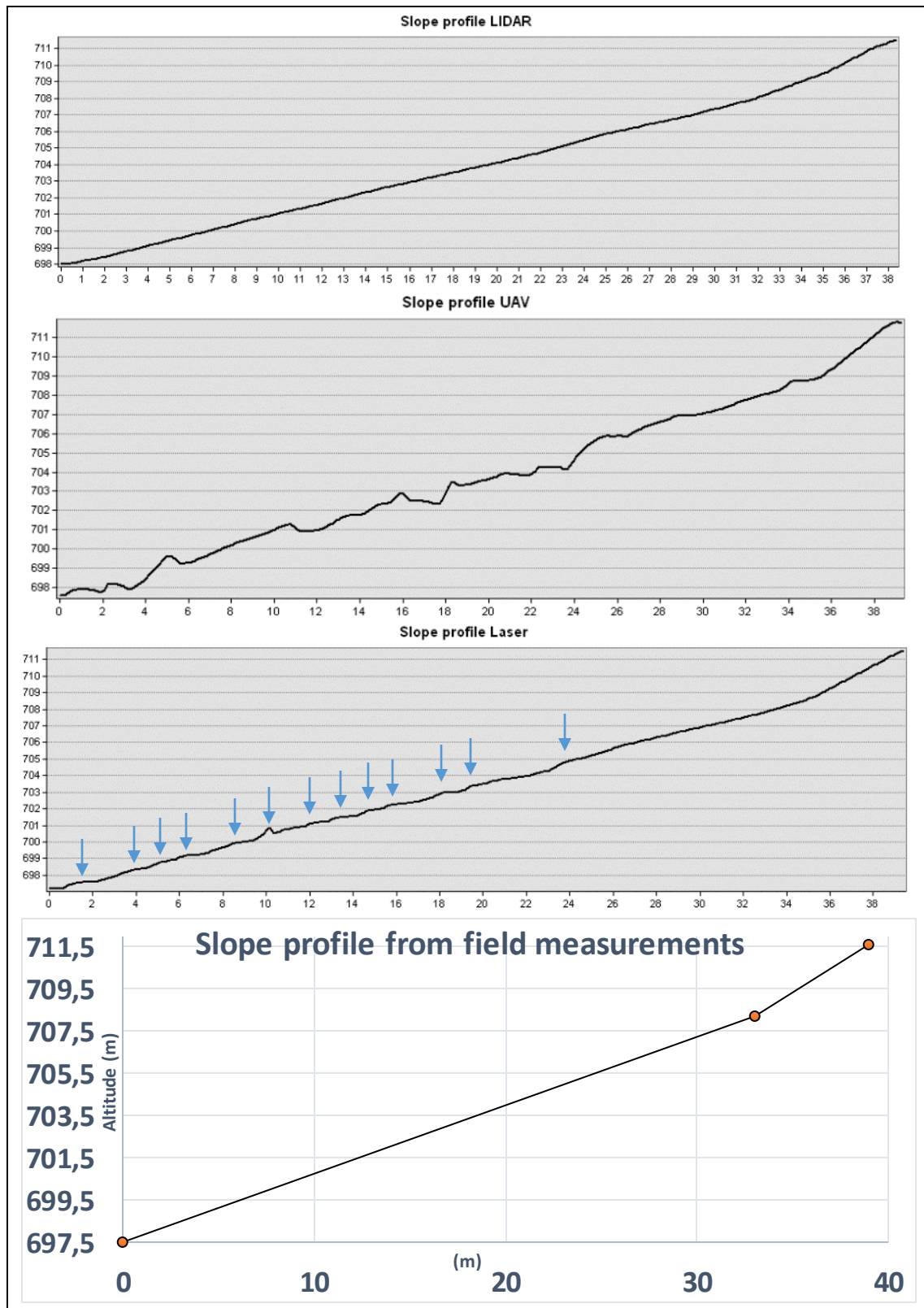


Figure 20: Longitudinal slope profiles derived from LIDAR, UAV, laser scanning and field measurements at H1, showing rip lines on laser scanning profile

Transverse profiles, matching one of the slope transects performed on site (Figure 21), were subtracted from the LIDAR, UAV and laser scanning DEM. UAV provided an unsmooth and irregular profile (Figure 22), which does not match the others, despite its DEM relatively matching the actual erosion features. Cross sections of erosion features have been represented as rectangular sections

in order to see them clearer on the slope transect profile, although erosion calculations were based on elliptical cross sections.



Figure 21: Transverse profile substracted at H1

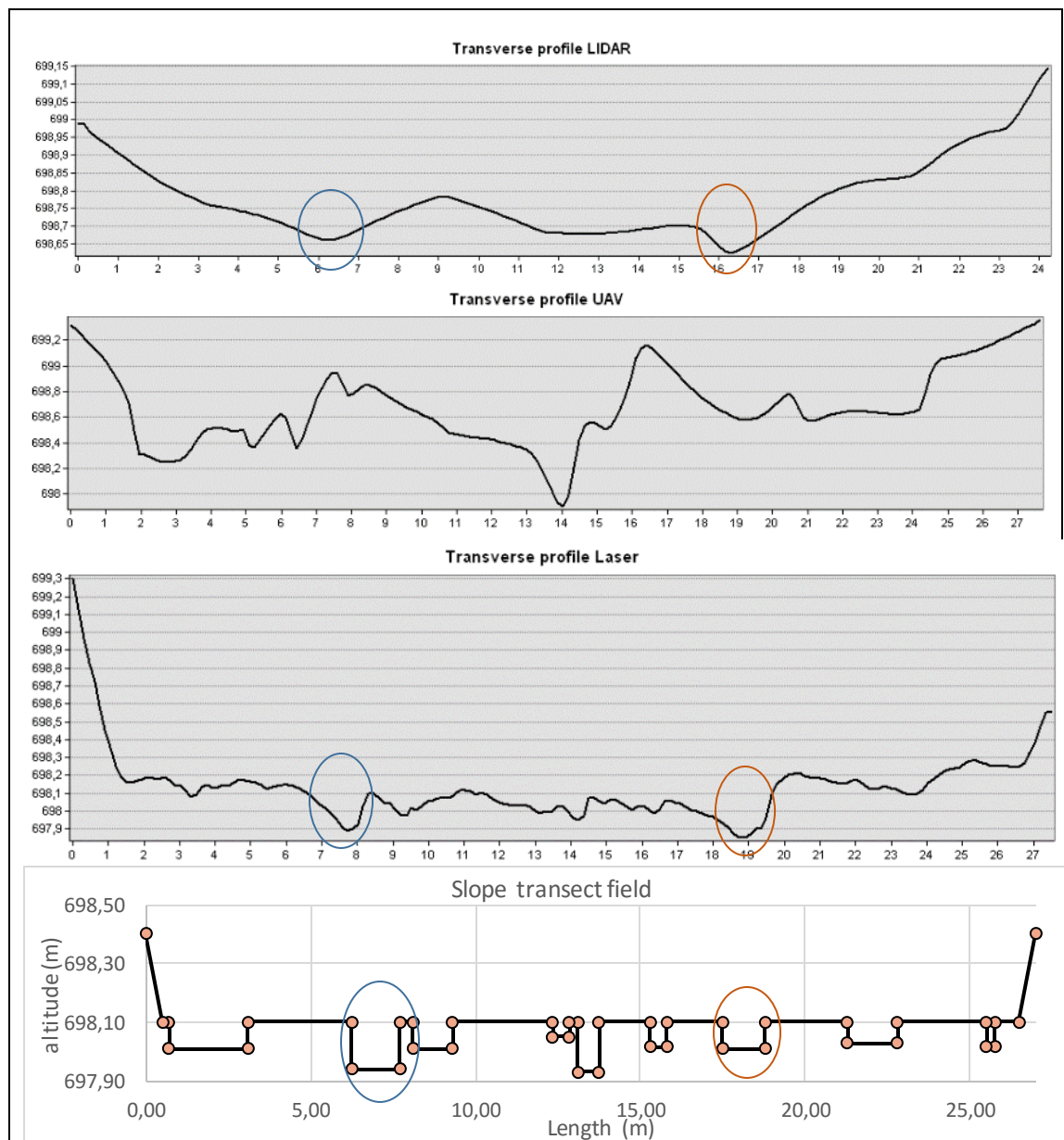


Figure 22: Transverse profiles from LIDAR, UAV, laser scanning and slope transects at H1 showing G1 in blue and another gully in red

As shown in Figure 22, the largest erosion features are detected by LIDAR, laser scanning and slope transects. Whereas the edges of G1 and the other marked erosion feature are not clearly defined on the LIDAR profile, laser scanning and slope transects provide very similar cross sections, which will be further analyzed at the gully scale surface assessment (Chapter 5.1.2).

Slope maps (in degrees) were generated from the study DEM to indicate the steepness of the H1 surface. The resulting UAV slope map shows substantial noise (Figure 23), as happened with the profiles (Figures 21 and 22). LIDAR provides a slope which matches some elements, however, erosion features cannot be discerned. In the case of laser scanning, a precise slope map was obtained (Figure 23), which shows how a single laser scanning can clearly detect rip lines and erosion features.

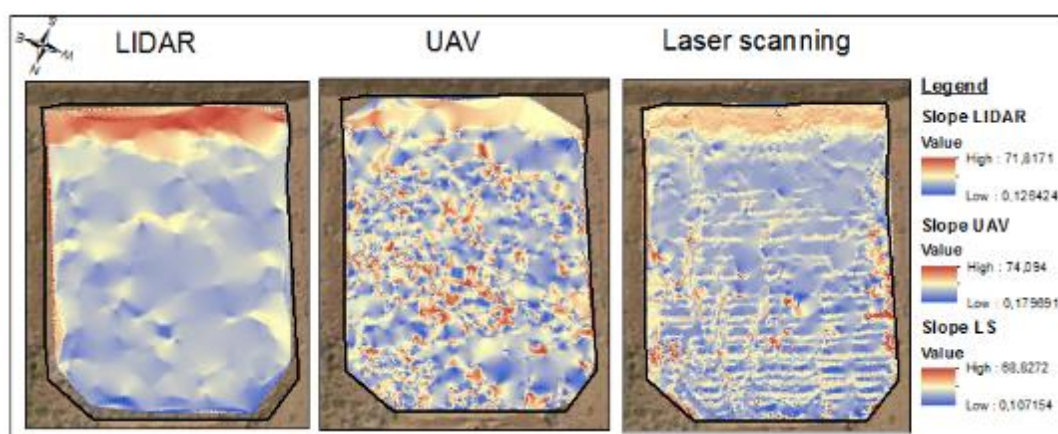


Figure 23: Comparison of LIDAR, UAV and laser scanning slope maps at H1 (degrees)

Different hydrological maps were generated in ArcGIS, including flow accumulation. Flow accumulation maps have been created from the direction water flows according to the study DEM. Water flows towards the lowest part of the plot, i.e. the northern corner of H1, accumulating on the erosion channels. Despite erosion features not being observed in the LIDAR slope map (Figure 23), water accumulates in areas where erosion features are and closely matches the laser scanning flow accumulation map (Figure 24). UAV, as in the previous analysis, does not provide an accurate hydrological assessment.

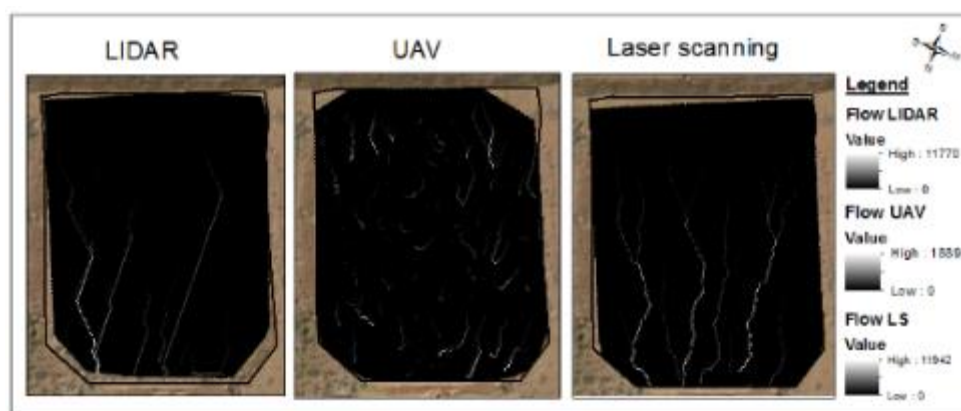


Figure 24: Comparison of LIDAR, UAV and laser scanning flow accumulation maps at H1



Figure 25: Difference of LIDAR and LS DEM at H1

Differencing DEM for consecutive years of data may provide an assessment of erosion and deposition distribution and volume (Tomczyk et al., 2012), from which soil loss could be calculated and then compared to actual erosion data from erosion plots or modelling predictions. However, as there is no accurate available surface data for accurately representing the initial situation, the subtraction of DEM was applied between current LIDAR and laser scanning, to detect differences in elevation patterns. Furthermore, mining waste dumps reduce their volume due to settlement of the soil over the first few years since rehabilitation. For this reason, differencing DEM would not be suitable for mining waste dumps unless volume loss is perceptible as a homogeneous loss along the hillslope.

In Figure 25, where black areas are where LIDAR is over laser scanning the surface, practically the whole surface generated from laser scanning is under the LIDAR DEM. LIDAR can barely detect gullies or rip lines, as it will be further verified at the gully scale. Although the differences in altitude were not large, in terms of erosion, a single mm makes a big difference. For instance, the difference of volume between both surfaces was estimated at 375 m³, which is almost 40 times the actual erosion rate (9.5 m³). Thus, this method does not provide an accurate landform assessment. Such a big difference could be associated with georeferencing errors in the laser scanning. However, Figure 25 does show how the detail of the LIDAR DEM is not very high compared to that generated from laser scanning.

Table 5: Erosion calculations from slope transects at H1

Ellipsoidal section		
Erosion volume per plot	m ³ /plot	31,59
Erosion rate per plot	t/plot	47,38
Erosion rate per hectare	t/ha	409,43
Erosion rate per hectare and year	t/ha/y	136,48

Slope transects provided an estimation of erosion volume at H1. Soil volume eroded from rills and gullies was estimated as 31.5 m³ since H1 construction or 136.5 t/ha/year (Table 5). Estimations could not be validated with data from erosion plots, as they do not consider deposition nor do they provide soil loss rates, but they were compared when making sediment rate estimations.

If actual average soil leaving the plot (43.8 t/ha/year) is subtracted from the estimated soil volume eroded (136.5 t/ha/year), then deposition was estimated as 92.7 t/ha/year; in other words 23.8 m³/plot since construction. As there are 24 rip lines at H1, and considering a homogeneous distribution of deposition between them, then 3.0 m³ have been deposited in each rip line since construction three years ago.

On the other hand, considering the initial and current rip line height (measured from the top of the rip line), 25 and 12 cm, respectively, and distance between rip lines, 1.25 m, deposition per rip line was estimated as 1.15 m³ for the three years. Deposition of 3.0 m³ would mean that rip lines had

been completely filled in. Rip lines implemented on the hillslope have been considerably filled in over the last three years (Figure 26), but not completely. Therefore, erosion volume estimates from slope transect data have probably been overestimated.

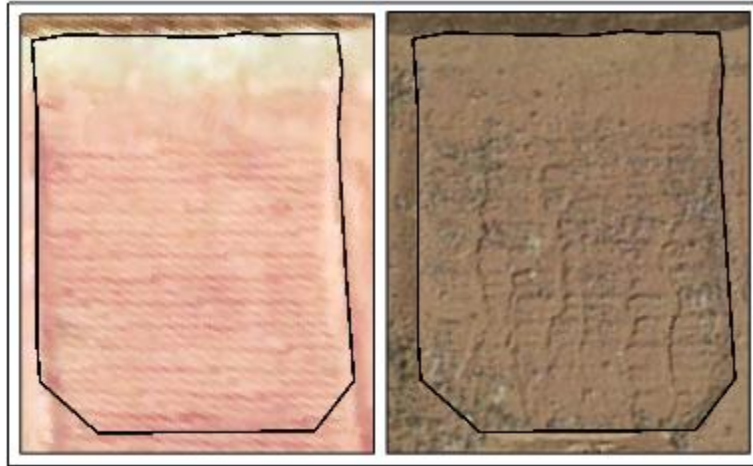


Figure 26: Orthophoto June 2012 (on the left) and satellite image September 2015 (on the right) showing how rip lines have been filled in since H1 construction

5.1.2. GULLY SCALE: G1 AND G2

5.1.2.1. *Gully 1(G1)*

LIDAR, UAV, laser scanning, 3D reconstruction and slope transects were applied for surface assessment at G1, an 18.5x1.5 m gully (Figure 27), covering a surface area of 28.0 m².



Figure 27: Satellite image of G1 (Sep 2015)

The slope maps provide a 3D picture in 2D of reconstructions for G1 and its surrounding surface (Figure 28). Despite its precision at the hillslope scale, UAV appeared to detect irregularities on the surface that could be useful for gully assessment, and will be further analysed. While LIDAR does not detect the gully channel or boundaries, laser scanning and 3D reconstruction provide a very accurate reconstruction showing G1 and rip lines around it (Figure 28).

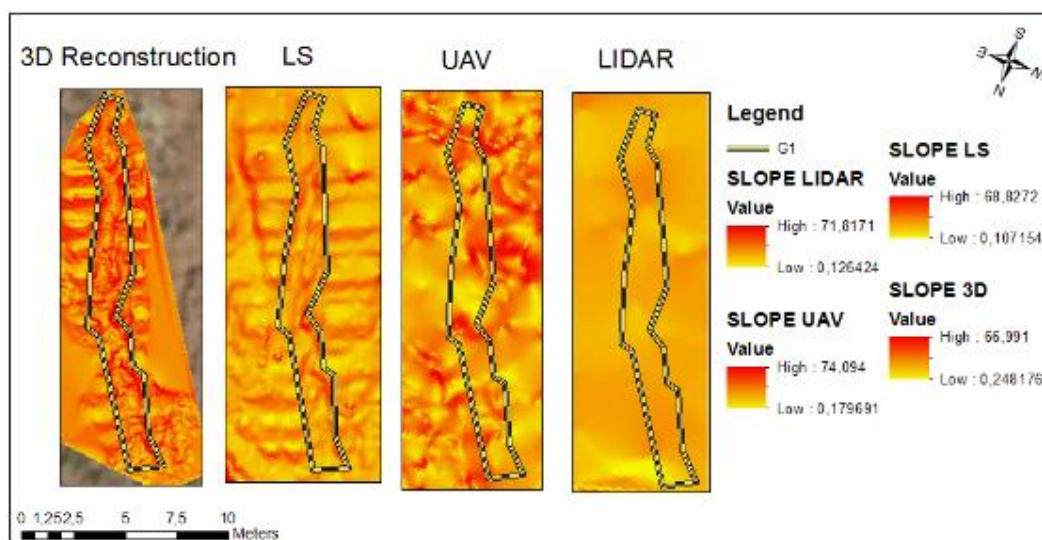


Figure 28: Comparison of slope maps derived from 3D reconstruction, laser scanning, UAV and LIDAR at G1 (degrees)

Although UAV seemed to detect some parts of G1 (Figure 28), attending to the cross sections (Figure 29), all profiles generated coincided with most aspects, except for UAV. The range of altitudes differ slightly between profiles (Figure 29). While G1 cross sections from 0.25 to 0.30 m deep for 3D reconstruction, laser scanning and LIDAR (in increasing order of depth), while depth was 0.4 m for

slope transects. According to these profiles, G1 was 1.3 m width, except for 3D Reconstruction, which was slightly wider (1.4 m).

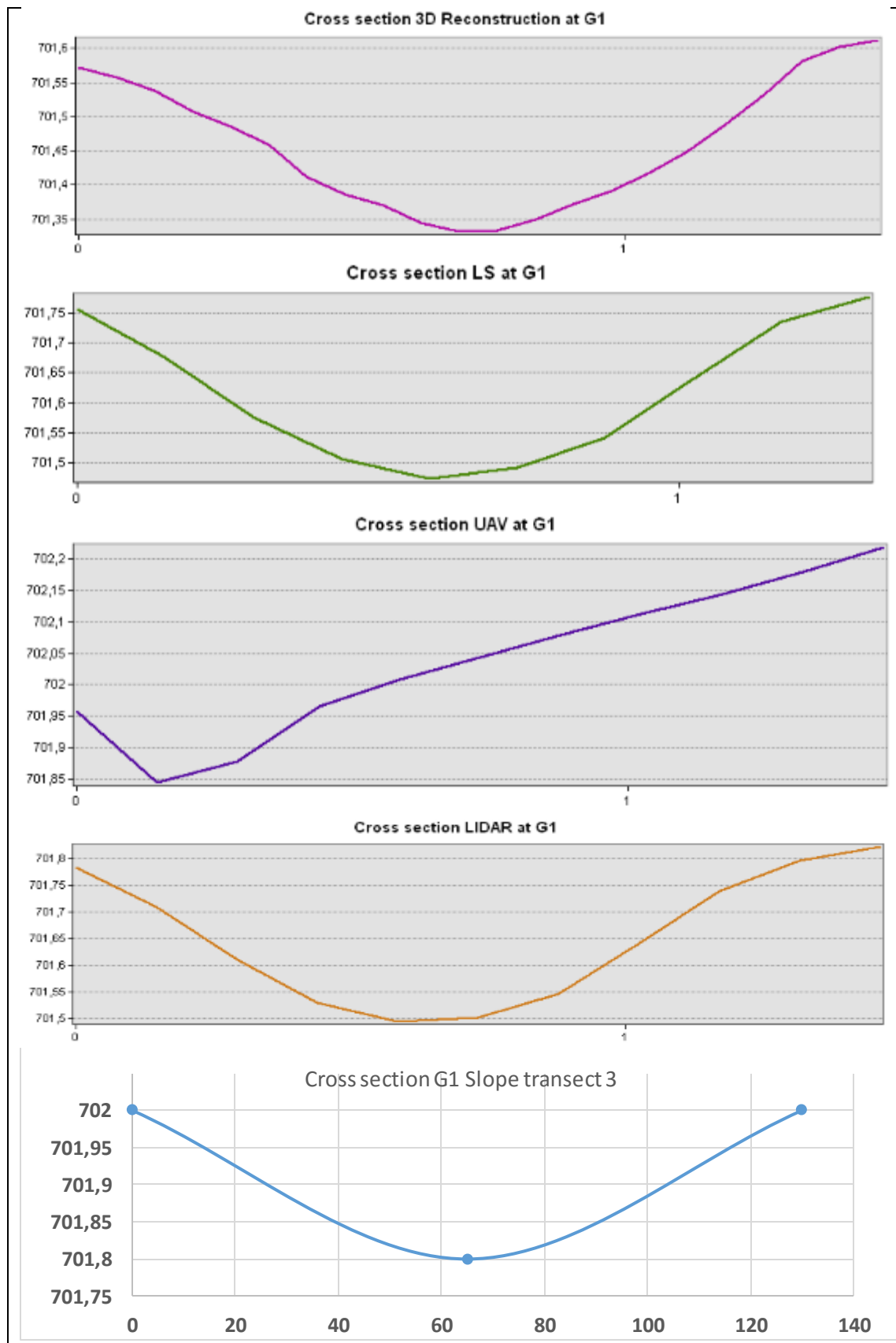


Figure 29: Cross section profiles derived from 3D reconstruction, laser scanning, UAV, LIDAR and slope transects at G1

Except for the slope transect, the volume of G1 was estimated from generated volume maps (Figure 30), in which whiter areas represent where more sediment has been eroded. 3D reconstruction and laser scanning provided fairly similar volume maps, showing the same erosion and deposition distribution patterns (Figure 30).

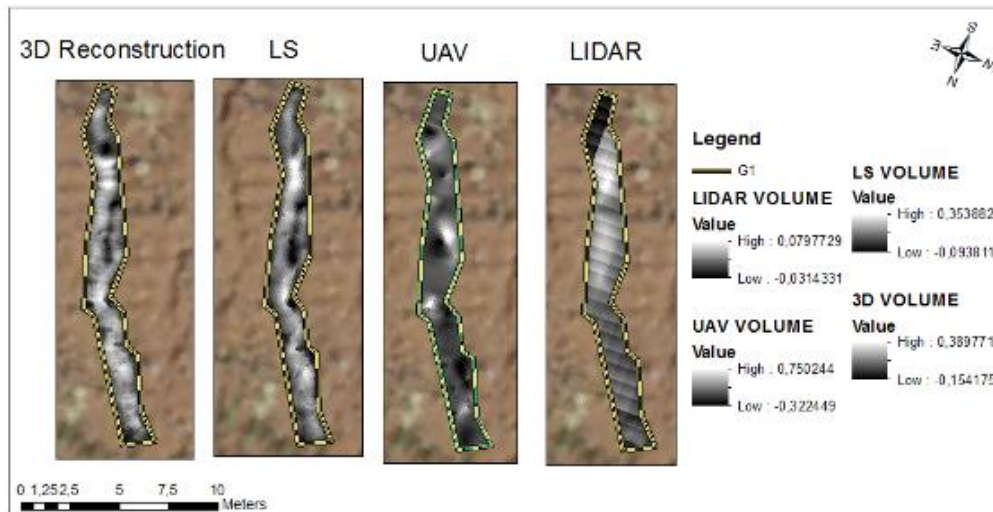


Figure 30: Comparison of volume maps created from 3D reconstruction, laser scanning, UAV and LIDAR at G1

Using the 3D reconstruction as the most accurate reference volume, the other study methods over or underestimated erosion volume (Table 6). While LIDAR and UAV do not provide accurate volume estimations (quantitatively underestimated), slope transects and laser scanning provided a closer volume estimation (20% overestimated), both giving the same volume estimation.

Table 6: Volume estimations relative to the 3D reconstruction for slope transects laser scanning, UAV and LIDAR at G1

Method	G1 Volume estimations (m ³)	% over or under
3D Reconstruction	2.5	0
Slope transects	3.0	+20
Laser scanning	3.0	+20
UAV	0.3	-90
LIDAR	0.4	-85

Although the cross section extracted from LIDAR represented an accurate profile of G1, LIDAR provided a rough estimation of the surface and erosion features at the gully scale. However, it could be more accurate for initial erosion assessments at the hillslope scale, it combined with more precise methods. In the case of UAV, noise in the point cloud led to not sufficient accuracy for this assessment.

Despite the observed similarity between 3D reconstruction and laser scanning analysis in the generated maps, G1 erosion rates derived from laser scanning were over-estimated (Table 6). This may be due to sinuosity of rills and gullies, which affect the visibility of the laser scanning and thus reduces detail in the scanning reconstruction. Slope transect also over-estimated erosion rates (Table 6), as happened when estimating H1 erosion rates. Laser scanning and slope transects results are suitable when assessing erosion depending on the purpose of the assessment and the required detail.

5.1.2.2. *Gully 2 (G2)*

As for G1, LIDAR, laser scanning, 3D reconstruction and slope transects were applied in G2, but only part of the gully was reconstructed due to the limited fieldwork time. However, enough detail was available for comparing the study methods for gullies with very different dimensions (G1 and G2). UAV was not available for this site.

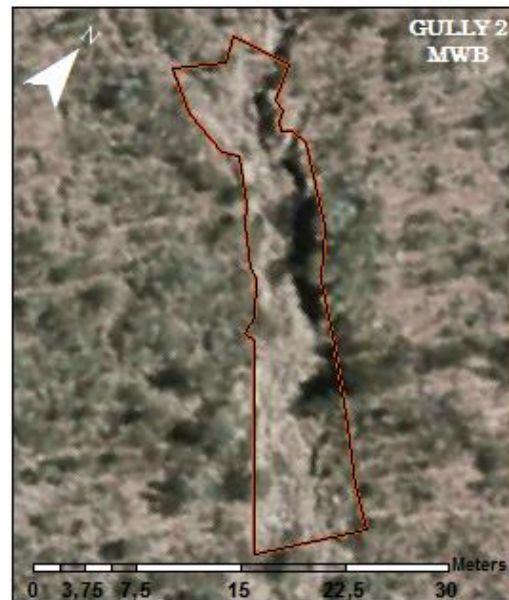


Figure 31: Satellite image of G2 (Sep 2015)

G2 is a 35 x 6 m gully covering an area of 223.3 m² (Figure 31). Vegetation cover on this hillslope is much higher than at H1 (65% canopy cover), but there was no vegetation growing at the gully channel.

Elevation points generated from a single laser scanning and 3D reconstruction, as at the other study sites, were linked to the images taken, providing very precise coloured 3D point cloud reconstructions when data was preprocessed (Figure 32). As for G1, even stones just a few square centimeters in size can be observed from the 3D reconstruction point cloud.

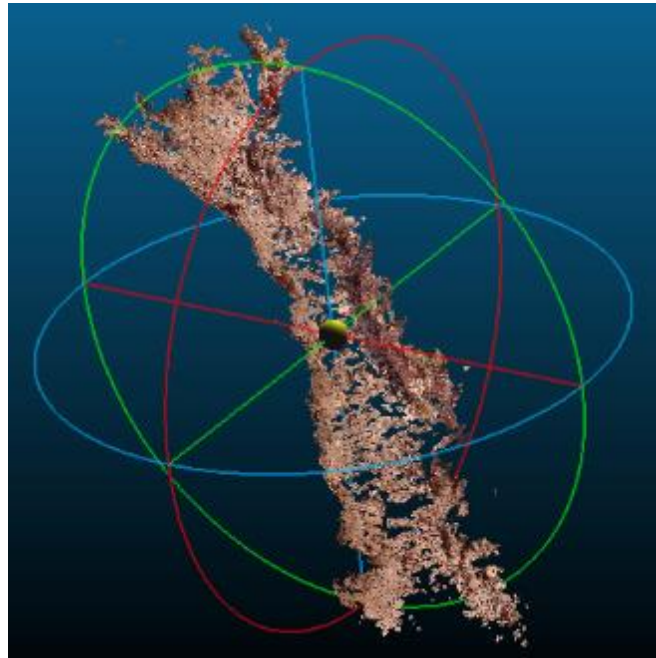


Figure 32: 3D view of point cloud generated from 3D reconstruction at G2, using *Cloud Compare* software

The generated DEM (Figure 33) have similar altitudes, varying from 561 to 572 masl, and follow similar elevation patterns, especially 3D reconstruction and laser scanning. Due to the sinuosity of G2, a single laser scanning could not cover the western part of the gully.

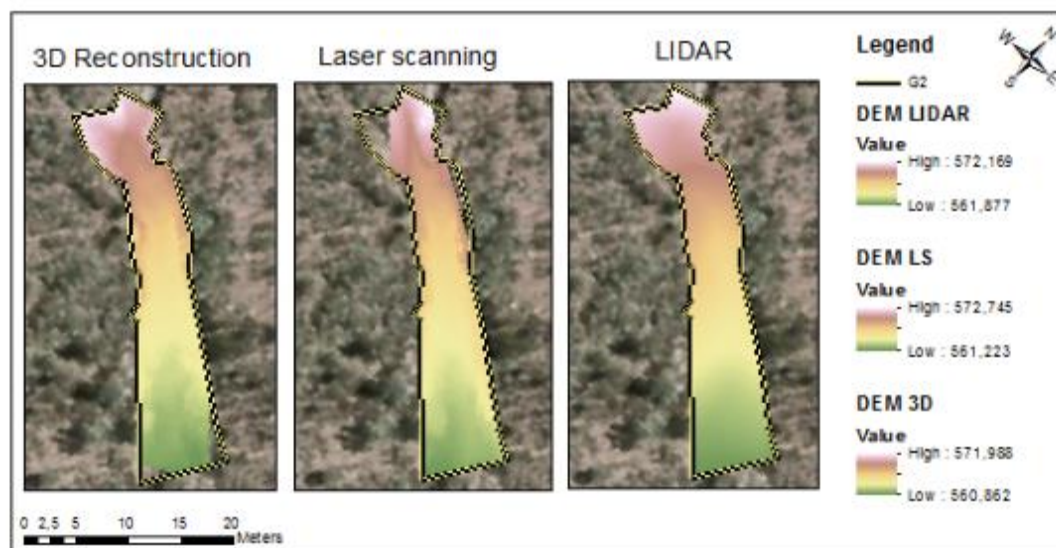


Figure 33: Comparison of DEM profiles derived from 3D reconstruction, laser scanning and LIDAR at G2

As for the previous assessments, slope maps provide a clear picture of the surface reconstruction, in which again laser scanning and 3D reconstruction provide a similar result (Figure 34). LIDAR slope map however does not coincide much with them; areas where slope is estimated low, relatively match with 3D reconstruction and laser scanning on the bottom of the gully. But, in any case, LIDAR seem not to provide an accurate reconstruction of the gully.

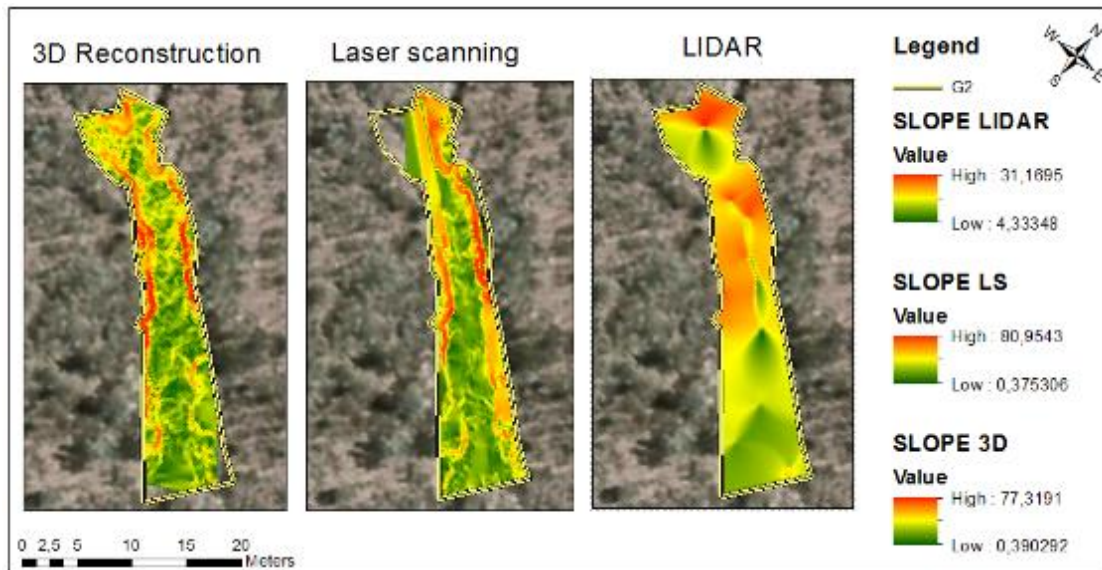
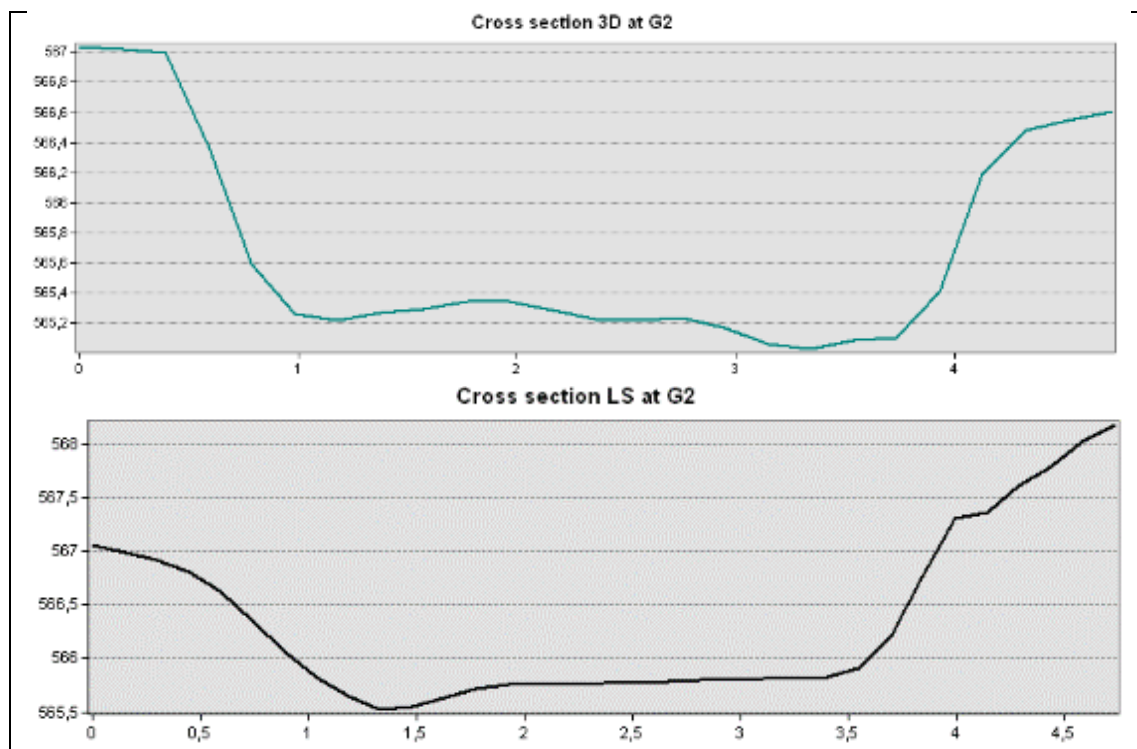


Figure 34: Maps of surface slope provided by 3D reconstruction, laser scanning and LIDAR at G2

Cross sections were applied to deeper analyze the precision of the surfaces reconstructed by the study methods. Although LIDAR detects G2, its cross section does not match at all with the others. Attending to the slope map and cross section provided by LIDAR (Figures 34 and 35), despite the big dimensions of G2, it does not provide an accurate reconstruction of the gully.



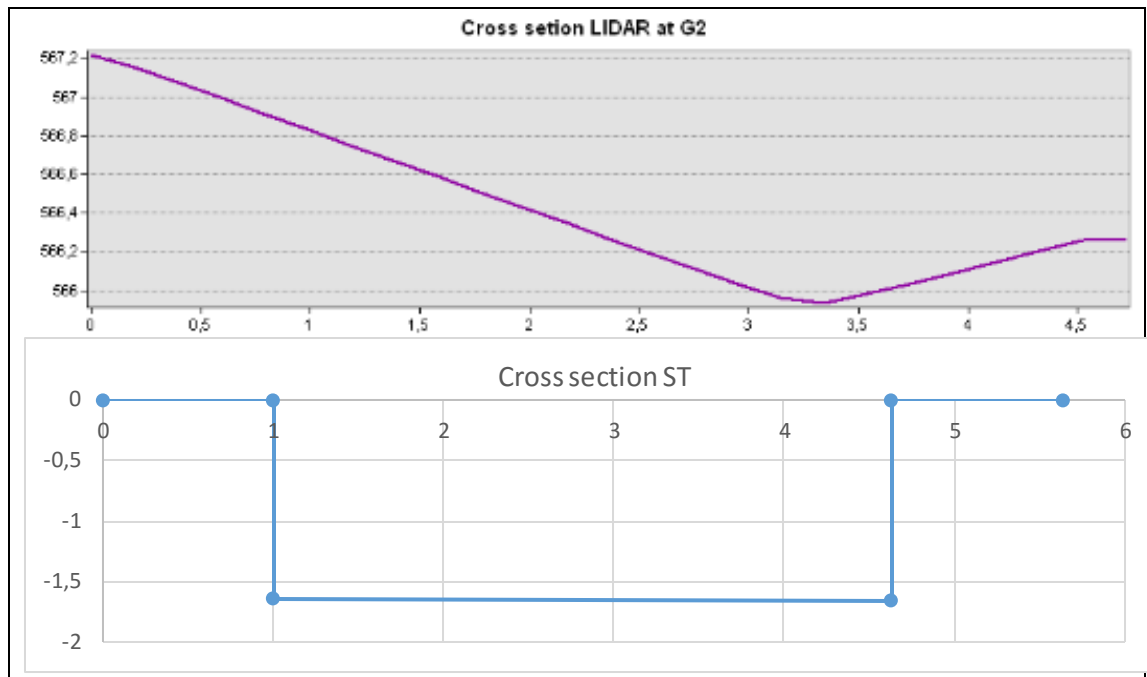


Figure 35: Cross section profiles derived from 3D reconstruction, laser scanning, LIDAR and slope transects at G2

Cross sections extracted from the other study methods were similar in shape and size though (Figure 35). Whereas a cross section of 3D 3.6x1.6 m was measured on site, LIDAR and laser scanning provided 3.75 x 1.6 and 3.5 x 1.5 m cross sections, respectively. Taking a closer look to the last two, and considering again 3D reconstruction as the reference surface, laser scanning underestimates quantitatively the size of G2. For instance, laser scanning does not detect the incision on the bed channel at the right of the profile that 3D reconstruction does perceive. This could probably be due to errors associated to angle of the scanner towards the surface and loss of visibility.

The volume of G2 was estimated from generated volume maps (Figure 36). The elevation difference values is similar for 3D reconstruction and laser scanning, as the distribution also is in the map. Meanwhile, the resulting LIDAR volume map (Figure 36), shows how the erosion feature is detected, but, as in the previous analysis, it does not provide an accurate assessment as the other methods.

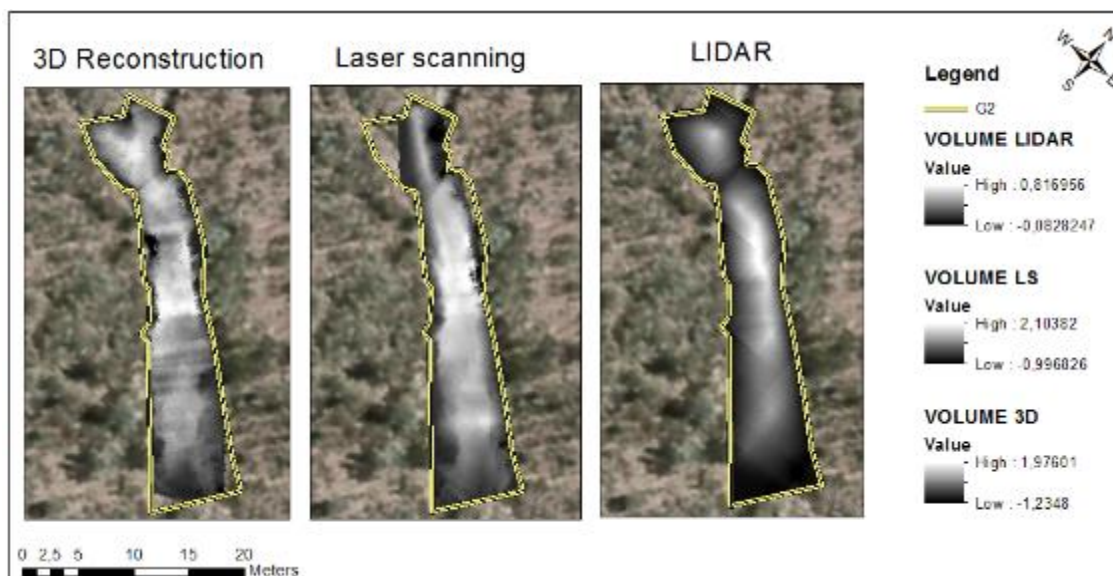


Figure 36: Comparison of volume map derived from 3D reconstruction, laser scanning and LIDAR at G2

G2 volume estimations provided by 3D reconstruction and laser scanning are very close (Table 7) despite differences seen in the previous analysis (e.g. cross sections). However, if laser scanning had covered the whole surface of the gully, volume would have been higher, being thus overestimated, as happened in G1. Although G2 volume from slope transect data was overestimated compared to volume estimations obtained from 3D reconstruction, laser scanning and LIDAR (Table 7), it gives an approximate estimation that could result in a quick erosion assessment. LIDAR however highly underestimated erosion rates, not being adequate for volume calculation of erosion features.

Table 7: Volume estimations relative to the 3D reconstruction for slope transects, laser scanning and LIDAR at G2

Method	G2 Volume estimations (m ³)	% under or over
3D Reconstruction	144.28	0
Slope transects	163.4	+13
Laser scanning	145.24	+1
LIDAR	49.46	-65

5.2. WEPP erosion modelling

The modelling outcomes should answer the following sub-research question: *In what ways does WEPP represent a useful tool for estimating erosion on mining waste dumps?* Erosion modelling was used to estimate soil loss since construction of erosion plots 3 years ago until the present day at H1, and then compared to actual erosion data from the plot, collected for the same period (Table 8).

Table 8: Comparison between erosion estimations with WEPP and H1 data from erosion plots

	Roughness	t/plot	t/plot/y	t/ha/y	% diff
Modelling	Initial: 9	11,08	3,69	33,95	-22
	Average: 7.3	16,47	5,49	50,48	+15
	Intermediate: 8	14,81	4,94	45,38	+4
Erosion plot (H1)	-	14,29	4,76	43,80	-

The model was calibrated with different values of random roughness (i.e. rip lines), including initial condition (rip lines when H1 was constructed) and values between the initial and the current rip line situation (Table 8). When the initial roughness conditions were considered, estimated soil loss at H1 was 3 t/plot less than actual soil loss. Predictions would have been different though if all the other initial input parameters would also have been implemented in the model (e.g. initial slope). Modelling outcomes successful resulted when simulating with an intermediate roughness value. Soil loss was 2 t/plot overestimated when considering average random roughness values. This shows how sensitive random roughness is when estimating erosion using WEPP.

Table 9: Comparison between runoff estimations with WEPP and H1 data from erosion plots

	Runoff (mm/y)	Accumulated runoff (mm)
Modelling	53.14	159.42
Erosion plot (H1)	45.00	135.00

Regarding runoff rates (Table 9), WEPP predicted a higher runoff than was measured, although predictions are based on actual climatic data (July 2012-April 2015). This could be because the model is not able to consider infiltration processes that are probably encouraged by rip lines. Deposition predicted by the model at H1 is 0, contradictory to the fact that rip lines have been considerably filled in since construction, as explained in chapter 5.1.1.

Rip lines could be included in the WEPP slope default conditions, instead of as a roughness value in management conditions, taking advantage of the possibility that WEPP gives to implement complex slopes. This way, more realistic simulations could be performed, as runoff and deposition processes encouraged by rip lines are considered by the model. This was not performed in this research because there was no accurate elevation data available. Laser scanning can provide complex slope profiles including rip lines that could be appropriate for predicting more feasibly erosion and assessing landform changes over time.

5.3. Qualitative analysis and comparison of methods

Once all surface data was collected, processed and analyzed, a structured summary of the study methods is provided based on the experience and information regarding the application of the techniques (Table 10). This addresses the last research question: *What are the strengths and weaknesses of the different methods in the assessment of erosion on rehabilitated waste dumps?* This overview of the various methods includes factors or criteria such as scale, affection of vegetation on the techniques, time of processing and cost. Processing time needs to be considered and thus computing power appropriate to the data needs to be used.

Table 10: Summary of methods (qualitative characteristics)

	WEPP Modelling	LIDAR	UAV	Laser scanning	3D reconst.	Slope transects
Cost	Cheap	-	-	Expensive 400 AUD/d	Cheap (standard camera)	Cheap, less than €10
Vegetation affection	-	No affection	Disturbed	Disturbed	Disturbed	Relatively disturbed
Scale	Hillslope	Hillslope	Hillslope	Hillslope Gully	Gully	Hillslope Gully
Collection time	Quick	-	-	Quick (8 min)	Slow (2 h)	Quick (20 min)
Pre- processing time	Slow (to obtain input parameters)	-	-	Medium (3h)	Very slow (6-8 h)	Very quick (20 min)
Processing time	Very quick (seconds)	Quick (seconds)	Quick (seconds)	Medium (seconds to minutes)	Slow (minutes)	
Weight of data	Very low (30Kb/H1 3 years)	Very low (30Kb/H1)	Low (75Kb/H1)	Very Heavy (0,3Gb/H1)	Very heavy (0,5Gb/gully)	Very low (20Kb/H1)
Precision	Depends on input data	Low (2m)	Medium- high (3.3cm)	High (7mm)	Very high (2mm)	-

Based on the characteristics of these methods (Table 10), the strengths, weaknesses, opportunities and threats of WEPP, remote sensing and ground-based methods for assessing erosion on rehabilitated waste dumps were analyzed.

5.3.1. WEPP MODEL

The Water Erosion Prediction Project (WEPP) model is a physically based erosion simulation model that provides approximate soil loss estimations which can be useful when making predictions. The model, which is very simple to use, requires a large amount of input data and needs a relatively long time for collecting and preprocessing data, especially regarding soil conditions and slope profiles (if a DEM needs to be generated). Daily climatic series data at 15-minute intervals can be incorporated into WEPP so that it can calculate peak rainfall and intensity, a crucial factor influencing erosion, when estimating soil loss by water erosion.

WEPP cannot account for some of the actual conditions occurring at the study sites, such as heterogeneities at hillslopes due to inappropriate design planning. When landforms are not well designed or implemented, rip lines instead of reducing hydrological connectivity along the slope can enhance it, leading to large erosion features, as in the case of G2. Poor landform design, in which landform and/or rip lines do not follow the natural contour, cannot be considered by WEPP model. Likewise, as happened in some of the erosion plots at MAC, hillslope can be formed by heterogeneous soil characteristics and substrate distribution (lots of topsoil on top and rocky material at the bottom of the hillslope), which WEPP is not able to model. Nonetheless, according to the approach that BHP-Billiton is applying currently for rehabilitation planning and implementation, problems associated with inappropriate landform design should not occur in the future.

The default management conditions applicable to the model in this study, assumed that vegetation was not growing in the area. In this case, as vegetation at MAC provides very limited canopy and ground cover for protecting the surface against erosion, this will not have repercussions on model outcomes. However, in the case of successfully rehabilitated waste dumps, vegetation progress should be considered in WEPP when predicting erosion, as it is an influencing factor on water erosion processes.

Random roughness was shown to be a sensitive input parameter into WEPP, which remains constant for the entire modelling, run not considering changes in rip lines over time. It would produce interesting result if the model could contemplate the actual influence of rip lines on runoff and deposition processes by interrupting the hydrological connectivity at the hillslope. As mentioned before, rip lines could be included in the WEPP slope input, taking full advantage of the opportunity WEPP gives to implement complex slope profiles.

5.3.2. LIDAR

LIDAR was a good method for making a general assessment of landform or to detect significant changes at the hillslope scale. It can thus potentially be applied to broad-scale erosion assessments taking full advantage of the extensive surface coverage by the aircraft, being also applicable to assessments, such as vegetation monitoring. Furthermore, as LIDAR is multispectral remotely sensed data, vegetation can be avoided when reconstructing surfaces by selecting the spectral response of bare soil. LIDAR data provided by BHP-Billiton in 00T format for previous years was not accurate enough for assessing the surface, as the files were already processed elevation files through a rough triangulation.

5.3.3. UAV

The UAV data, due to noise in the elevation point cloud, was not accurate enough for assessing the surface or erosion at the hillslope scale. This might be because data was collected or preprocessed for a different purpose at a larger scale. Furthermore, UAV gave a low calibration rate when data was preprocessed.

5.3.4. LASER SCANNING

Laser scanning can provide, in the absence of vegetation, a complex surface reconstruction applicable to future mining waste dump rehabilitation, in order to analyze landform surfaces, predict erosion or assess landform changes over time more precisely. When laser scanning was applied to plots with higher vegetation cover than the study areas proved to be ineffective, as vegetation obscures visibility to the scanner. Scanning also loses detail or precision with geomorphology of the land (e.g. meandering erosion features, slopes or rip lines) and the distance from the scanner.

Laser scanning has potential for being applied at both the gully and hillslope scale. A combination of various laser scans can be useful for assessing a large hillslope or a complex meandering erosion feature, and it probably would have provided a more accurate reconstruction of G2. However, *Scene* software was not successful when combining successive scans as the resulting point cloud was a very heavy file that was difficult to work with despite being cropped for the study area.

The scanner used for the field work was relatively heavy and took up considerable space, making it uncomfortable for field work if it needs to be carried on foot to remote areas. Collection and preprocessing of data in *Scene* was quick and easy, although point clouds were not well geo-referenced, so more pre-processing time was required.

5.3.5. 3D RECONSTRUCTION

Very accurate reconstructions were obtained from pictures taken with a consumer grade camera. 3D reconstruction was applied to more gullies than the study ones, which were not included because it was not possible to process more data given the limited research time. Despite the guidelines and requirements for 3D reconstruction being followed as much as possible, some reconstructions were not very satisfactory. This could be due to the bright conditions that characterize the Pilbara region, translated into high reflection and shadowiness when taking pictures; the structure of the erosion features (deep and narrow gullies); or that too many pictures were provided for the reconstruction, making the processing too heavy that *Visual SFM* software could not reconstruct the whole structure.

This 3D method provided very accurate reconstructions, in which even stones could be discerned from the point cloud, and could be applied for monitoring specific features or implemented into 3D erosion models. This technique is effective at the gully or smaller scale, due to the large amount of data needed to be collected and processed for reconstructing large features as the study gullies. As for the laser scanning, 3D reconstruction has the potential for assessing gully erosion where vegetation is not growing, or cover is very low.

A GPS was applied to scale and georeference the 3D point cloud, but the positions provided were not accurate enough for this purpose, as also happened for the slope transects and soil samples location. In order to avoid future issues related to GPS precision and thus monitor accurately hillslopes and erosion features, it is recommended to use a different device such as a total station in order to precisely determine the position of control points or other locations related to the study. The point cloud had to be georeferenced, scaled and edited with *Cloud Compare* software which increases the preprocessing time.

5.3.6. SLOPE TRANSECTS

Slope transects involves quick and simple data collection, which only requires a measuring tape, and subsequent processing (very simple calculations in an *Excel* spread sheet), and provide approximate erosion (over)estimations. Therefore, they can provide a quick erosion assessment at the hillslope (or smaller) scale. While laser scanning and 3D reconstruction are not suitable when vegetation is growing successfully, slope transects can be applied where vegetation is not too dense. It can also be applied despite the sinuosity of erosion features. This method though can only consider erosion, but not deposition.

6. CONCLUSIONS

The potential of remotely sensed data and ground based methods for erosion assessment have been tested and described at the hillslope and gully scale. The research outcomes provide tools for assessing erosion at different scales, monitoring landform changes over time and supporting or justifying future decision-making in rehabilitation planning at mining waste landforms. The study methods can potentially be applied to all the phases of waste dump rehabilitations: design, implementation and monitoring.

Waste dump rehabilitation must insure that the constructed structure shows no signs of significant erosion and is stable. Good rehabilitation planning remains essential for creating and keeping stable, productive and self-sustaining conditions, taking future land use into account. Therefore, BHP-Billiton should continue applying and enhancing their current rehabilitation guidelines, ensuring landform stability.

One of the most important factors to consider when planning rehabilitation is the landform design. Laser scanning can potentially be applied when waste dumps are implemented for accurately reconstructing landform, as there is no vegetation that can disturb the scanning, in order to more precisely analyze landform surface, predict erosion or assess landform changes over time.

Unlike Fletcher et al. (2013), UAV did not have the ability to identify erosion from the surface models, due to the noise in its elevation point cloud. LIDAR is a good method to get an overview at the hillslope scale in order to make a general assessment of landform or detect significant changes, as in the case of G2. However, in contradiction to the results from Perroy et al. (2010), LIDAR had no potential for producing and monitoring erosion estimations. The combination of LIDAR, observation from aerial images and field work encourages the detection of degraded areas. If further assessment needs to be done, then other methods such as slope transects, laser scanning or 3D reconstruction can give a more accurate analysis of the surface.

Laser scanning and slope transects gave the most accurate surface assessment at the hillslope scale. Laser scanning allows one to assess erosion at the hillslope scale and gives the opportunity of combining several scans, even though attention should be paid to data preprocessing and the size of the resulting files. Slope transects provide approximate estimations of soil loss through simple and quick data collection and processing, and thus can be considered as suitable for quick erosion assessment at the hillslope scale.

Gully scale assessment might be interesting for assessing physical characteristics of the feature; analyzing if a gully is active or not over time or estimating erosion rates by using precise gully reconstructions. If erosion features need to be assessed where no vegetation is growing, which is a big concern for rehabilitators and mining companies (Fletcher et al., 2013), laser scanning and 3D provide very accurate surface reconstructions. 3D reconstruction was the most accurate study method for assessing erosion at the gully scale and thus can be applied for precisely analyzing specific erosion features. Other resources could be applied where erosion appears in an area covered by vegetation, such as slope transects (if vegetation not too dense) or multispectral methods.

In order to develop a system of adequate landform monitoring, data must be collected frequently, so that trends over time or significant changes can be detected. Therefore landform stability could be more precisely assessed at hillslopes or specific erosion features. Overlaying and differencing consecutive DEMs, which provide a spatial distribution of erosion processes and estimations of soil loss (Tomczyk et al., 2012), may provide an effective way for assessing water erosion on waste dumps. But it should be kept in mind that waste dumps reduce their volume during the first few years after construction due to settling of the soil.

WEPP provides approximate soil loss estimations which can be useful when making predictions once a new waste dump is implemented or over already degraded areas. However, WEPP cannot account for some of the actual conditions occurring on the study sites such as inadequate landform design or heterogeneous substrate. By implementing complex slope profiles derived from laser scanning in WEPP, the model could consider actual runoff and deposition processes occurring between rip lines. This way, rip lines would be considered as a WEPP slope input instead of random roughness.

GIS provides powerful tools for assessing the surface that need to be combined because a single analysis might not provide all the information that could be inferred by combining different assessments, for instance, slope and flow behavior.

All these methods are merely estimations of real life. Models make it possible to bridge the existing gap between theory and data and to understand specific processes of real life better, but it always is a simplified representation. The output of any analysis can be only as good as the quality of the data. Erosion follows complex processes which are even more difficult to fully understand on site, making its assessment complicated. Thus, erosion assessment and monitoring must always go hand in hand with field data.

7. REFERENCES

- Aly, M. K. (2010). *MINErosion 4: A user-friendly catchment/landscape erosion prediction model for post mining sites in Central Queensland*. Griffith School of Engineering, Griffith University. M.Sc. of Soil Resources, Cairo University, Egypt.
- Bagyaraj M., Ramkumar T., Venkatramanan S., Chung S. Y. and Gurugnanam B. (2014). *Assessment of soil erosion probability in Kodaikanal, India using GIS and remote sensing*. Available online on:
[http://www.academia.edu/6228298/Assessment of soil erosion probability in Kodaikanal India using GIS and remote sensing](http://www.academia.edu/6228298/Assessment_of_soil_erosion_probability_in_Kodaikanal_India_using_GIS_and_remote_sensing). Retrieved at: 26/03/2015.
- BHP Billiton Iron Ore (2013). *Mine Closure Plan (draft)*. Available online on:
https://consultation.epa.wa.gov.au/seven-day-comment-on-referrals/orebody-29-30-35-mining-below-water-table/supporting_documents/Appendix%20F%20%20Mine%20Closure%20Plan.pdf. Retrieved at: 24/03/2015.
- Boggs, G.S., Devonport, C.C., Evans K.G., Saynor, M.J., and Moliere, D.R. (2001). *Development of a GIS based approach to mining risk assessment*. Supervising Scientist, Environment Australia, Commonwealth Department of Environment and Heritage.
- Castillo, C., Pérez, R., James, M. R., Quinton, J. N., Taguas, E. V., and Gómez, J. A. (2012). *Comparing the accuracy of several field methods for measuring gully erosion*. Soil Science Society of America Journal, 76(4), 1319-1332.
- Claughton D. (2014). *Rehabilitation of mine land by Stratford Coal*. ABC. Available online on:
<http://www.abc.net.au/news/2014-12-04/nsw-rehabilitation-of-mine-land-04-12-14/5943162>. Retrieved at: 23/03/2015.
- Darwish T.M., Stehouwer R., Miller D., Sloan J., Jomaa I., Shaban A., Khater C. and Hamzé M. (2010). *Assessment of abandoned quarries for revegetation and water harvesting in Lebanon, East Mediterranean*. Available online on:
<http://ecosystems.psu.edu/research/labs/environmental-soils/publications/aassessment-of-abandoned-quarries-for-revetetation-and-water-harvesting-in-lebanon-east-mediterraeen>. Retrieved at: 28/03/2015.
- Department of Agriculture and Food (2014). *An inventory and condition survey of the Pilbara region, Western Australia*. Government of Western Australia. Available online on:
<https://www.agric.wa.gov.au/rangelands/inventory-and-condition-survey-pilbara-region-western-australia>
- Department of Industry, Tourism and Resources (2006). *Rehabilitaci3n de minas*. Programa de desarrollo sostenible Leading Practice para la industria minera. Translated by eTranslate Rafael de la Figuera Von Wichmann. Available online on:
<http://www.industry.gov.au/resource/Documents/LPSDP/LPSDP-MineRehabSpanish.pdf>

- Department of Mines and Petroleum (2009). *Waste Rock Dumps*. Environmental Notes on Mining. Government of Western Australia. Available online on: <http://www.dmp.wa.gov.au/documents/ENV-MEB-223.pdf>
- Ecoscape (2011). *Pilbara Iron Ore Project – Blacksmith Vertebrate Fauna and Short Range Endemic Survey*. Ecoscape (Australia) Pty Ltd. Available online on: [http://www.epa.wa.gov.au/EIA/EPAREports/Documents/1456/App%2010%20-%20Ecoscape%20\(2010\)%20Fauna%20Report\[1\]%20.pdf](http://www.epa.wa.gov.au/EIA/EPAREports/Documents/1456/App%2010%20-%20Ecoscape%20(2010)%20Fauna%20Report[1]%20.pdf). Retrieved at: 06/11/2015.
- Environmental Protection Authority, EPA (2006). *Guidance for the Assessment of Environmental Factors: Rehabilitation of Terrestrial Ecosystems*, Guidance No. 6, Environment Protection Authority, Perth, Australia.
- ESRI (2013). *Surface creation and analysis*. ArcGIS 10.1 Resources. Available online on: http://resources.esri.com/help/9.3/arcgisengine/java/gp_toolref/geoprocessing/surface_creation_and_analysis.htm
- Evans, K.G., Willgoose, G.R., Saynor, M.J. and House, T. (1998). *Effect of vegetation and surface amelioration on simulated landform evolution of the post-mining landscape at ERA Ranger Mine, Northern Territory*. Supervising Scientist Report 134, Supervising Scientist, Canberra.
- Evans, K. G. (2000). *Methods for assessing mine site rehabilitation design for erosion impact*. Soil Research, 38(2), 231-248.
- Flanagan, D.C., Gilley, J. E. and Franti, T.G. (2007). *Water Erosion Prediction Project (WEPP): Development history, model capabilities and future enhancements*. American Society of Agricultural and Biological Engineers ISSN 0001-2351. Vol. 50(5): 1603-1612. Available online on: http://www.epa.wa.gov.au/EIA/EPAREports/Documents/1413/3.%20Landloch%20Draft_Rehabilitation%20Guidelines%202010.pdf
- Fletcher, A. T., & Erskine, P. D. (2013). *Rehabilitation Closure Criteria Assessment Using High Resolution Photogrammetrically Derived Surface Models*. ISPRS-International Archives of the Photogrammetry, Remote Sensing and Spatial Information Sciences, 1(2), 137-140. Available online on: <http://www.int-arch-photogramm-remote-sens-spatial-inf-sci.net/XL-1-W2/137/2013/isprsarchives-XL-1-W2-137-2013.pdf>. Retrieved at: 27/01/2016.
- Hazarika M.K., and Honda K. (1999). *Estimation of Soil Erosion Using Remote Sensing and GIS, Its Validation and Economic Implications on Agricultural Production*. Available online on: <http://topsoil.nserl.purdue.edu/nserlweb-old/isco99/pdf/ISCOdisc/SustainingTheGlobalFarm/P068-Hazaika.pdf>. Retrieved at: 23/03/2015.
- Hudson, N. (1993). *Field measurement of soil erosion and runoff* (Vol. 68). Chapter 2 Reconnaissance methods. Food & Agriculture Organisation (FAO). Available online on: <http://www.fao.org/docrep/T0848E/t0848e-07.htm>

- James, M. R., and Robson, S. (2012). *Straightforward reconstruction of 3D surfaces and topography with a camera: Accuracy and geoscience application*. Journal of Geophysical Research: Earth Surface (2003–2012), 117(F3).
- Jasper, D.A. (1994). *Management of mycorrhizas in revegetation*. Management of Mycorrhizas in Agriculture, Horticulture and Forestry. Eds Robson, A.D., Abbott, L.K. and Malajczuk, N., Kluwer Academic Publishers, Dordrecht, the Netherlands (pp. 211-219).
- Johnson, C. K., Mortensen, D. A., Wienhold, B. J., Shanahan, J. F., & Doran, J. W. (2002). *Soil Electrical Conductivity Classification: A Basis For Site-Specific Management In Semiarid Cropping Systems*. Available online on: <http://digitalcommons.unl.edu/cgi/viewcontent.cgi?article=2061&context=usdaarsfacpub>
- Landloch Pty Ltd (2010), *Rehabilitation guidelines for the Jack Hills waste landform*. Report prepared for Crosslands Resources Ltd. Available online on: http://riawa.com.au/wordpress/wp-content/uploads/2014/10/2014-ROBINSON_WARDMAN_GOLOS_Closure-planning-at-the-Nifty-Copper-Mine-Site.pdf
- Minnesota Geospatial Information Office, MnGeo (2001). *How is LIDAR Data Used to Protect Water Quality in Minnesota?* Available online on: http://www.mngeo.state.mn.us/chouse/elevation/uses/LIDAR_uses_waterquality.html. Retrieved at: 27/08/2015.
- Moliere, D. R., Evans, K. G., and Willgoose, G. R. (2002). *Temporal trends in erosion and hydrology for a post-mining landform at Ranger Mine*. Research Institute, 31. Available online on: <http://www.environment.gov.au/system/files/resources/48efb9e4-5bf8-45f0-ba88-dd8e1b3ed7b5/files/ssr166-erosion-hydrology.pdf>
- Morgan, R. P. C. (2009). *Soil erosion and conservation*. John Wiley & Sons.
- Niemiec, M. (2009). *Satellite remote sensing for water erosion assessment*. Roczniki Geomatyki, 7(2), 99-106.
- Perroy, R. L., Bookhagen, B., Asner, G. P., and Chadwick, O. A. (2010). *Comparison of gully erosion estimates using airborne and ground-based LIDAR on Santa Cruz Island, California*. Geomorphology, 118(3), 288-300. Available online on: http://www.geog.ucsb.edu/~bodo/pdf/perroy10_gully_erosion_santa_cruz_island.pdf. Retrieved at: 27/08/2015.
- Printemps, J., Ausseil, A. G., Dumas, P., Mangeas, M., Dymond, J. R., and Lille, D. (2007). *An erosion model for monitoring the impact of mining in New Caledonia*. MODSIM, New Zealand, 2562-2568.
- Raval, S., Merton, R. N. and Laurence, D. (2011). *Mine environmental monitoring using CHRIS Proba imagery of the Dexing Copper Mine, China*. Proceedings 34th International Symposium on Remote Sensing of Environment, Sydney, Australia.

- Raval S., Merton R.N. and Laurence D. (2013). *Satellite based mine rehabilitation monitoring using WorldView-2 imagery*. Mining Technology. 122 (4): 200-207. Available online on: <http://www.acsmp.unsw.edu.au/satellite-based-mine-rehabilitation-monitoring-using-worldview-2-imagery>. Retrieved at: 04/04/2015.
- Red Dirt Seeds: Mine Site Rehabilitation (n.d.). *Revegetation: Before and After*. Available online on: <http://www.reddirtseeds.com.au/examples.aspx>. Retrieved at: 21/03/2015.
- Satellite Imaging Corporation, SIC (n.d.). *Satellite Imagery and GIS for Land Cover and Change Detection*. Available online on: <http://www.satimagingcorp.com/applications/environmental-impact-studies/land-cover-and-change-detection/>. Retrieved at: 23/03/2015.
- Schmid, T., Schack-Kirchner, H., and Hildebrand, E. (2004, October). *A case study of terrestrial laser scanning in erosion research: calculation of roughness and volume balance at a logged forest site*. In Proceedings of the ISPRS Working Group VIII/2: Laser-Scanners for Forest and Landscape Assessment (pp. 03-06).
- Singh, R. B., and Haigh, M. J. (Eds.). (1995). *Sustainable Reconstruction of Highland and Headwater Regions: Proceedings of the third international symposium*, New Delhi 6-8 October 1995. CRC Press.
- State Law Publisher, SLP (2015). *Mining Act 1978*. Department of the Premier and Cabinet. Government of Western Australia. Available online on: [http://www.slp.wa.gov.au/pco/prod/FileStore.nsf/Documents/MRDocument:28226P/\\$FILE/Mining%20Act%201978%20-%20\[08-i0-00\].pdf?OpenElement](http://www.slp.wa.gov.au/pco/prod/FileStore.nsf/Documents/MRDocument:28226P/$FILE/Mining%20Act%201978%20-%20[08-i0-00].pdf?OpenElement)
- Tomczyk, A., and Ewertowski, M. (2012). *Digital Elevation Models of Differences (DODs): implementation for assessment of soil erosion on recreational trails*. In EGU General Assembly Conference Abstracts (Vol. 14, p. 843).
- United States, USA (1985). *Final environmental impact statement for the Jackpile-Paguate uranium mine reclamation project, Laguna Indian Reservation, Cibola County, New Mexico*. United States. Bureau of Land Management. Rio Puerco Resource Area; United States. [b] Bureau of Land Management. Albuquerque District; United States. Bureau of Indian Affairs. Albuquerque Area Office.
- Valentin, C., Poesen, J., & Li, Y. (2005). *Gully erosion: impacts, factors and control*. Catena, 63(2), 132-153.
- Verdonk, S.C. (2015). *Gully volume estimates using UAV Photometry in the Salagou area*. Research Thesis at University of Utrecht.
- Vrieling, A. (2006). *Satellite remote sensing for water erosion assessment: A review*. Catena, 65(1), 2-18.

- Weesies, G. A., McCool, D. K., & Yoder, D. C. (1997). *Predicting soil erosion by water: a guide to conservation planning with the Revised Universal Soil Loss Equation (RUSLE)* (Vol. 703). Washington, DC: United States Department of Agriculture.
- Woldai, T. (2001). Application of Remotely Sensed data and GIS in Assessing the Impact of Mining Activities on the Environment. In *Proceedings—17th International Mining Congress & exhibition of Turkey*. Ed.: E. Unal, B. Ünver & E. Tercam, IMCET (pp. 75-84).
- Wu, C. (2011). *VisualSFM: A Visual Structure from Motion System*. Available online on: <http://ccwu.me/vsfm/>
- Wu, C., Agarwal, S., Curless, B., and Seitz, S.M. (2011). *Multicore Bundle Adjustment*. CVPR.

8. APPENDICES

Additional information, such as plans with a surface analysis per method and scale, which provides details to support the methodology, results and discussion is included in the Appendices, at the end of the document.

Appendix 1: Project support

This research required data, equipment, licenses and expertise/knowledge from a number of agencies including Landloch, BHP Billiton and WUR.

Permission to access different waste dump locations was needed from BHP Billiton, including many inductions, i.e. specific training for visiting mining sites in order to accomplish access requirements. This training mainly consists of explanations through online interactive videos on hazard and risks, and safety basics on site. Landloch provided insurance that assures coverage during the field work on mine sites.

Three different mining sites were visited. This required transportation and accommodation from BHP Billiton. Appropriate working clothing i.e. PPE, including working helmet, boots with steel caps, protective glasses, gloves, high visibility shirts and long works pants was provided by Landloch. In order to measure or estimate erosion rates on site and collect other needed data for the model, adequate equipment was needed, including tape measures, GPS equipment, digital camera and laser rangefinder. A laptop and a cellphone was provided in order to facilitate field work and data processing on site.

WEPP model has been used extensively by Landloch. Expertise was provided by Landloch in order to correctly run the model under mining waste dump conditions, as WEPP was designed for erosion studies in agricultural lands. Running erosion models with different sources of information (remote sensing techniques) requires a computer with a high processing and storage capacity. Therefore, a powerful computer provided with the WEPP software and *ArcGIS* was needed to further develop this project which Landloch provided. For estimation of erosion rates at the sites, available WEPP input data from the study sites was provided by Landloch and BHP-Billiton, such as soil and climatic data, remotely sensed resources, including satellite imagery, LIDAR and UAV data. Runoff and erosion data collected during 3 years (2012-2015) from the erosion plots at MAC was used for validating the model erosion estimations.

Appendix 2: Research Planning

Time	Location	Research activity
Aug-Sep 2015	Madrid	Proposal writing Preliminary literature review Research preparation i.e. organise the stay in Perth and making contact with Evan Howard, Landloch, and BHP-Billiton
Sep-Dec 2015	Perth	Refine and adjust proposal Collect all digital data needed for the assessment Run the WEPP model DATA COLLECTION Visit the Pilbara to get overview, select study sites and collect data needed for all the methods DATA ANALYSIS Estimate erosion rates from on-site data Compare measured and predicted erosion rates Comparison of different methods Presentation to Landloch and BHP-Billiton
Jan-Feb 2016	Wageningen	Complete data analysis Report writing Presentation

Appendix 2: Rill and gully erosion collection and calculation sheet

SLOPE TRANSECTS

Site: _____

Date: _____

	Transect	EFA Transect Distance (m)	rill number	Start of Rill Edge (m)	End of Rill Edge (m)	Rill Depth (m)	Comments
1							
2							
3							
4							
5							
6							
7							
8							
9							
10							
11							
12							
13							
14							
15							

Calculations:

- 1 Calculate rill width by deducting the start from the end rill edge distance (m)

$$\text{Rill width (m)} = \text{End of Rill Edge (m)} - \text{Start of Rill Edge (m)}$$

- 2 Calculate the cross-sectional area of each rill, using the formula for the appropriate cross-section i.e. triangle, semicircle or rectangle. Thus, assuming a rectangular section it is:

$$\text{Cross-section area (m}^2\text{)} = \text{Width (m)} * \text{Depth (m)}$$

- 3 Calculate the eroded cross-section for each transect by adding all the cross sections

$$\text{Transect cross-section} = \sum \text{Cross-section areas}$$

- 4 Calculate the average cross-section per transect

$$\text{Transect cross-section area (m}^2\text{)} = \frac{\sum_{i=1}^n \text{Transect cross-section area}_i}{n}$$

- 5 Calculate volume eroded in the hillslope by multiplying by the hillslope length covered by slope transects

$$\text{Soil loss (m}^3\text{/m}^2\text{)} = \text{Transect cross-section area (m}^2\text{)} * L \text{ (m)}$$

- 6 Convert the volume per hillslope surface to kilogrames per square meter or tonnes per hectare

$$\text{Soil loss (m}^3\text{/m}^2\text{)} * \text{Bulk density (}\frac{\text{Kg}}{\text{m}^3}\text{)} = \text{Soil loss (}\frac{\text{Kg}}{\text{m}^2}\text{)} * 10 = \text{Soil loss (}\frac{\text{T}}{\text{ha}}\text{)}$$

Appendix 3: Field activities

Field activities

Site:

Date:

3D Reconstruction		Material
<input type="checkbox"/>	Install control points	6 Metal sticks as control point
<input type="checkbox"/>	Pictures (including control points)	Camera
<input type="checkbox"/>	GPS control points	GPS
<input type="checkbox"/>	Mark feature and control points in map (number, note it down)	Map
<input type="checkbox"/>	Measure total length	Measurement tape

Processing:

- ☐ Download pictures
- ☐ Charge camera battery

Laser scanning

<input type="checkbox"/>	Run laser scanner	Laser scanner
<input type="checkbox"/>	Mark in map & GPS where it was settled	Map
<input type="checkbox"/>	Write down details of scanning	GPS

After:

- ☐ Charge and download data

Slope transects

<input type="checkbox"/>	Measure rills/gullies	Measurement tapes
<input type="checkbox"/>	Mark specific feature for gully scale assessment	GPS
<input type="checkbox"/>	GPS start and end of transects	

After:

- ☐ Process data into excel

Modelling

Roughness

<input type="checkbox"/>	Rip measurements		Measurement tape
<input type="checkbox"/>	Height	_____ cm	Camera
<input type="checkbox"/>	Width	_____ cm	Soil bags
<input type="checkbox"/>	Distance	_____ cm	Spade
		From ridge to ridge	Marker
			GPS

Soil properties

- ☐ Picture of soil surface & any weird surface
- ☐ Soil samples (4-5)
 - ☐ H1&G1 (MAC)
 - ☐ G2 (MWB)
 - ☐ Weird materials
- ☐ GPS soil sample location
- ☐ Mark in map where they were taken

Vegetation cover

- ☐ Check type of vegetation _____
- ☐ Relation canopy-ground cover _____
- ☐ Take pictures

Slope

- ☐ Measure hillslope
- ☐ Slope of batter on top

Appendix 4: Field equipment check list

CHECK LIST

Site: _____

Date: _____

PPE

- ☐ Pants
- ☐ Shirts
- ☐ Belt
- ☐ Helmet + hat
- ☐ Gloves + clip
- ☐ Glasses
- ☐ Socks
- ☐ Boots
- ☐ Access card

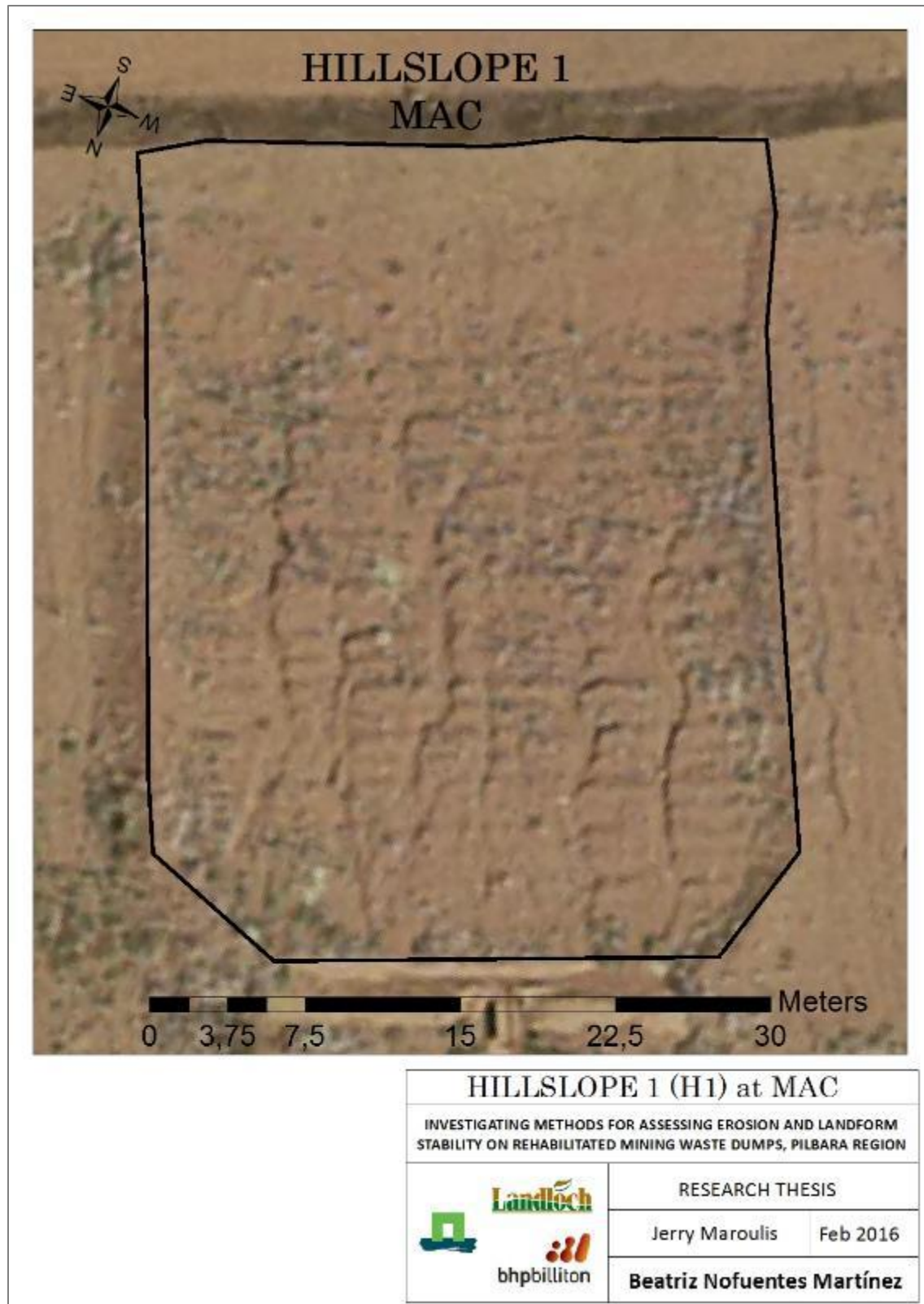
Field equipment

- ☐ Camera + charger + cable
- ☐ GPS + cable to download data
- ☐ Sticks for georeferencing
- ☐ Laser scanner & tripod
- ☐ Measurement tape
 - ☐ 3-5m
 - ☐ 50m
- ☐ Note pad
- ☐ Pens
- ☐ Fly net
- ☐ Maps
- ☐ Folder

- ☐ 30 soil bags
- ☐ Spade
- ☐ Markers
- ☐ Batteries for GPS
- ☐ Flanges for closing laser scanning
- ☐ Check list
- ☐ Slope transect template
- ☐ Sunscreen
- ☐ Phone
- ☐ Hard drive
- ☐ Laptop + charger
- ☐ Laser Rangefinder

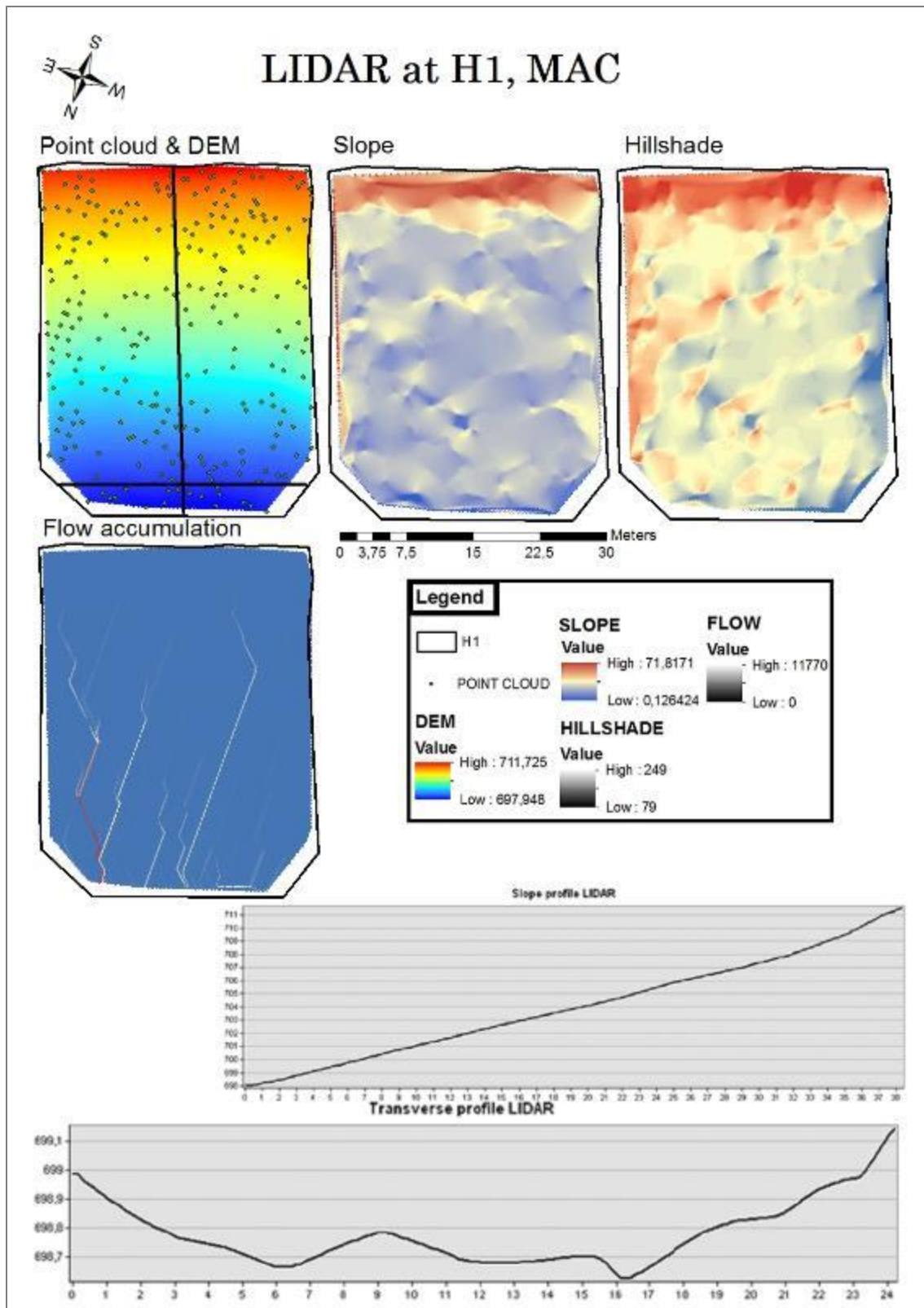
Appendix 5: Surface assessments

AP5.1. HILLSLOPE SCALE



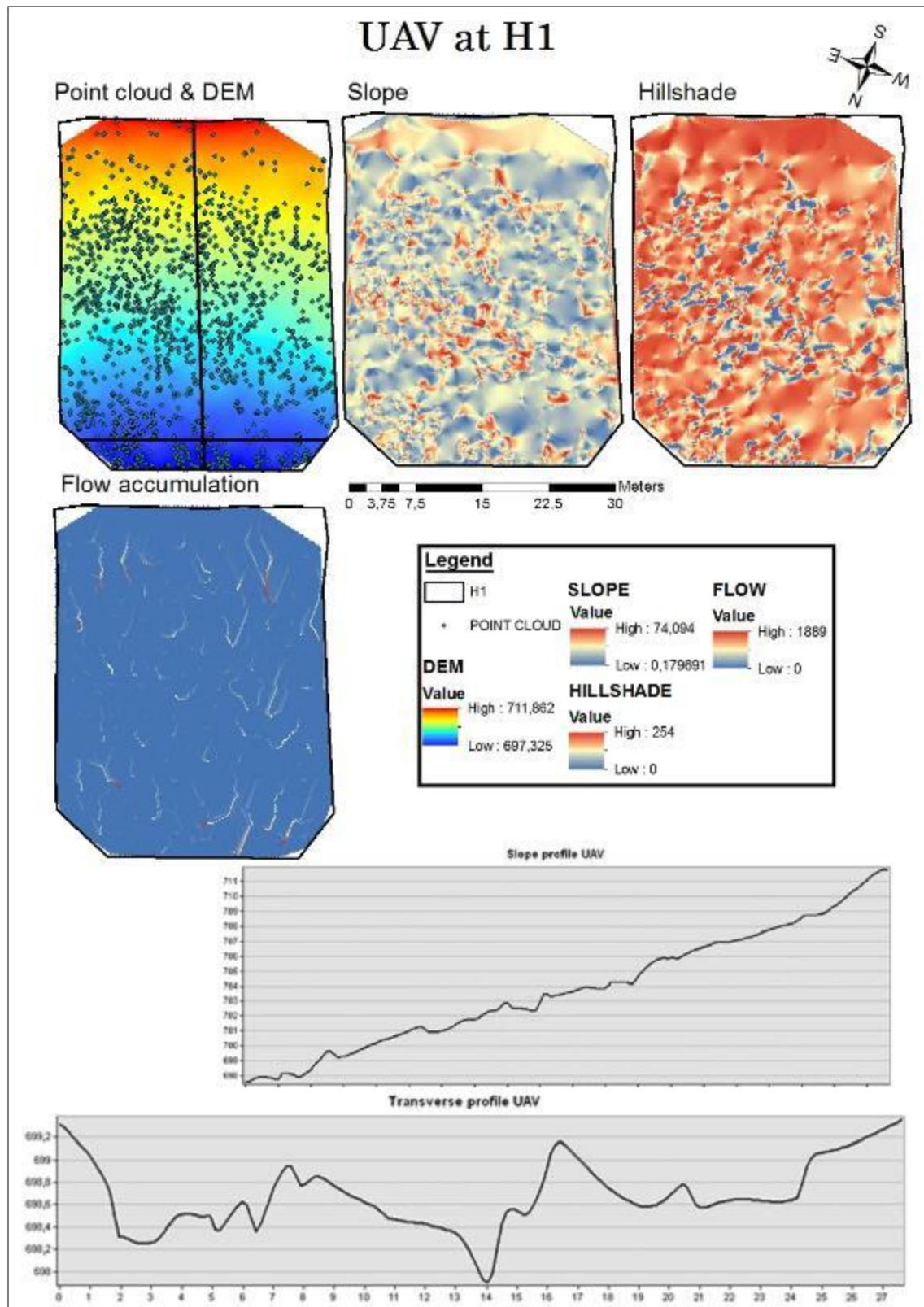
Plan 1: Hill Slope 1 (H1, MAC)

NOTE: Spatial image of H1 and its associated erosion features.

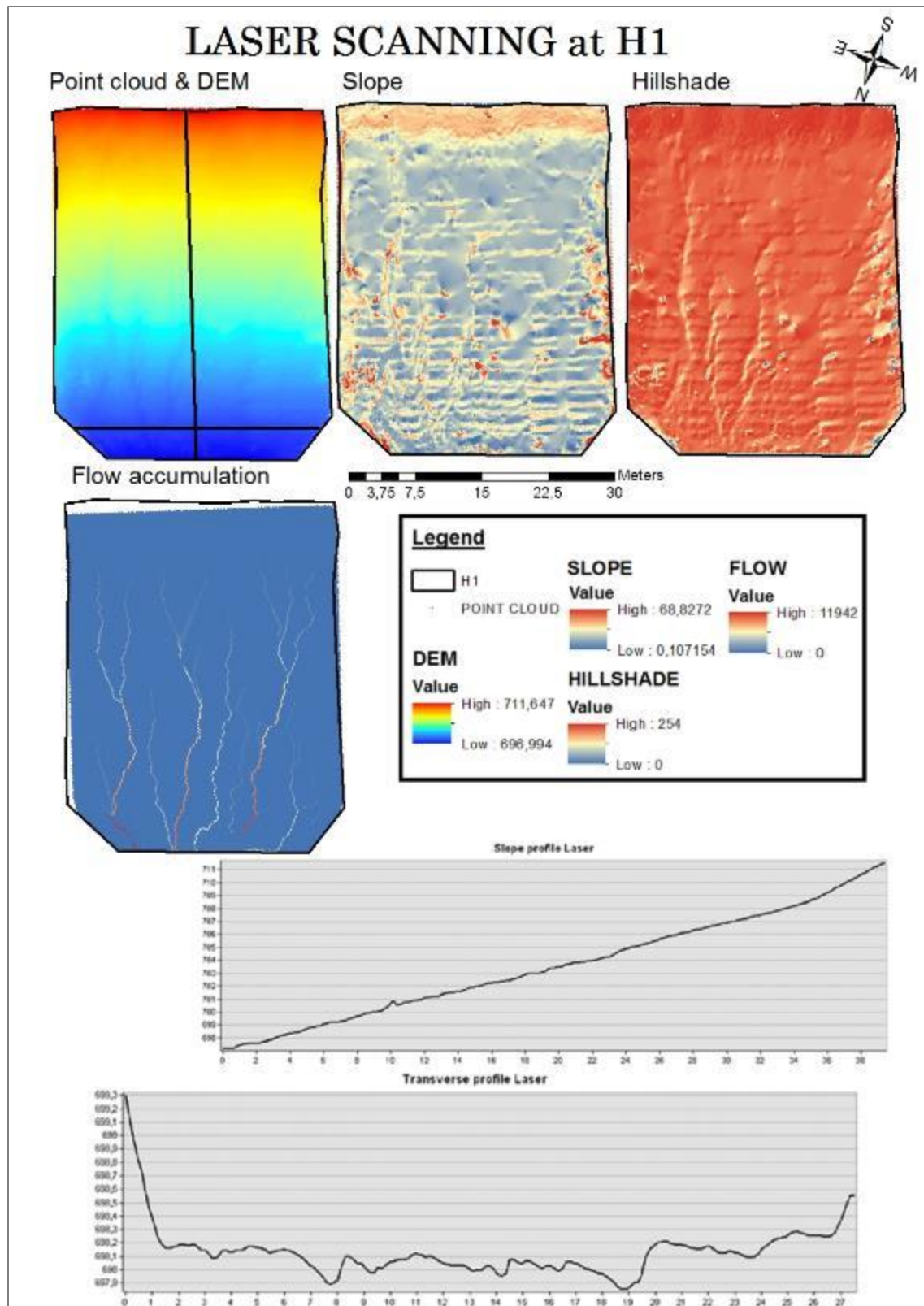


Plan 2: LIDAR surface assessment at H1 (MAC)

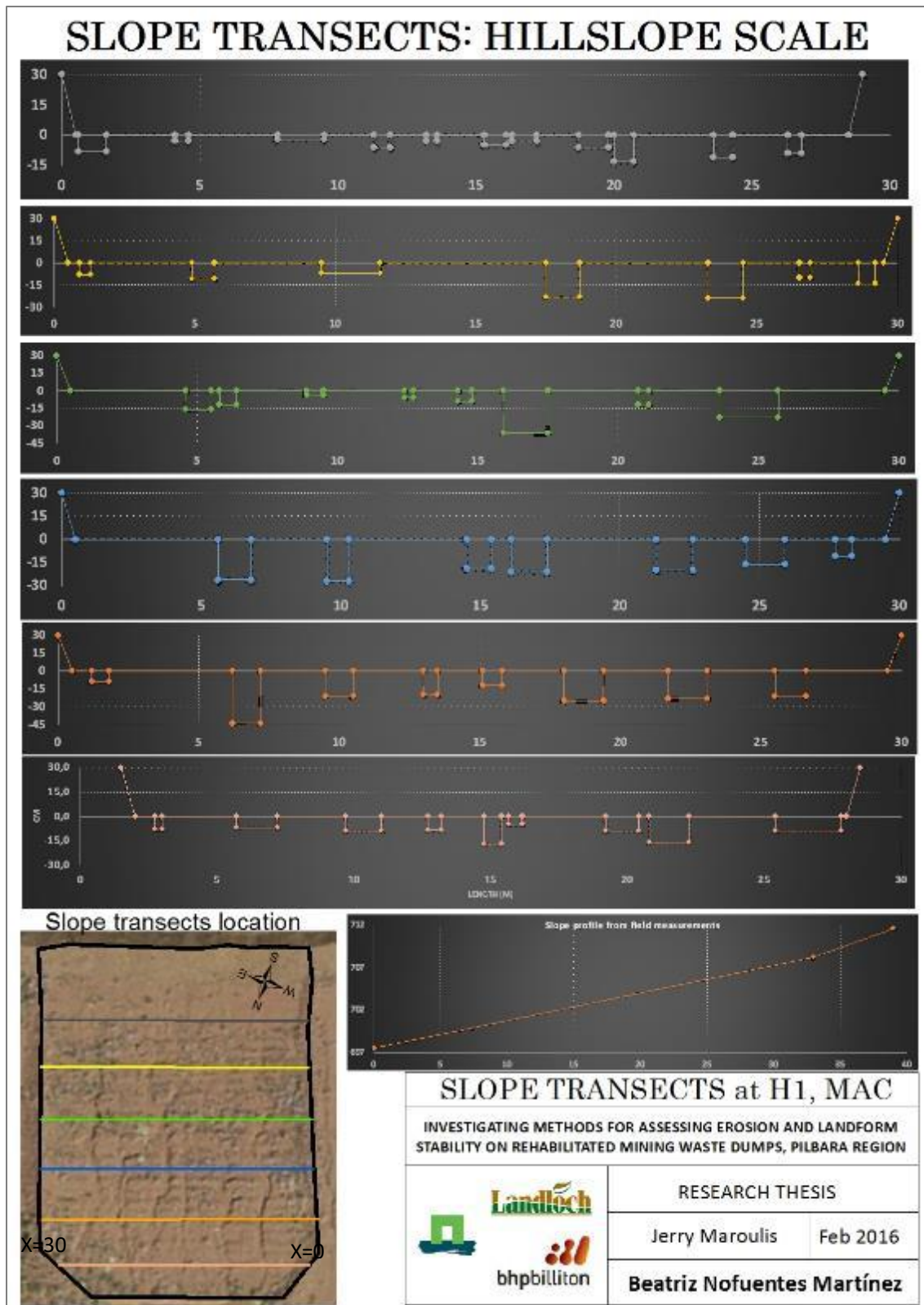
NOTE: All the slope maps attached to this study are in degrees.



Plan 3: UAV surface assessment at H1 (MAC)



Plan 4: Laser scanning surface assessment at H1 (MAC)

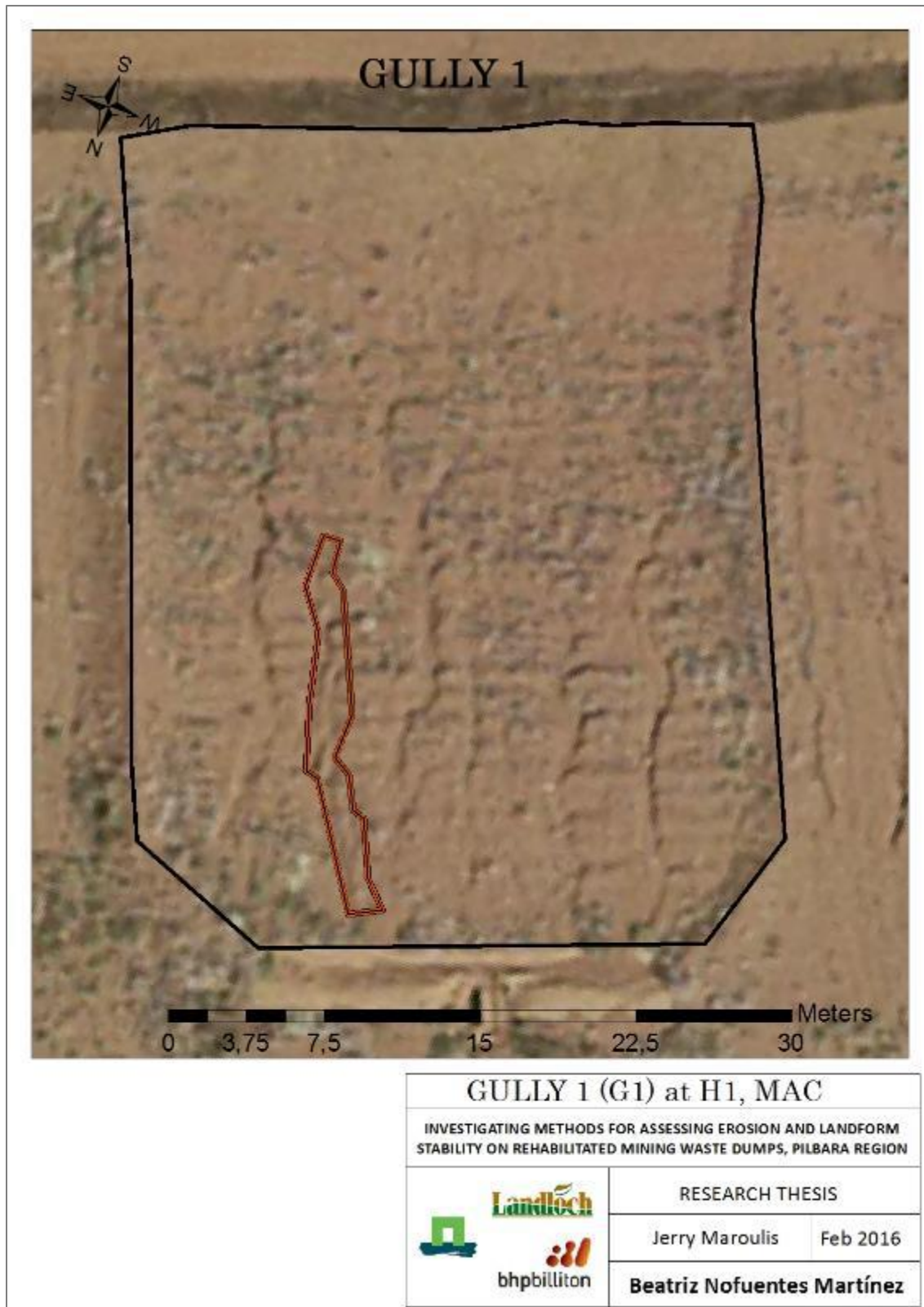


Plan 5: Cross sections from slope transect data at H1 (MAC)

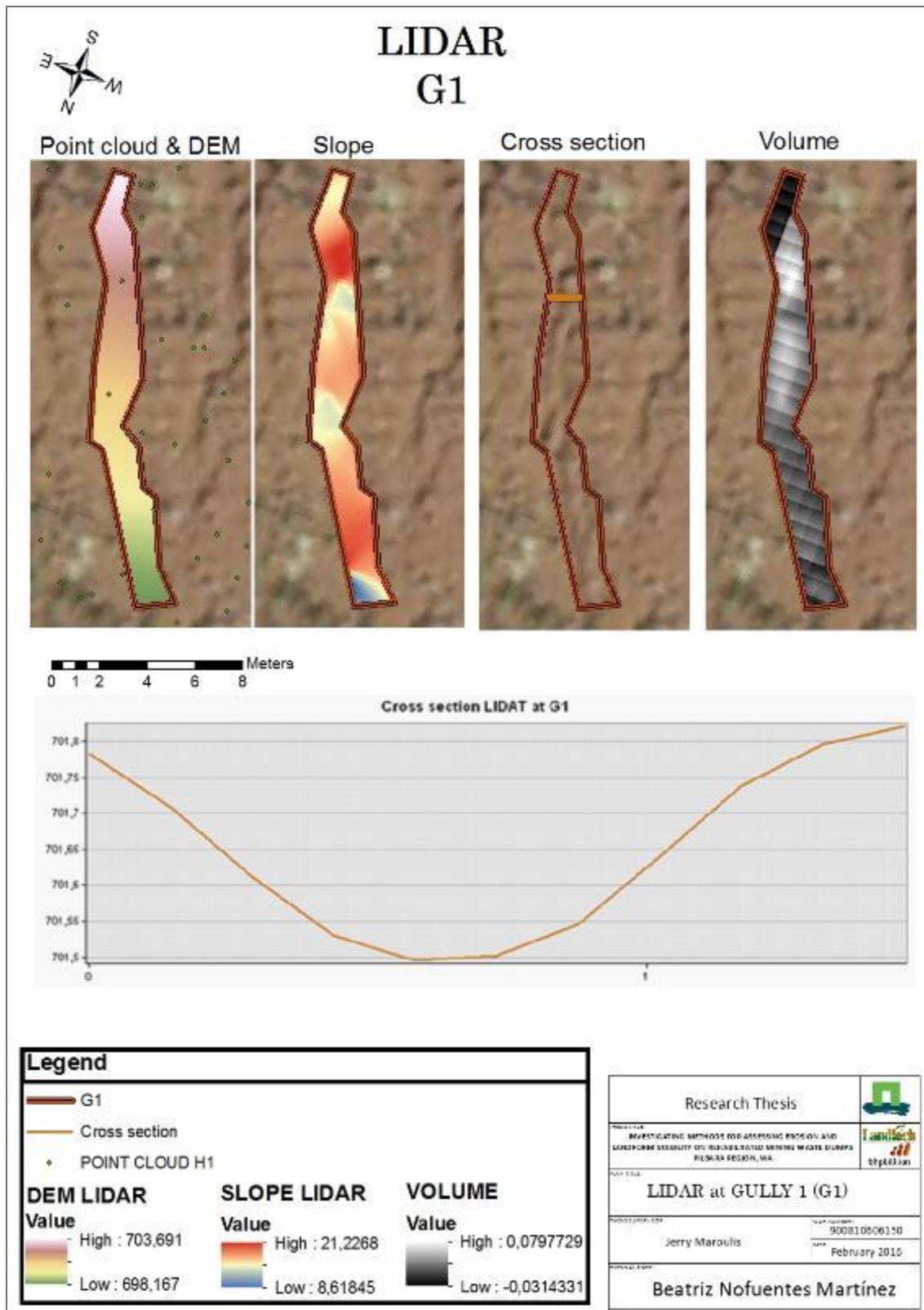
NOTE: All the slope transects graphs contain values from 0 to 30 m length in the X axis, and from 30 to -45 m a litude in the Y axis, assuming hillslope surface (altitude 0) is flat. An extra slope transect was included at H1 considering erosion volume 0 when making the calculations, so that the hillslope was covered homogeneously. Although cross section of erosion features are represented as rectangular sections for the slope transect profile, erosion calculations were based on elliptical cross sections.

AP5.2. GULLY SCALE

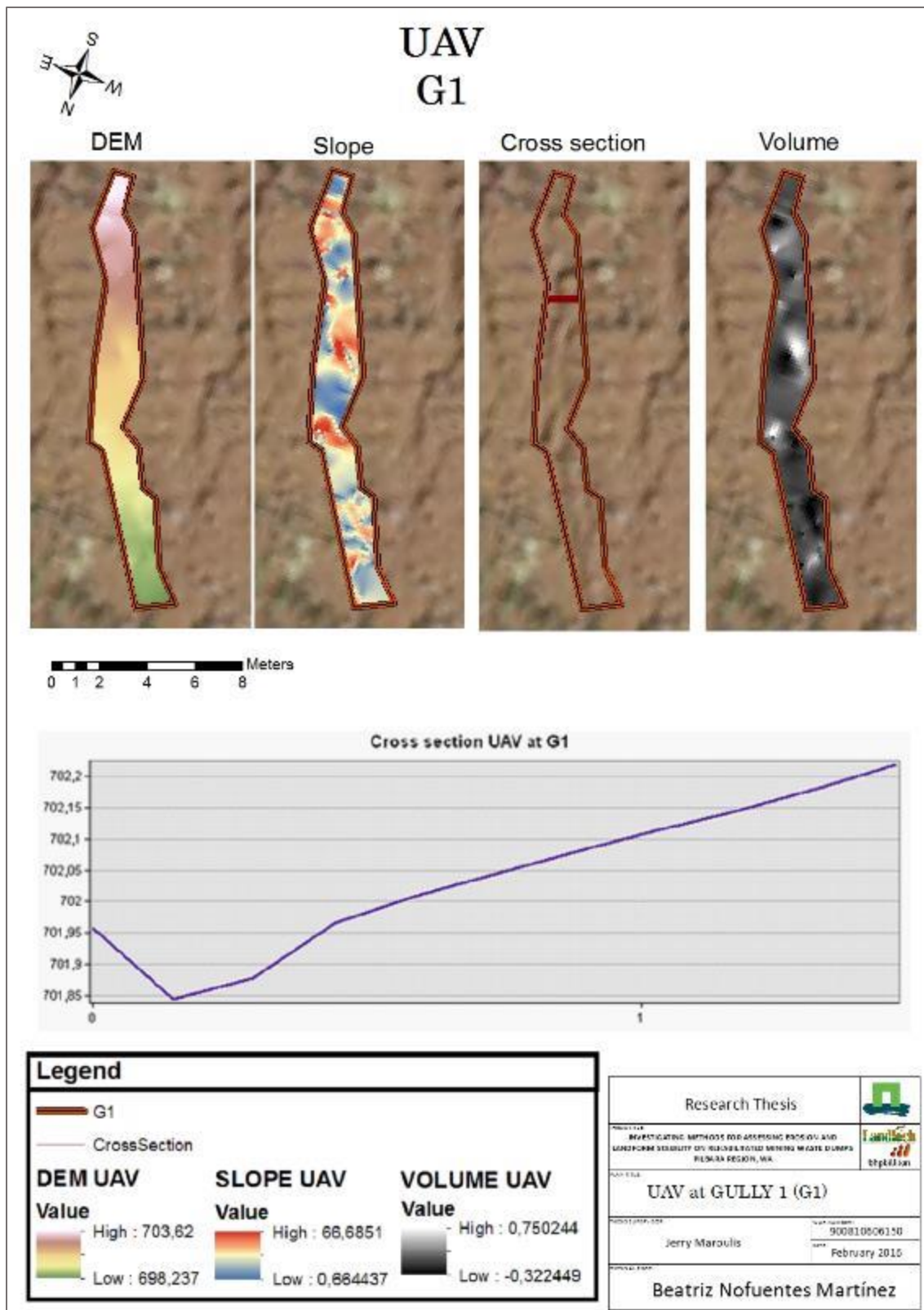
AP5.2.1. Gully 1 (MAC)



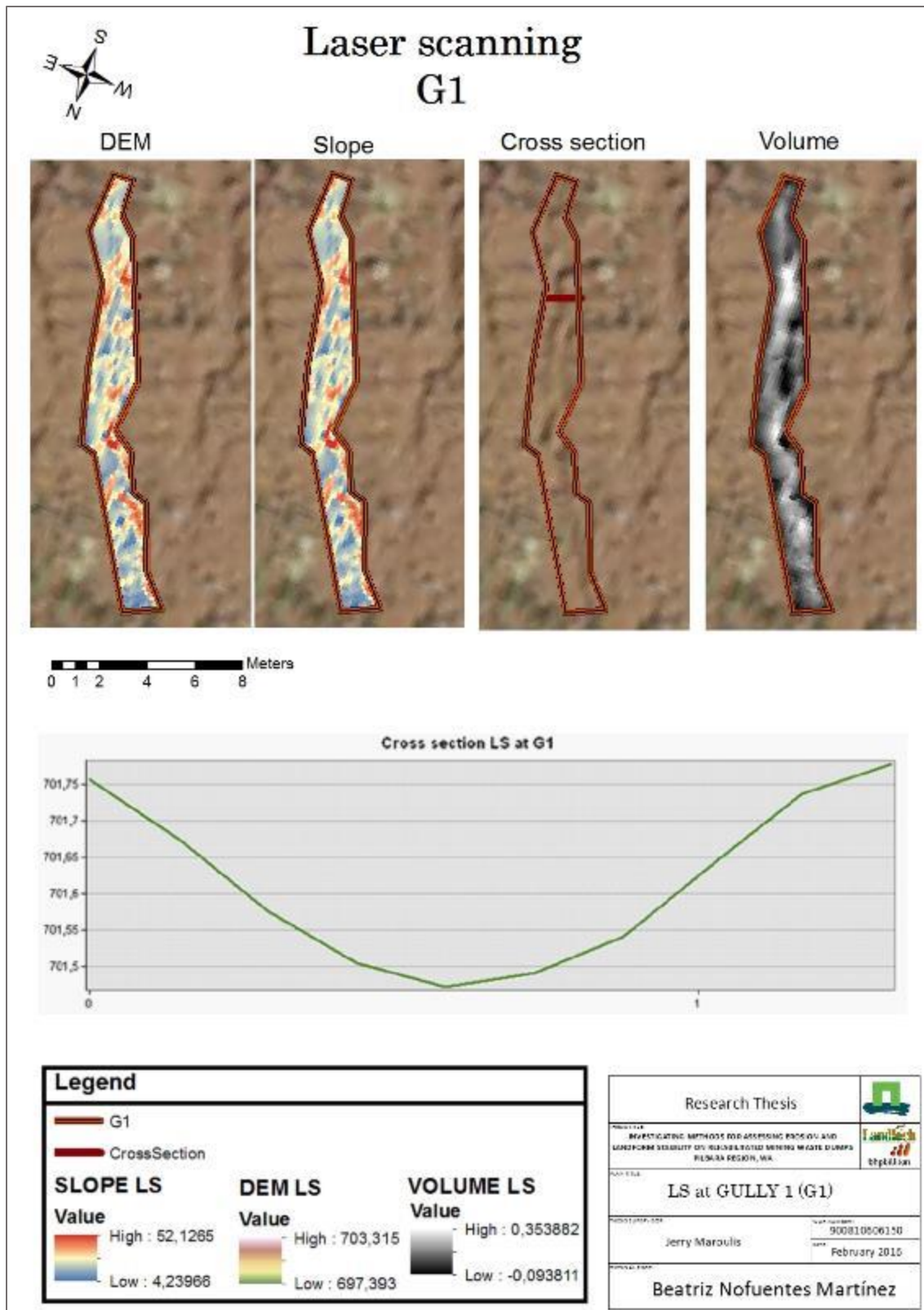
Plan 6: Gully 1 (G1, MAC)



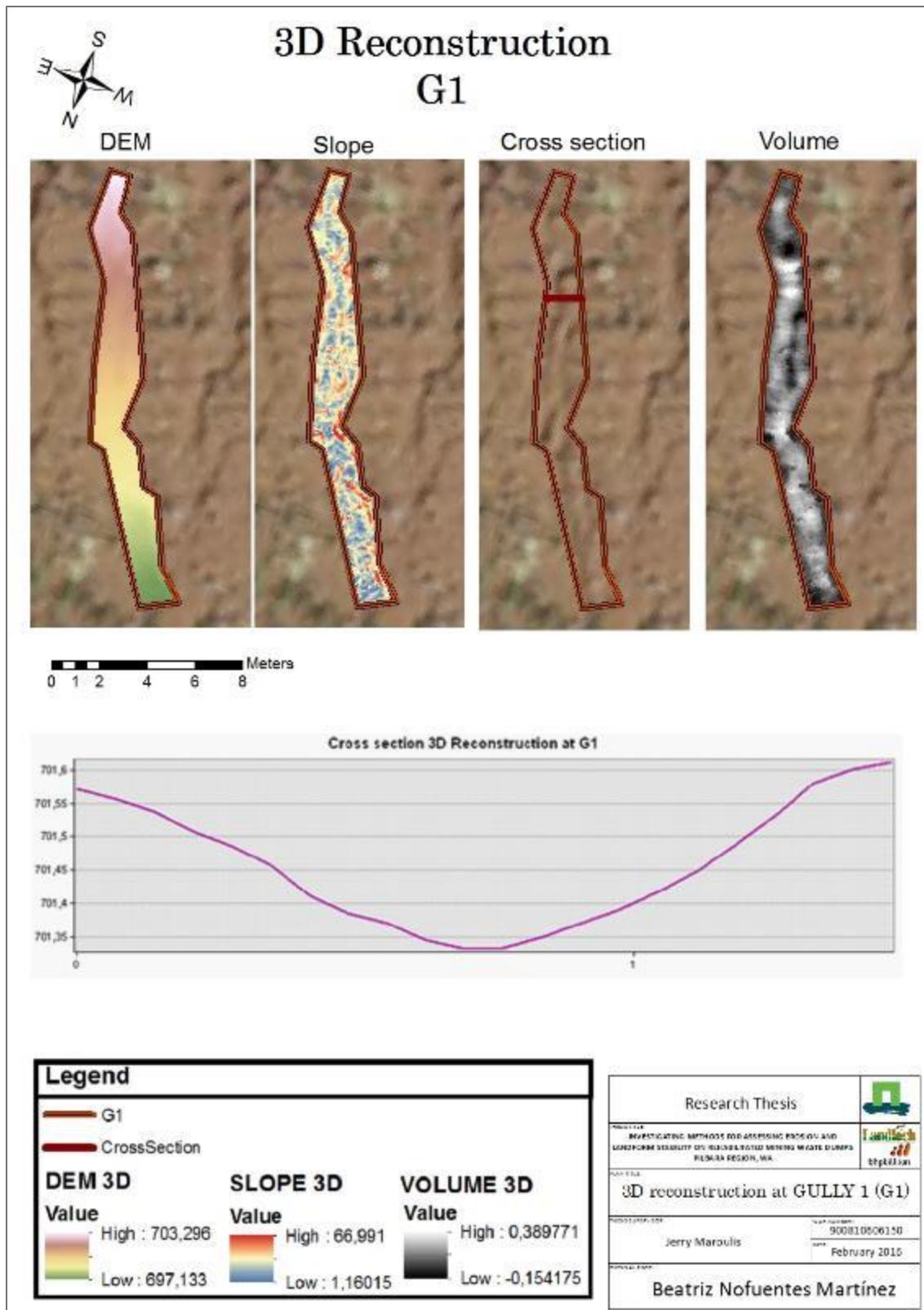
Plan 7: LIDAR surface assessment at G1 (MAC)



Plan 8: UAV surface assessment at G1 (MAC)

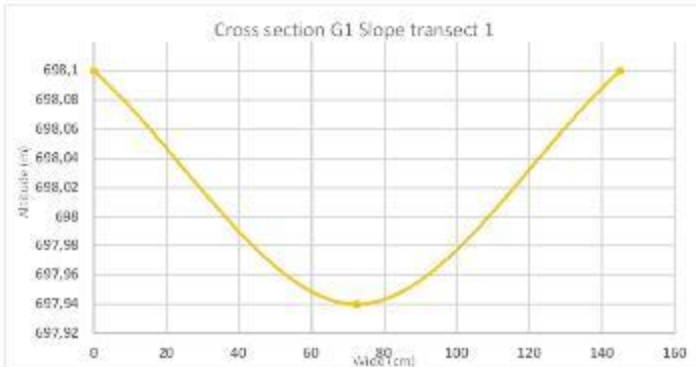
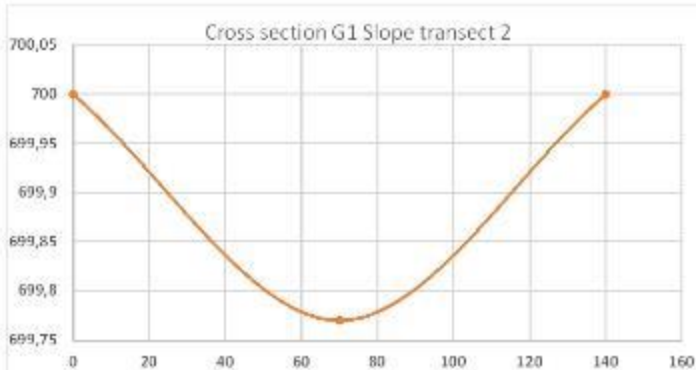
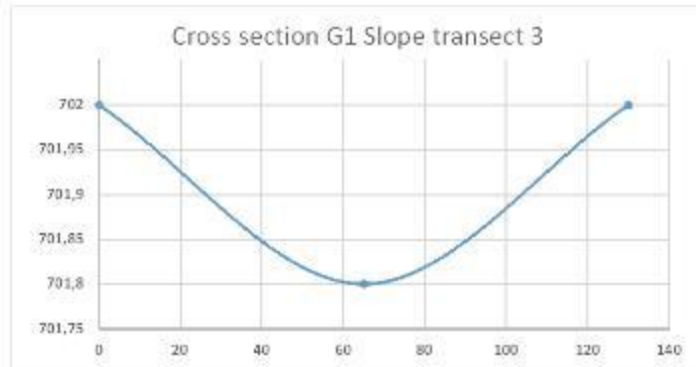


Plan 9: Laser scanning surface assessment at G1 (MAC)

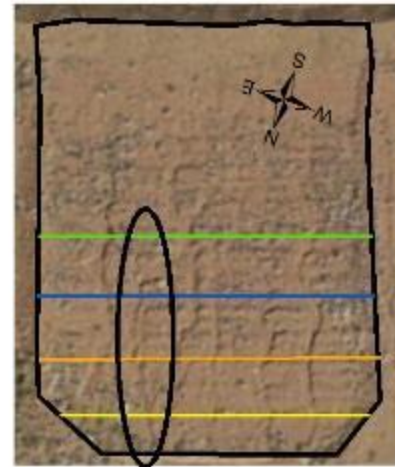


Plan 10: 3D reconstruction surface assessment at G1 (MAC)

SLOPE TRANSECTS: GULLY SCALE (G1)



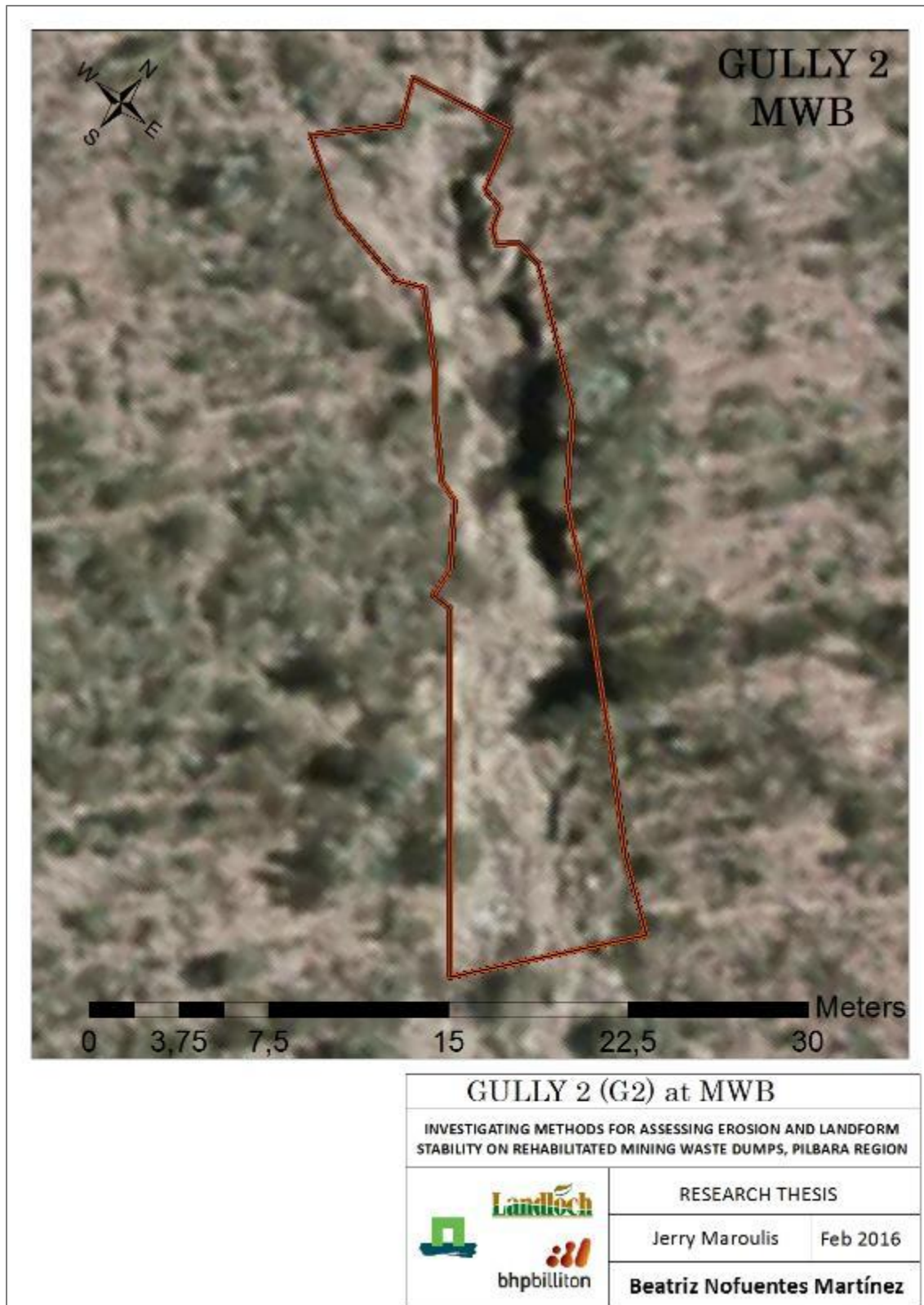
Slope transects location



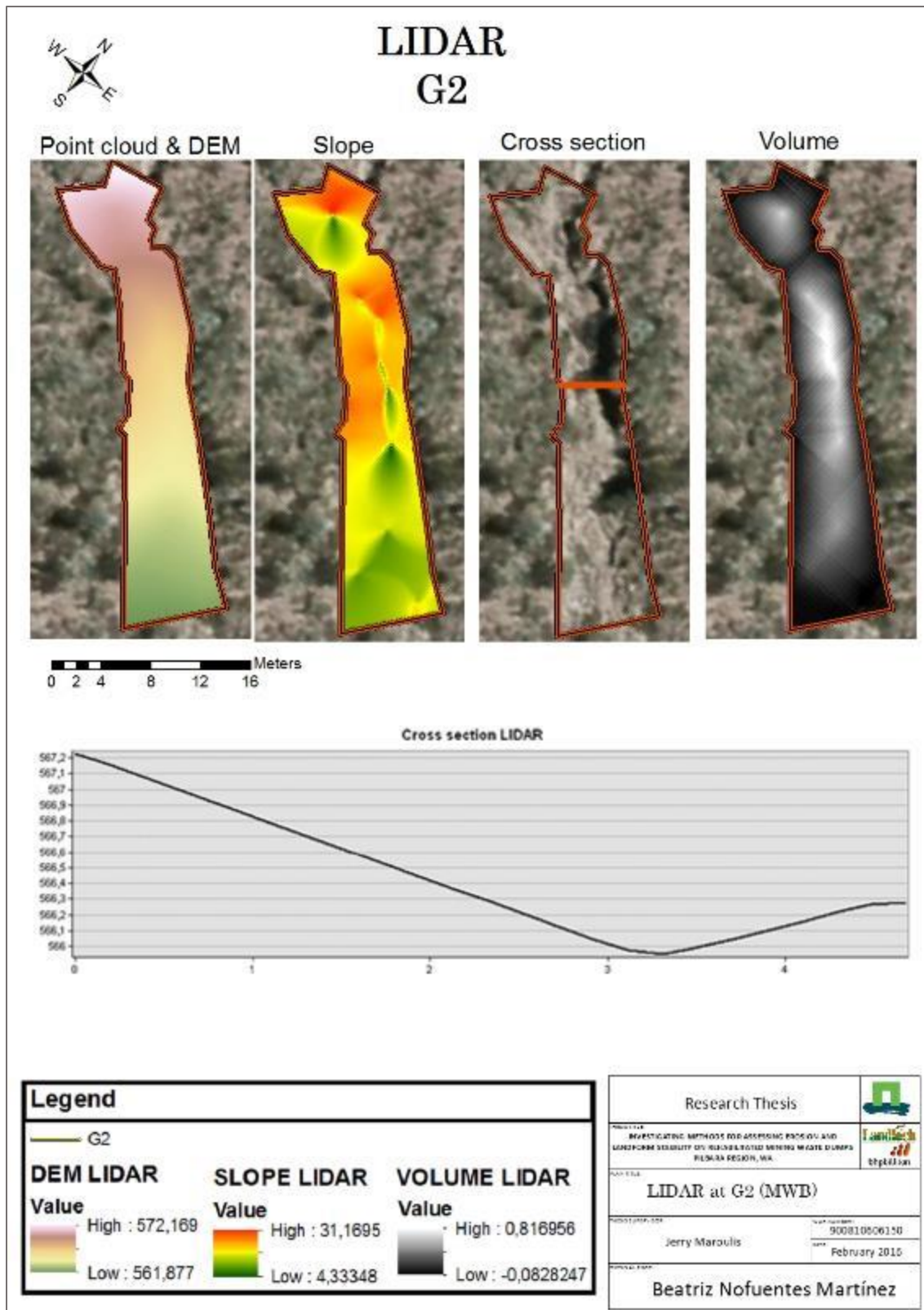
Research Thesis		
HYDROLOGIC APPROACH TO THE SOILS OF THE MAC AND LANDFILL WASTEWATER TREATMENT PLANT WASTE TREATMENT PLANT, WA		
SLOPE TRANSECTS GULLY SCALE (G1)		
Jerry Marcule	900810605150	
February 2016		
Beatriz Nofuentes Martínez		

Plan 11: Cross sections from slope transect data at G1 (MAC)

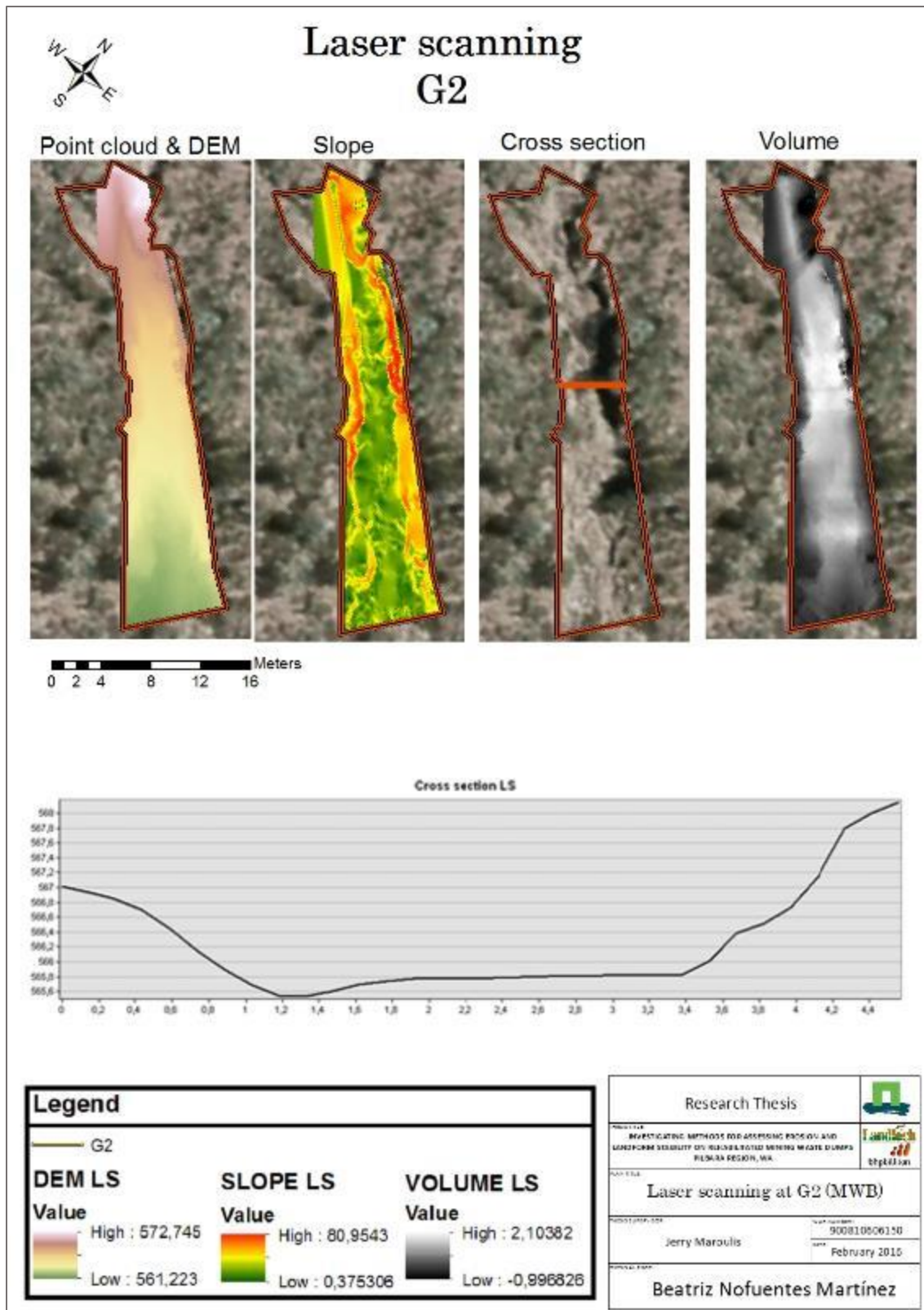
AP5.2.2. Gully 2 (MWB)



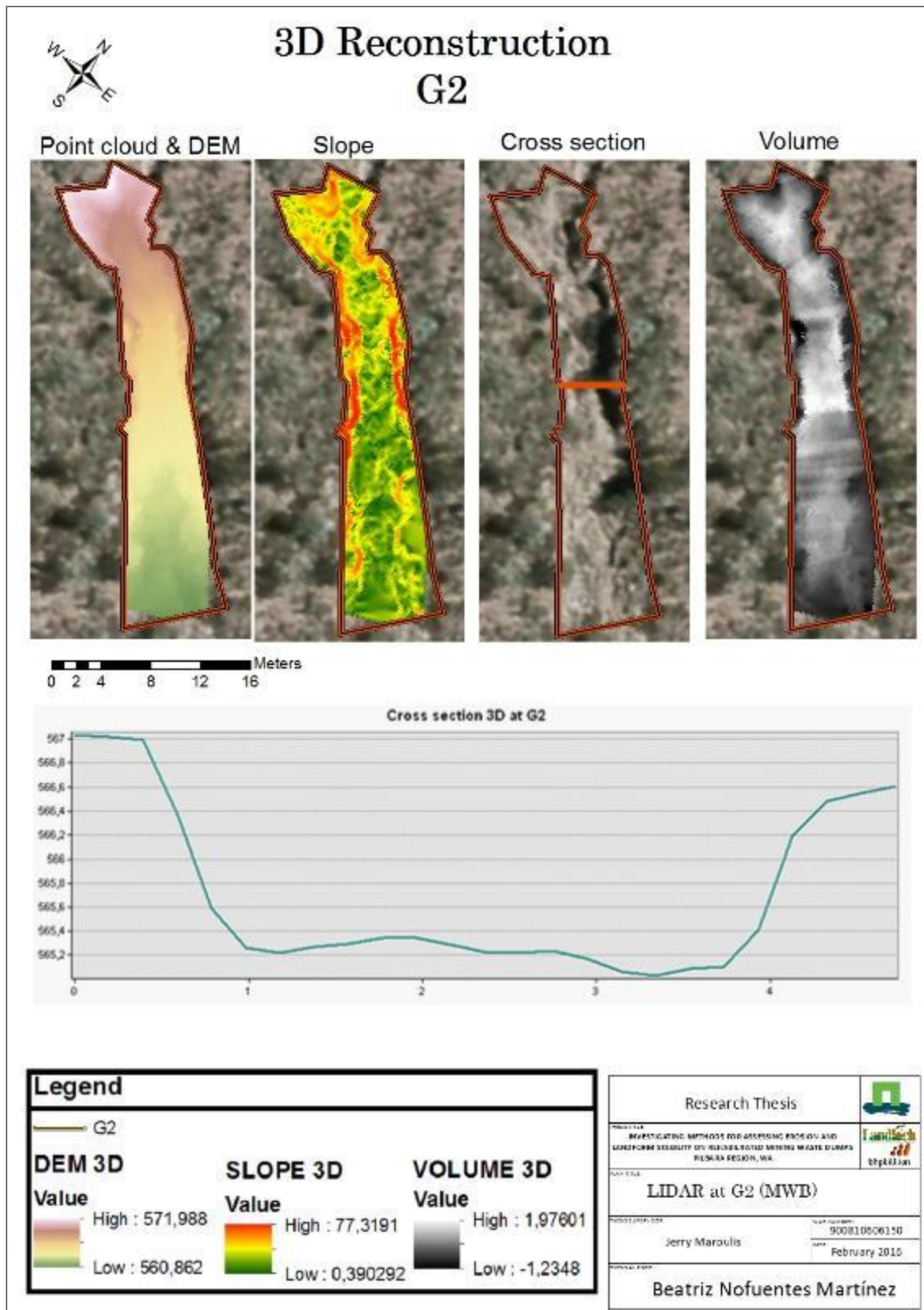
Plan 12: Gully 2 (G2, MWB)



Plan 13: LIDAR surface assessment at G2 (MWB)



Plan 14: Laser scanning surface assessment at G2 (MWB)



Plan 15: 3D Reconstruction surface assessment at G2 (MWB)

Appendix 6: Site pictures



Picture 1: Results of revegetation efforts at Albatross Flamingo Waste Dump

Comparison of revegetation in a plutonic gold mining waste dump immediately after seed harvesting (2004; left) and six years later (2010; right). Source: Red Dirt Seeds. In order to prevent soil loss and support any possible future land use, revegetation based on enhancing native and local species (BHP Billiton Iron Ore, 2013; Red Dirt Seeds, n.d.) is applied to waste dumps in the region.



Picture 2: Status of vegetation after rehabilitation on a waste dump in the Pilbara region

The ideal species in terms of rehabilitation are the spinifex (*Triodia* sp.), as they stabilize soil and create dense masses, controlling runoff and erosion (green masses in the picture). The brownish masses around it are buffel species, which are not original from the region. Although this hillslope is covered with dense vegetation, suffers heavily from erosion in some areas due to a non-adequate design of the landform.



Picture 3: Rip lines implementation after waste dumps rehabilitation at MWB

BHP-Billiton installs rip lines on contour across the slope using a wheeled tractor as contour barriers in order to interrupt the hydrological connectivity at the hillslope scale. This rehabilitated waste dump was initially going to be studied, however the rehabilitation finished in 2015 and no erosion has occurred since then. It was designed following the current rehabilitation planning of BHP-Billiton, by combining different hillslopes along the waste dump.



Picture 4: Eroded waste dump at MWB (1)



Picture 5: Eroded waste dump at MWB (2)

The materials left over from mining give shape to waste dumps, which a part from being the most visual landform left after mining closure, are the most susceptible to erosion (Department of Mines and Petroleum, 2009).

AP6.1. MAC Hillslope 1 (H1)



Picture 6: H1 view from the bottom of the hillslope



Picture 7: View of H1 from the top of the hillslope



Picture 8: Erosion bucket at H1

A bucket collecting runoff and suspended load is located at the plot outlet, after the fabric; it is a tipping box with a magnetic counter that counts the number of times the box has tipped, i.e. runoff volume. H1 erosion plot data could be slightly under-estimated due to a leak associated to the maintenance of the plot outlet.



Picture 9: View from top of H1

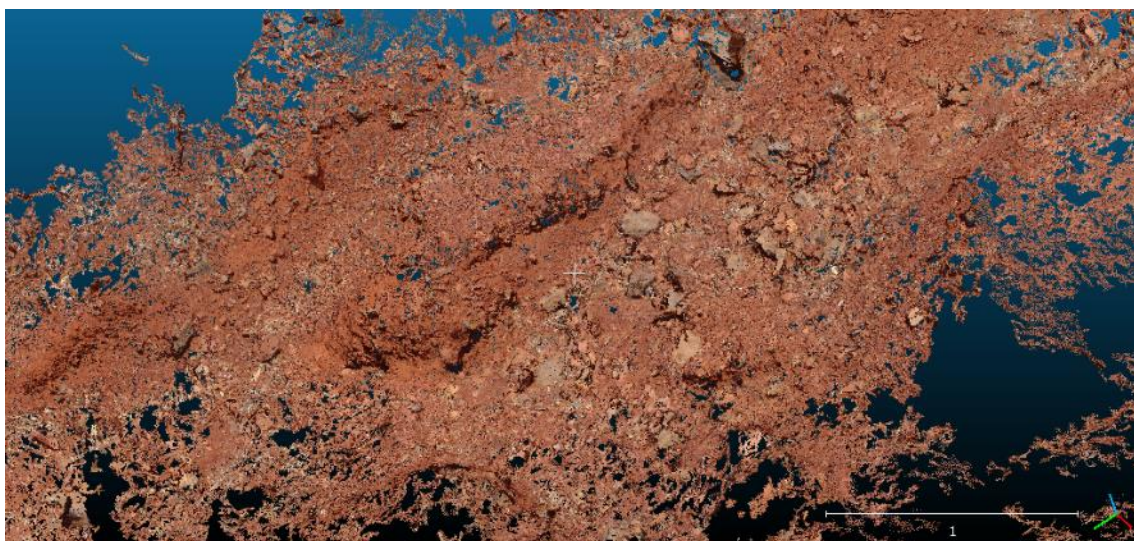
Mound on top of a waste dump hillslope (left of the image) disconnecting hydrological connectivity within mining waste batters.

Gully 1



Picture 10: G1 at MAC from top

Control points used for scaling and georeferencing the 3D reconstructions can be seen.



Picture 11: Precision of the point cloud generated from 3D reconstruction at G1

Even stones just a few square centimeters in size can be observed from the 3D reconstruction point cloud.



AP6.2. MWB

Gully 2 (G2)



Picture 12: G2 from the bottom of the hillslope



Picture 13: G2 from the middle of the hillslope looking downhill



Picture 14: G2 from the middle of the hillslope looking uphill



Picture 15: G2 from the top of the hillslope (1)



Picture 16: G2 from the top of the hillslope (2)